Centro de Investigación y de
Estudios Avanzados del Instituto
Politécnico Nacional
Unidad Zacatenco

Departamento de Matemáticas

Redes Neuronales Celulares p-ádicas y Aplicaciones

Una disertación presentada por

M. en C. Brian Andres Zambrano Luna

para obtener el Grado de

Doctor en Ciencias en la Especialidad de Matemáticas

Asesor de tesis:

Dr. Wilson A. Zúñiga Galindo

Ciudad de México, México Mayo 18, 2023

Centro de Investigación y de
Estudios Avanzados del Instituto
Politécnico Nacional
Unidad Zacatenco

Department of Mathematics

p-Adic Cellular Neural Networks and Applications

A dissertation presented by

M. Sc. Brian Andres Zambrano Luna

to obtain the Degree of

Doctor en Ciencias en la Especialidad de Matemáticas

Thesis Advisor:

Dr. Wilson A. Zúñiga Galindo

Mexico City, Mexico May 18, 2023

Doctoral Dissertation Jury

Dr. Carlos G. Pacheco

Departamento de Matemáticas
Cinvestav-Zacatenco, México

Dr. Michael Porter

Departamento de Matemáticas
Cinvestav-Zacatenco, México

Dr. Miriam Bocardo Gaspar

Departamento de Matemáticas
Universidad de Guadalajara, México

Dr. Sergii Torba

Departamento de Matemáticas
Cinvestav-Zacatenco, México

Dr. Wilson A. Zúñiga Galindo

Departamento de Matemáticas
Cinvestav-Zacatenco, México

Reviewers

Dr. Andrei Khrennikov

Department of Mathematics
Linnaeus University, Sweden

Dr. Leonardo Fabio Chacón Cortés

Departamento de Matemáticas
Universidad Javeriana, Colombia

Dr. Vladimir S. Anashin

Department of Mathematics
Lomonosov Moscow State University, Russia

Resumen

En esta tesis, presentamos las redes neuronales celulares p-adic, que son generalizaciones matemáticas de las redes neuronales celulares clásicas (CNN) introducidas por Chua y Yang en la década de 1980. Las nuevas redes tienen infinitas celdas que están organizadas jerárquicamente en árboles enraizados, y también tienen infinitas capas ocultas. También presentamos dos tipos de CNN que pueden realizar cálculos con datos reales y cuya dinámica se puede entender casi por completo. El primer tipo puede detectar el borde de las imágenes grises. El segundo tipo es una nueva clase de redes de reacción-difusión. Investigamos la estabilidad de estas redes y demostramos que pueden usarse como filtros para reducir el ruido, conservando los bordes, en imágenes contaminadas con ruido gaussiano aditivo.

Esta tesis se basa en las publicaciones [70, 71] escritas en colaboración con mi supervisor Dr. Wilson Zúñiga-Galindo.

Abstract

In this thesis, we introduce the p-adic cellular neural networks, which are mathematical generalizations of the classical cellular neural networks (CNNs) introduced by Chua and Yang in the 1980s. These new networks have infinitely many cells which are organized hierarchically in rooted trees, and also they have infinitely many hidden layers. We also present two types of CNNs that can perform computations with real data, and whose dynamics can be understood almost completely. The first type can detect the edge of gray images. The second type is a new class of reaction-diffusion networks. We investigate the stability of these networks and show that they can be used as filters to reduce noise, preserving the edges, in images polluted with additive Gaussian noise.

This thesis is based on the publications [70, 71] written in collaboration with my supervisor Dr. Wilson Zúñiga-Galindo.

Acknowledgment

This project would not have been possible without the support of many people. Many thanks to my adviser, Dr. Wilson Alvaro Zúñiga Galindo. Without all his advice and talks, we had, all this project would not be what it is.

Thanks to CONACYT for providing me with the financial means to complete this project through their scholarship program.

Thanks to my parents, brothers, family, and numerous friends, especially those part of our student seminary Angel, Angela, Victor, Edgar, and Carlos, who endured this long process with me, always offering support and love.

I would like to thank also to Dr. John Rodrigez, Dr. Oswaldo Lezama, and Dr. Armando Reyes the best mathematicians I met at Universidad Nacional de Colombia and who guided me at the start of this journey.

Finally, thanks to Cinvestav-IPN and the Mexican government for being my home for these three years.

Overview

In the late 80s, Chua and Yang introduced a new natural computing paradigm called the cellular neural networks (or nonlinear cellular networks) CNN, which includes the cellular automata as a particular case [17, 19, 20]. From the beginning, the CNN paradigm was intended for applications such as integrated circuits. This paradigm has been highly successful in various applications in vision, robotics, and remote sensing. See, e.g., [18, 59], and the references therein.

In this work, we present a mathematical generalization of the CNNs of Chua and Yang called *p-adic cellular neural networks*. The p-adic continuous CNNs offer a theoretical framework to study the emergent patterns of hierarchical discrete CNNs having arbitrarily many hidden layers.

This work was carried out in collaboration with Dr. Wilson A. Zuñiga Galindo, and it was published in the Journal of Nonlinear Mathematical Physics, [70].

Nowadays, it is widely accepted that the analysis of ultrametric spaces is the natural tool for formulating models where the hierarchy plays a central role. An ultrametric space (M, d) is a metric space M with a distance satisfying $d(A, B) \leq \max\{d(A, C), d(B, C)\}$ for any three points A, B, C in M. Ultrametricity in physics means the emergence of ultrametric spaces in physical models. Ultrametricity was discovered in the 1980s by Parisi and others in the theory of spin glasses and by Frauenfelder and others in the physics of proteins. In both cases, the space of states of a complex system has a hierarchical structure that plays a central role in the physical behavior of the system, see e.g. [21, 23, 29, 34, 41, 52, 64, 72], and the references therein.

On the other hand, Khrennikov and his collaborators have studied neural network models where p-state neurons take their values in p-adic numbers, see [1, 35]. These models are entirely different from the ones considered here. In addition, Khrennikov has developed non-Archimedean models of brain activity and mental processes, see, e.g., [31] and the references therein.

Among the ultrametric spaces, the field of p-adic numbers $\mathbb{Q}_p$ plays a central role. A p-adic number is a series of the form

$$x = x_{-k}p^{-k} + x_{-k+1}p^{-k+1} + \ldots + x_0 + x_1 p + \ldots, \text{ with } x_{-k} \neq 0, \tag{0.0.1}$$

where p is a prime number, the x_js are p-adic digits, i.e. numbers in the set $\{0, 1, \ldots, p-1\}$. The set of all the possible series of form (0.0.1) constitutes the field of p-adic numbers $\mathbb{Q}_p$. There are natural field operations, sum and multiplication, on series of form (0.0.1), see e.g. [37]. There is also a natural norm in $\mathbb{Q}_p$ defined as $|x|_p = p^k$, for a nonzero p-adic number x of the form (0.0.1). The field of p-adic numbers with the distance induced by $|\cdot|_p$ is a complete ultrametric space. The ultrametric property refers to the fact that $|x-y|_p \leq \max\left\{|x-z|_p, |z-y|_p\right\}$ for any x, y, z in $\mathbb{Q}_p$.

We denote by G_M the set of all the p-adic numbers of the form $\boldsymbol{i} = \boldsymbol{i}_{-M}p^{-M} + \boldsymbol{i}_{-M+1}p^{-M+1} + \cdots + \boldsymbol{i}_0 + \cdots + \boldsymbol{i}_{M-1}p^{M-1}$, where the $\boldsymbol{i}_j$s belong to $\{0, 1, \ldots, p-1\}$. Then $(G_M, |\cdot|_p)$ is a finite ultrametric space. Geometrically speaking, G_M is a regular rooted tree with $2M$ layers, here regular means that exactly p edges emanate from each vertex. We study N-dimensional, discrete hierarchical CNNs having arbitrarily many layers. In particular, a (1-dimensional) p-adic discrete CNN is a dynamical system of the form

$$\frac{\partial}{\partial t}X(\boldsymbol{i},t) = -X(\boldsymbol{i},t) + \sum_{\boldsymbol{j}\in G_M} \mathbb{A}(\boldsymbol{i},\boldsymbol{j})Y(\boldsymbol{j},t) + \sum_{\boldsymbol{j}\in G_M} \mathbb{B}(\boldsymbol{i},\boldsymbol{j})U(\boldsymbol{j}) + Z(\boldsymbol{i}), \tag{0.0.2}$$

$\boldsymbol{i} \in G_M$, where $Y(\boldsymbol{j},t) = f\left(X(\boldsymbol{j},t)\right)$, with $f(x) = \frac{1}{2}\left(|x+1| - |x-1|\right)$. Here $X(\boldsymbol{i},t), Y(\boldsymbol{i},t) \in \mathbb{R}$ are the state, respectively the output, of cell $\boldsymbol{i}$ at the time t. The function $U(\boldsymbol{i}) \in \mathbb{R}$ is the input of the cell $\boldsymbol{i}$, $Z(\boldsymbol{i}) \in \mathbb{R}$ is the threshold of cell $\boldsymbol{i}$, and the matrices $\mathbb{A}, \mathbb{B} : G_M \times G_M \to \mathbb{R}$ are the feedback operator and feedforward operator, respectively. Note that the matrices $\mathbb{A}$, $\mathbb{B}$ are functions on the Cartesian product of two rooted trees. The Chua-Yang CNNs are a particular case of (0.0.2), see e.g. [18, 59].

For the sake of simplicity, we focus on space-invariant networks, i.e. in the case in which

$$\mathbb{A}(\boldsymbol{i},\boldsymbol{j}) = \mathbb{A}(|\boldsymbol{i}-\boldsymbol{j}|_p), \quad \mathbb{B}(\boldsymbol{i},\boldsymbol{j}) = \mathbb{B}(|\boldsymbol{i}-\boldsymbol{j}|_p). \tag{0.0.3}$$

We study the emergent patterns produced by the p-adic discrete CNNs. Since we are interested in arbitrary large trees, the description of these networks requires literally millions of integro-differential equations, consequently, a numerical approach seems not suitable for an exploration of the theoretical properties. Instead of this, we construct a p-adic continuous model that can be very well approximated by (0.0.2).

Intuitively, in the space-invariant case, the continuous model corresponding to (0.0.2) is obtained by taking the limit as M tends to infinity:

$$\frac{\partial X(x,t)}{\partial t} = -X(x,t) + \int_{\mathbb{Q}_p} A(|x-y|_p)Y(y,t)dy + \int_{\mathbb{Q}_p} B(|x-y|_p)U(y)dy + Z(x), \tag{0.0.4}$$

with $Y(x,t) = f(X(x,t))$.

The study of the qualitative behavior of differential equations on large graphs is a relevant matter due to its applications. In [47] Nakao and Mikhailov proposed using continuous models to study reaction-diffusion systems on networks and the corresponding Turing patterns. In [74] the second author showed that p-adic analysis is the natural tool to carry out this program. Models constructed using energy landscapes naturally drive to a large system of differential equations (the master equation of the system), see e.g. [9, 34, 41]. p-Adic continuous versions of some of these systems were constructed by Avetisov, Kozyrev and others in connection with models of protein folding, see e.g. [34, 41] for a general discussion. Another relevant system is the Eigen-Schuster model in biology, see e.g. [49]. In [73] a p-adic continuous version of this model was introduced, this p-adic version allows to explain the Eigen paradox. Recently Hua and Hovestadt pointed out that the p-adic number system offers a natural representation of hierarchical organization of complex networks [29].

We now describe in detail the results and contributions presented in this thesis. In Chapter 1 we present the essential aspects of p-adic analysis, including the definitions of the field of p-adic numbers and the Bruhat-Schwartz space. We also define the integration over $\mathbb{Q}_p^n$ and the change of variables theorem. Chapter 2 introduces semilinear differential equations over Banach spaces, a natural theory to study integro- differential Equations that describe p-adic CNN.

Chapter 3 we present the results concern to p-adic CNN. For the sake of simplicity, in the introduction we discuss our results in dimension one. We study the case where $A(|x|_p)$, $B(|x|_p)$ are integrable, and U, Z are continuous functions vanishing at infinity. Under these hypotheses the initial value problem attached to (0.0.4) with initial datum X_0 (a continuous function vanishing at infinity) has a unique solution $X(x,t)$ which is a continuous function vanishing at infinity in x for every $t \geq 0$, satisfying $|X(x,t)| \leq X_{\max}$, where the constant $X_{\max}$ is completely determined by A, B, U, Z and f, see Theorem 9. An analogous result is valid for discrete CNNs, see Theorem 10.

The solution $X(x,t)$ can be very well approximated in the $\|\cdot\|_\infty$-norm as

$$\sum_{\boldsymbol{j}\in G_M} X(\boldsymbol{j},t)\Omega\left(p^M |x-\boldsymbol{j}|_p\right).$$

By using standard techniques of approximation of semilinear evolution equations, we show that the solution of the Cauchy problem attached to (0.0.2), under condition (0.0.3), is arbitrarily close in the $\|\cdot\|_\infty$-norm to the solution of the Cauchy problem attached to (0.0.4), if M is sufficiently large, see Theorem 11. This implies that the p-adic continuous CNNs have infinitely many hidden layers, and that they are continuous versions of suitable p-adic discrete CNNs. It is relevant to mention that equation (0.0.4) makes sense over the real numbers, i.e., by replacing $\mathbb{Q}_p$ by $\mathbb{R}$ in (0.0.4) we get an equation modeling a continuous network. But, there are no natural discretizations of the real version of (0.0.4) that can be interpreted as hierarchical CNNs, because the real numbers are a completely ordered field, and thus the natural hierarchy is only the linear one.

In practical applications it is natural to assume that the radial functions A, B have compact support or that they are test functions. Under this hypothesis we study the patterns produced by p-adic continuous CNNs when U, Z and X_0 are test functions. The hypothesis that X_0 is a test function means that at time $t = 0$ only certain clusters of cells are excited. Each cluster corresponds to a p-adic ball centered at some cell with radius, say p^{-L}. The intensity of the excitation is the same for all cells in a given cluster. The fact that U, Z are test functions can be interpreted in an analogous way. Let B_{M_0} denote the ball centered at the origin with radius p^{M_0}, which the smallest ball containing the supports of A, B, U, Z, X_0. Then the solution $X(x,t)$ of the initial value problem attached to (0.0.4) is a test function supported in B_{M_0} of the form $\sum_{\boldsymbol{j}\in G_{M_0}} X(\boldsymbol{j},\boldsymbol{t})\Omega\left(p^{M_0}|x-\boldsymbol{j}|_p\right)$ for $t \geq 0$, with $M_0 \geq L$, see Theorem 8. This means that a p-adic continuous CNN produces a pattern which is organized in a finite number of disjoint clusters, each of them supporting a time varying pattern. We also show the existence of two steady state patterns $X_+(x)$, $X_-(x)$, which are test functions, such that $X_-(x) \leq \lim_{t\to\infty} X(x,t) \leq X_+(x)$, see Theorem 9. We conjecture that for generic p-adic continuous CNNs, $\lim_{t\to\infty} X(x,t)$ is a test function, which means that the steady state pattern is organized in a finite number of disjoint clusters, each of them supporting a constant pattern. This is exactly the multistability property reported in [47], see also [74], for reaction-diffusion networks.

We have conducted a large number of numerical simulations. Such simulations require solving integro-differential equations on a tree. The numerical study of p-adic continuous CNNs offers two big challenges. The first, the need of dealing with matrices having millions of entries, the second, the visualization of functions depending on p-adic variables. Due to the first problem, we use small trees with 16 to 64 leaves. The p-adic numbers have a fractal nature, so, it is necessary to visualize real-valued functions defined on the Cartesian product of a fractal times the real line. To deal with this problem we systematically use heat maps which allow us to get a glimpse of the hierarchical nature of the CNNs. Our numerical simulations show that the solutions of continuous CNNs exhibit a very complex behavior, including self-similarity and multistability, depending on the interaction of all the parameters defining the network and initial datum.

In the last Chapter 4, we show that p-adic CNNs can perform computations using real data and that the dynamics can be understood entirely. We present two types of p-adic CNNs, one for edge detection of gray images and the other for denoising gray images polluted with Gaussian noise. This work was carried on in collaboration with Dr. Wilson Zuñiga Galindo, [71]. It is important to emphasize that our goal is not to produce new techniques for image processing but to use these tasks to verify that p-adic CNNs can perform relevant computations. On the other hand, classical CNNs have been implemented in hardware for performing certain image-processing tasks. We have used some of the ideas introduced in [18], but our results go in a completely new direction.

We found experimentally that p-adic CNNs of the form

$$\begin{cases} \frac{\partial}{\partial t}X(x,t) = -X(x,t) + aY(x,t) + (B * U)(x) + Z(x), \quad x \in \mathbb{Z}_p, t \geq 0; \\ \\ Y(x,t) = f(X(x,t)), \end{cases} \tag{0.0.5}$$

can be used as edge detectors. Here $\mathbb{Z}_p$ is the p-adic unit ball, and U is an image. We develop numerical algorithms for solving the Cauchy problem attached to (0.0.5), with initial datum $X(x,0) = 0$. The simulations show that after a time sufficiently large the network outputs a white and black image approximating the edges of the original image $U(x)$. The performance of this edge detector is comparable to the Canny detector and other well-known detectors. But most importantly, we can explain reasonably well how the network detects the edges of an image.

We determine all the stationary states of (0.0.5), i.e., the solutions of $\frac{\partial}{\partial t}X(x,t) = 0$, for all $a \in \mathbb{R}$, see Lemma 8 and Theorem 12. We show that for $a > 1$, the set of all possible stationary states $\mathcal{M}$ of (0.0.5) has a hierarchical structure; more precisely, $(\mathcal{M}, \preccurlyeq)$ is a lattice, where $\preccurlyeq$ is a partial order. Furthermore, we determine the set of minimal elements of $(\mathcal{M}, \preccurlyeq)$, see Theorem 13. The dynamics of the network consists of transitions in a hierarchically organized landscape $(\mathcal{M}, \preccurlyeq)$ toward of some minimal state. This is a reformulation of the classical paradigm asserting that the dynamics of a large class of complex systems can be modeled as a random walk on its energy landscape.

We found experimentally that p-adic CNNs of the form

$$\frac{\partial X(x,t)}{\partial t} = \mu X(x,t) + (\lambda I - \boldsymbol{D}_0^{\alpha})X(x,t) + \int_{\mathbb{Z}_p} A(x-y)f(X(y,t))dy + \int_{\mathbb{Z}_p} B(x-y)U(y)dy + Z(x), \tag{0.0.6}$$

can be used for denoising gray images poluted with Gaussian noise. In this case, $X(x,0)$ is the input image, and $X(x,t_0)$ for a suitable (typically small) t_0 is the output image.

The CNN (0.0.6) is a reaction-diffusion network. The diffusion part corresponds to

$$\frac{\partial X(x,t)}{\partial t} = (\lambda I - \boldsymbol{D}_0^{\alpha})X(x,t),\ x \in \mathbb{Z}_p, t \geq 0, \tag{0.0.7}$$

here $\boldsymbol{D}_0^{\alpha}$ is the Vladimirov operator acting on functions supported in the unit ball, $\alpha > 0$. The equation (0.0.7) is a p-adic heat equation in the unit ball: this means that there is a stochastic Markov process attached to it. The paths of this stochastic process are discontinuous. p-Adic heat equations and the associated stochastic processes have been studied intensively in the last thirty years in connection with models of complex systems, see, e.g., [7, 8, 21, 34, 38, 41, 63, 64, 72, 75].

The reaction term in (0.0.6) gives an estimation of the edges of the image, while the diffusion term produces a smoothed version of the image. Under suitable hypotheses, see Theorem 14, we show that a solution of the initial value problem attached to (0.0.6) is bounded at very time if $\mu \leq 0$, otherwise, the solution is bounded by $Ce^{\mu t}$, where C is a positive constant. Some numerical simulations show that our filter effectively reduces the noise while preserving the edges of the image. However, its performance is inferior to the Perona-Malik filter, see, e.g., [57].

Finally, we want to mention that Prof. Adrei Khrenikov and his collaborators have studied extensively the applications of p-adic analysis to image processing, see [10] and related papers [11, 33, 40]

Contents

Resumen I

Abstract II

1 Essential aspects of p-adic analysis 1
1.1 The field of p-adic numbers 1
1.2 Topology of $\mathbb{Q}_p^N$ 1
1.3 Integration over $\mathbb{Q}_p^N$ 2
1.4 The Bruhat-Schwartz space 3
1.5 The Spaces $\mathcal{X}_\infty$, $\mathcal{X}_M$ 4
1.6 Tree-like structures and p-adic numbers 5

2 Semilinear differential equations 7
2.1 Strongly continuous semigroups 7
2.2 Semilinear partial differential equations 9
2.3 Approximation for Semilinear differential Equations 9

3 p-adic Cellular Neural Networks 11
3.1 p-Adic CNNs: basic definitions 11
3.1.1 p-Adic discrete CNNs 11
3.1.2 p-Adic continuous CNNs 12
3.1.3 Discretization of p-adic continuous CNNs 13
3.2 Stability of p-adic continuous CNN 15
3.3 Stability of p-adic discrete CNN and Approximation of Continuous CNNs 21
3.3.1 The operators $\boldsymbol{P}_M$, $\boldsymbol{E}_M$ 21
3.4 Numerical Simulations of p-Adic Continuous CNNs 24
3.4.1 Numerical Scheme A 24
3.4.2 Numerical Scheme B 25
3.4.3 A remark on the visualization of finite rooted trees 26
3.4.4 First Simulation 26
3.4.5 Second Simulation 28
3.4.6 Third Simulation 30
3.4.7 Fourth Simulation 31

4 p-adic Cellular Neural Network: Application to Image Processing 36
4.1 A type p-adic continuous CNNs for edge detection . . . 36
4.1.1 Stationary states . . . 37
4.2 Hierarchical structure of the space of stationary states . . . 39
4.3 Edge detection . . . 40
4.3.1 A new class of edge detectors . . . 40
4.3.2 Discretization . . . 41
4.4 Numerical Examples . . . 44
4.5 Reaction-diffusion Cellular Neural Networks . . . 44
4.5.1 The p-adic heat equation . . . 44
4.5.2 The p-adic heat equation on the unit ball . . . 46
4.5.3 Reaction-diffusion CNNs . . . 47
4.6 Denoising . . . 50
4.7 Images and test functions . . . 51
4.7.1 Finite rooted trees and test functions . . . 51
4.7.2 Images and finite rooted trees . . . 53

5 Conclusions 56

A Cellular Neural Networks 58
A.1 General Cellular Neural Network . . . 58
A.2 Chua-Yang CNN model . . . 59

B Image processing 61
B.1 Canny Edge detector . . . 61
B.2 Perona-Malik Equation . . . 62

Bibliography 63

Chapter 1

Essential aspects of p-adic analysis

In this document, p will be a fixed prime number. In this chapter, we present some important results about of p-adic numbers. For an in-depth review of p-adic analysis, the reader may consult [2, 64], and the references therein.

1.1 The field of p-adic numbers

The field of p-adic numbers $\mathbb{Q}_p$ is defined as the completion of the field of rational numbers $\mathbb{Q}$ with respect to the $p-$adic norm $|\cdot|_p$, which is defined as

$$|x|_p = \begin{cases} 0 & \text{if} \quad x = 0 \\ p^{-\gamma} & \text{if} \quad x = p^{\gamma}\frac{a}{b}, \end{cases}$$

where a and b are integers coprime with p. The integer $\gamma := ord(x)$, with $ord(0) := +\infty$, is called the *$p-$adic order of x*. We extend the $p-$adic norm to $\mathbb{Q}_p^N$ by taking

$$||x||_p := \max_{1\leq i\leq N} |x_i|_p, \qquad \text{for } x = (x_1, \dots, x_N) \in \mathbb{Q}_p^N.$$

We define $ord(x) = \min_{1\leq i\leq N}\{ord(x_i)\}$; then $||x||_p = p^{-ord(x)}$. The metric space $\left(\mathbb{Q}_p^N, ||\cdot||_p\right)$ is a complete ultrametric space. As a topological space $\mathbb{Q}_p$ is homeomorphic to a Cantor-like subset of the real line, see e.g. [2, 64].

Any $p-$adic number $x \neq 0$ has a unique expansion of the form

$$x = p^{ord(x)} \sum_{j=0}^{\infty} x_j p^j,$$

where $x_j \in \{0, 1, \dots, p-1\}$ and $x_0 \neq 0$.

1.2 Topology of $\mathbb{Q}_p^N$

For $r \in \mathbb{Z}$, denote by $B_r^N(a) = \{x \in \mathbb{Q}_p^N; ||x-a||_p \leq p^r\}$ *the ball of radius p^r with center at* $a = (a_1, \dots, a_N) \in \mathbb{Q}_p^N$, and take $B_r^N(0) := B_r^N$. Note that $B_r^N(a) = B_r(a_1) \times \cdots \times B_r(a_N)$, where $B_r(a_i) := B_r^1(a_i) = \{x \in \mathbb{Q}_p; |x_i - a_i|_p \leq p^r\}$ is the one-dimensional ball of radius p^r with center at $a_i \in \mathbb{Q}_p$. The ball B_0^N equals the product of N copies of $B_0 = \mathbb{Z}_p$, *the ring of $p-$adic integers*. We also denote by $S_r^N(a) = \{x \in \mathbb{Q}_p^N; ||x-a||_p = p^r\}$ *the sphere of radius p^r with center at $a = (a_1, \dots, a_N) \in \mathbb{Q}_p^N$*, and take $S_r^N(0) := S_r^N$. We notice that $S_0^1 = \mathbb{Z}_p^\times$ (the group of units of $\mathbb{Z}_p$), but $\left(\mathbb{Z}_p^\times\right)^N \subsetneq S_0^N$. The balls and spheres are both open and closed subsets in $\mathbb{Q}_p^N$. In addition, two balls in $\mathbb{Q}_p^N$ are either disjoint or one is contained in the other.

As a topological space $\left(\mathbb{Q}_p^N, ||\cdot||_p\right)$ is totally disconnected, i.e. the only connected subsets of $\mathbb{Q}_p^N$ are the empty set and the points. A subset of $\mathbb{Q}_p^N$ is compact if and only if it is closed and bounded in $\mathbb{Q}_p^N$, see e.g. [64, Section 1.3], or [2, Section 1.8]. The balls and spheres are compact subsets. Thus $\left(\mathbb{Q}_p^N, ||\cdot||_p\right)$ is a locally compact topological space.

We will use $\Omega\left(p^{-r}||x-a||_p\right)$ to denote the characteristic function of the ball $B_r^N(a)$. For more general sets, we will use the notation 1_A for the characteristic function of a set A.

1.3 Integration over $\mathbb{Q}_p^N$

We now review Haar's theorem for locally compact topological groups, which allow us to develop an integration theory over $\mathbb{Q}_p^N$. For further details, the reader may consult [64, Chapter 4] and [2, Chapter 3].

Theorem 1. *[28, Thm B. Sec.58] Let $(G, +)$ be a locally compact topological group. There exists a Borel measure dx, unique up to multiplication by a positive constant, such that $\int_U dx > 0$ for every non empty Borel open set U, and $\int_{x+E} dx = \int_E dx$, for every Borel set E.*

The measure dx is called a Haar measure of G. Since $(\mathbb{Q}_p, +)$ is a locally compact topological group, by Theorem 1, it has a Haar measure dx. We normalize this measure using the condition $\int_{\mathbb{Z}_p} dx = 1$.

In the N-dimensional case, we denote by $d^N x$ the product measure $\underbrace{dx \cdots dx}_{N-times}$. This measure satisfies that $d^N(x+a) = d^n x$, for $a \in \mathbb{Q}_p^N$, and $\int_{\mathbb{Z}_p^N} d^N x = 1$.

Example 1. *1. $\int_{p\mathbb{Z}_p} dx = p^{-1}$. Indeed,*

$$1 = \int_{\mathbb{Z}_p} dx = \int_{\bigsqcup_{i=0}^{p-1} i+p\mathbb{Z}_p} dx = \sum_{i=0}^{p-1} \int_{i+p\mathbb{Z}_p} dx = \sum_{i=0}^{p-1} \int_{p\mathbb{Z}_p} dx = p \int_{p\mathbb{Z}_p} dx.$$

2. $\int_{B_{-1}^N} d^N x = p^{-N}$.

3. $\int_{S_{-1}^N} d^N x = (1 - p^{-N})$, this formula is obtained as follows:

$$\int_{S_{-1}^N} d^N x = \int_{\mathbb{Z}_p^N \setminus B_{-1}^N} d^N x = \int_{\mathbb{Z}_p^N} d^N x - \int_{B_{-1}^N} d^N x = 1 - p^{-N}.$$

4. $\int_{B_r^N(a)} d^N x = p^{rN}$.

5. $\int_{S_r^N(a)} d^N x = p^r(1-p^{-N})$.

6. Let $s \in \mathbb{C}$ *with* $Re(s) > 0$. *Then*

$$\int_{a+p^l\mathbb{Z}_p} |x|_p^{s-1}\, dx = \begin{cases} p^{-ls}\left(\frac{1-p^{-1}}{1-p^{-s}}\right) & \text{if} \quad a \in p^l\mathbb{Z}_p \\ p^{-l}\,|a|_p^{s-1} & \text{if} \quad a \notin p^l\mathbb{Z}_p. \end{cases} \tag{1.3.1}$$

Indeed,

If $a \notin p^l\mathbb{Z}_p$, *by changing variables* $x \mapsto y - a$ *we have*

$$\int_{a+p^l\mathbb{Z}_p} |x|_p^{s-1}\, dx = \int_{p^l\mathbb{Z}_p} |-a+y|_p^{s-1}\, dy = |a|_p^{s-1} \int_{p^l\mathbb{Z}_p} dy = p^{-l}\,|a|_p^{s-1}.$$

If $a \in p^l\mathbb{Z}_p$ *then* $a + p^l\mathbb{Z}_p = p^l\mathbb{Z}_p$, *by changing variables* $x \mapsto yp^l$ *we have*

$$\begin{aligned} \int_{a+p^l\mathbb{Z}_p} |x|_p^{s-1}\, dx &= p^{-l}\int_{\mathbb{Z}_p} \left|p^l y\right|_p^{s-1} dy = p^{-ls}\int_{\mathbb{Z}_p} |y|_p^{s-1}\, dy \\ &= p^{-ls}\sum_{k=0}^{\infty}\int_{S_k} |y|_p^{s-1}\, dy = p^{-ls}\sum_{k=0}^{\infty} p^{-k(s-1)}p^{-k}(1-p^{-1}) \\ &= p^{-ls}(1-p^{-1})\sum_{k=0}^{\infty} p^{-ks} = p^{-ls}\frac{1-p^{-1}}{1-p^{-s}}. \end{aligned}$$

1.4 The Bruhat-Schwartz space

A real-valued function φ defined on $\mathbb{Q}_p^N$ is *called locally constant* if for any $x \in \mathbb{Q}_p^N$ there exists an integer $l(x) \in \mathbb{Z}$ such that

$$\varphi(x + x') = \varphi(x) \text{ for } x' \in B_{l(x)}^N. \tag{1.4.1}$$

A function $\varphi : \mathbb{Q}_p^N \to \mathbb{R}$ is called a *Bruhat-Schwartz function (or a test function)* if it is locally constant with compact support. Any test function can be represented as a linear combination, with real coefficients, of characteristic functions of balls. The $\mathbb{R}$-vector space of Bruhat-Schwartz functions is denoted by $\mathcal{D}(\mathbb{Q}_p^N)$. For $\varphi \in \mathcal{D}(\mathbb{Q}_p^N)$, the largest number $l = l(\varphi)$ satisfying (1.4.1) is called *the exponent of local constancy (or the parameter of constancy) of* φ.

If U is an open subset of $\mathbb{Q}_p^N$, $\mathcal{D}(U)$ denotes the space of test functions with supports contained in U, then $\mathcal{D}(U)$ is dense in

$$L^\rho(U) = \left\{\varphi : U \to \mathbb{R};\ \left(\int_{\mathbb{Q}_p^N} |\varphi(x)|^\rho\, d^N x\right)^{\frac{1}{\rho}} < \infty\right\},$$

where $d^N x$ is the Haar measure on $\mathbb{Q}_p^N$ normalized by the condition $vol(B_0^N) = 1$, for $1 \leq \rho < \infty$, see e.g. [2, Section 4.3]. In the case $U = \mathbb{Q}_p^N$, we will use the notation L^ρ instead of $L^\rho\left(\mathbb{Q}_p^N\right)$. For an in depth discussion about p-adic analysis the reader may consult [2, 38, 62, 64].

1.5 The Spaces $\mathcal{X}_\infty$, $\mathcal{X}_M$

We define $\mathcal{X}_\infty(\mathbb{Q}_p^N) := \mathcal{X}_\infty = \overline{\left(\mathcal{D}(\mathbb{Q}_p^N), \|\cdot\|_\infty\right)}$, where $\|\phi\|_\infty = \sup_{x\in\mathbb{Q}_p^N} |\phi(x)|$ and the bar means the completion with respect the metric induced by $\|\cdot\|_\infty$. Notice that all functions in $\mathcal{X}_\infty$ are continuous and that

$$\mathcal{X}_\infty \subseteq \mathcal{C}_0 := \left(\left\{ f : \mathbb{Q}_p^N \to \mathbb{R}; f \text{ continuous with } \lim_{\|x\|_p \to \infty} f(x) = 0 \right\}, \|\cdot\|_\infty \right).$$

On the other hand, since $\mathcal{D}(\mathbb{Q}_p^N)$ is dense in $\mathcal{C}_0$, cf. [62, Chap.II, Proposition 1.3], we conclude that $\mathcal{X}_\infty = \mathcal{C}_0$.

For $M \geq 1$, we set $G_M^N := B_M^N / B_{-M}^N$, which is a finite additive group with $\#G_M^N := p^{2NM}$ elements. Any element $\boldsymbol{i} = (\boldsymbol{i}_1, \ldots, \boldsymbol{i}_N)$ of G_M^N can be represented as

$$\boldsymbol{i}_j = \boldsymbol{i}_{-M}^j p^{-M} + \boldsymbol{i}_{-M+1}^j p^{-M+1} + \ldots + \boldsymbol{i}_0^j + \boldsymbol{i}_1^j p + \ldots + \boldsymbol{i}_{M-1}^j p^{M-1}, \tag{1.5.1}$$

for $j = 1, \ldots, N$, with $\boldsymbol{i}_k^j \in \{0, 1, \ldots, p-1\}$. From now on, we fix a set of representatives in $\mathbb{Q}_p^N$ for G_M^N of the form (1.5.1). Notice that

$$\boldsymbol{i}_j = p^{-M}\left(\boldsymbol{a}_0^j + \boldsymbol{a}_1^j p + \cdots + \boldsymbol{a}_{2M-1}^j p^{2M-1}\right),$$

where $\boldsymbol{a}_0^j + \boldsymbol{a}_1^j p + \cdots + \boldsymbol{a}_{2M-1}^j p^{2M-1} \in \mathbb{Z}_p / p^{2M}\mathbb{Z}_p = B_0 / B_{-2M}$.

The characteristic functions of the balls $B_{-M}^N(\boldsymbol{i})$ for $\boldsymbol{i} \in G_M^N$

$$\left\{\Omega\left(p^M \|x - \boldsymbol{i}\|_p\right)\right\}_{\boldsymbol{i}\in G_M^N} \tag{1.5.2}$$

are orthogonal with respect to the standard L^2 inner product, since

$$\Omega\left(p^M \|x - \boldsymbol{i}\|_p\right)\Omega\left(p^M \|x - \boldsymbol{j}\|_p\right) = 0, \text{ for } \boldsymbol{i}, \boldsymbol{j} \in G_M^N,\ \boldsymbol{i} \neq \boldsymbol{j} \text{ and for any } x \in B_M^N.$$

We denote by $\mathcal{D}^M\left(\mathbb{Q}_p^N\right) := \mathcal{D}^M$ the $\mathbb{R}$-vector space spanned by (1.5.2). We set

$$\mathcal{X}_M := \left(\mathcal{D}^M, \|\cdot\|_\infty\right) \text{ for } M \geq 1.$$

Notice that $\mathcal{X}_M$ is isomorphic as a Banach space to $\left(\mathbb{R}^{\#G_M^N}, \|\cdot\|_\mathbb{R}\right)$, where

$$\left\|\left(t_1, \ldots, t_{\#G_M^N}\right)\right\|_\mathbb{R} = \max_{1\leq j\leq \#G_M^N} |t_j|.$$

1.6 Tree-like structures and p-adic numbers

Take $N=1$ and fix $M\in\mathbb{N}\smallsetminus\{0\}$, then $G_M^1:=G_M=p^{-M}\mathbb{Z}_p/p^M\mathbb{Z}_p$ is an additive group consisting of elements of the form

$$\boldsymbol{i}=\boldsymbol{i}_{-M}p^{-M}+\boldsymbol{i}_{-M+1}p^{-M+1}+\cdots+\boldsymbol{i}_0+\cdots+\boldsymbol{i}_{M-1}p^{M-1}, \tag{1.6.1}$$

where the $\boldsymbol{i}_j$ belong to $\{0,1,\ldots,p-1\}$. Furthermore, the restriction of $|\cdot|_p$ to G_M induces an absolute value such that $|G_M|_p=\left\{0,p^{-(M-1)},\cdots,p^{-1},1,\cdots,p^M\right\}$. We endow G_M with the metric induced by $|\cdot|_p$, and thus G_M becomes a finite ultrametric space. In addition, G_M can be identified with the set of branches (vertices at the top level) of a rooted tree with $2M+1$ levels and p^{2M} branches. Any element $\boldsymbol{i}\in G_M$ can be uniquely written as $p^{-M}\widetilde{\boldsymbol{i}}$, where

$$\widetilde{\boldsymbol{i}}=\widetilde{\boldsymbol{i}}_0+\widetilde{\boldsymbol{i}}_1p+\cdots+\widetilde{\boldsymbol{i}}_{2M-1}p^{2M-1}\in\mathbb{Z}_p/p^{2M}\mathbb{Z}_p,$$

with the $\widetilde{\boldsymbol{i}}_j$s belonging to $\{0,1,\ldots,p-1\}$. The elements of the $\mathbb{Z}_p/p^{2M}\mathbb{Z}_p$ are in bijection with the vertices at the top level of the above mentioned rooted tree. By definition the root of the tree is the only vertex at level 0. There are exactly p vertices at level 1, which correspond with the possible values of the digit $\widetilde{\boldsymbol{i}}_0$ in the p-adic expansion of $\widetilde{\boldsymbol{i}}$. Each of these vertices is connected to the root by a non-directed edge. At level ℓ, with $1\leq\ell\leq 2M$, there are exactly p^ℓ vertices, each vertex corresponds to a truncated expansion of $\widetilde{\boldsymbol{i}}$ of the form $\widetilde{\boldsymbol{i}}_0+\cdots+\widetilde{\boldsymbol{i}}_{\ell-1}p^{\ell-1}$. The vertex corresponding to $\widetilde{\boldsymbol{i}}_0+\cdots+\widetilde{\boldsymbol{i}}_{\ell-1}p^{\ell-1}$ is connected to a vertex $\widetilde{\boldsymbol{i}}'_0+\cdots+\widetilde{\boldsymbol{i}}'_{\ell-2}p^{\ell-2}$ at the level $\ell-1$ if and only if $\left(\widetilde{\boldsymbol{i}}_0+\cdots+\widetilde{\boldsymbol{i}}_{\ell-1}p^{\ell-1}\right)-\left(\widetilde{\boldsymbol{i}}'_0+\cdots+\widetilde{\boldsymbol{i}}'_{\ell-2}p^{\ell-2}\right)$ is divisible by $p^{\ell-1}$.

In conclusion, $\mathbb{Z}_p/p^{2M}\mathbb{Z}_p$ is a rooted tree, and $\mathbb{Z}_p$ is an infinite rooted tree. Now, the 1-dimensional unit sphere $\mathbb{Z}_p^\times$ is the disjoint union of sets of the form $j+p\mathbb{Z}_p$, for $j\in\{1,\ldots,p-1\}$. Each set of the form $j+p\mathbb{Z}_p$ is an infinite rooted tree. Then, $\mathbb{Z}_p^\times$ is a forest formed by the disjoint union of $p-1$ infinite rooted trees. On the other hand, $\mathbb{Q}_p^\times=\mathbb{Q}_p\smallsetminus\{0\}$ is a countable disjoint union of scaled versions of the forest $\mathbb{Z}_p^\times$, more precisely, $\mathbb{Q}_p^\times=\bigsqcup_{k=-\infty}^{k=+\infty}p^k\mathbb{Z}_p^\times$. The field of p-adic numbers has a fractal structure, see e.g. [2, 64].

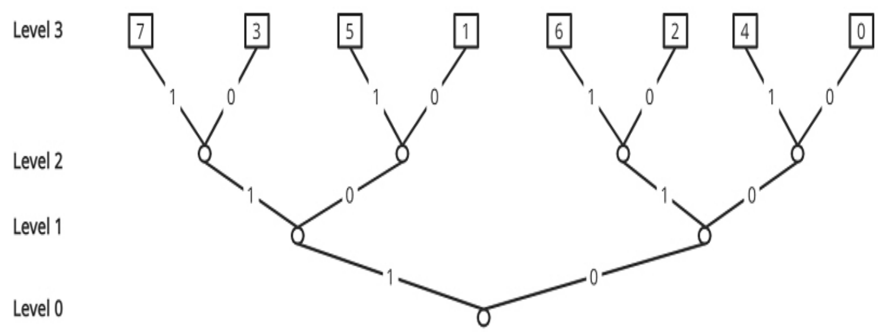

Figure 1.1: The rooted tree associated with the group $\mathbb{Z}_2/2^3\mathbb{Z}_2$. We identify the elements of $\mathbb{Z}_2/2^3\mathbb{Z}_2$ with the set of integers $\{0,\ldots,7\}$ with binary representation $\boldsymbol{i} = \boldsymbol{i}_0 + \boldsymbol{i}_1 2 + \boldsymbol{i}_3 2^2$, $\boldsymbol{i}_0, \boldsymbol{i}_1, \boldsymbol{i}_2 \in \{0,1\}$. Two leaves $\boldsymbol{i}, \boldsymbol{j} \in \mathbb{Z}_2/2^3\mathbb{Z}_2$ have a common ancestor at level 2 if and only if $\boldsymbol{i} \equiv \boldsymbol{j} \bmod 2^2$, i.e., $\boldsymbol{i} = \boldsymbol{a}_0 + \boldsymbol{a}_1 2 + \boldsymbol{i}_2 2^2$ and $\boldsymbol{j} = \boldsymbol{a}_0 + \boldsymbol{a}_1 2 + \boldsymbol{j}_2 2^2$ with $\boldsymbol{i}_2, \boldsymbol{j}_2 \in \{0,1\}$. Now, for $\boldsymbol{i}, \boldsymbol{j} \in \mathbb{Z}_2/2^3\mathbb{Z}_2$ have a common ancestor at level 1 if and only if $\boldsymbol{i} \equiv \boldsymbol{j} \bmod 2$. Notice that that the p-adic distance satisfies $-\log_2 |\boldsymbol{i} - \boldsymbol{j}|_2 =$ (level of the first common ancestor of $\boldsymbol{i}$, $\boldsymbol{j}$).

Chapter 2

Semilinear differential equations

This chapter will regard the main ideas about semi-linear partial differential equations that we will apply during all the remaining chapters. The explanation is based on the reference [46, Chapter 4, Chapter 5], [67, Chapter 1, Chapter 2].

Through this chapter, X will denote a Banach space over $\mathbb{K} = \mathbb{R}$ or $\mathbb{C}$ with norm $\|\cdot\|$.

For a linear operator $A : \mathrm{Dom}(A) \subseteq X \to X$ we denote $\rho(A)$ as the resolvent of A, i.e., all $\lambda \in \mathbb{K}$ such that $R(\lambda, A) := (\lambda I - A)^{-1} : X \to Dom(A)$ exists and is bounded. We denote $\sigma(A) := \mathbb{K} \setminus \rho(A)$ as the spectrum of A.

2.1 Strongly continuous semigroups

In this section, we will summarize the theory of strongly continuous semigroups.

Definition 1. *Let $\{T(t)\}_{t\geq 0}$ be a family of bounded linear operators on X. $\{T(t)\}_{t\geq 0}$ is called a strongly continuous semigroup or C_0-semigroup if*

- *T_0 is the identity I.*
- *For all $t, s \geq 0$, $T(t)T(s) = T(s+t)$.*
- *For all $x \in X$, $\lim_{t\to 0^+} \|T(t)x - x\| = 0$.*

Given a strongly continuous semigroup $\{T(t)\}_{t\geq 0}$, its infinitesimal generator A is defined as $x \in Dom(A)$ if and only if $\lim_{t\to 0^+} \frac{T(t)x-x}{t}$ exists and Ax is the limit.

Theorem 2. *Assume that $\{T(t)\}_{t\geq 0}$ is a strongly continuous semigroup with infinitesimal generator A. Then*

1. *There exist constants $w \in \mathbb{R}$ and $M \geq 0$ such that*

$$\|T(t)\| \leq Me^{wt} \text{ for } t \geq 0.$$

2. *For $x \in X$ and $t \geq 0$, we have $\int_0^t T(s)xds \in Dom(A)$ and*

$$T(t)x - x = A\left(\int_0^t T(s)xds\right).$$

3. *For all $x \in Dom(A)$ an $t \geq 0$, $T(t)x \in Dom(A)$ and*

$$\frac{dT(t)x}{dt} := \lim_{h\to 0} \frac{T(t+h)x - T(t)x}{h} = AT(t)x = T(t)Ax.$$

4. *$Dom(A)$ is dense in X and A is a closed linear operator, i.e., $\{(x, Ax);\ x \in Dom(A)\}$ is closed in $X \times X$.*

5. *For every $x \in Dom(A)$ and $t \geq s \geq 0$*

$$T(t)x - T(s)x = \int_s^t T(\tau)Axd\tau = \int_s^t AT(\tau)xd\tau.$$

The following well-known theorem due to Hill-Yosida-Phillips tells us how we can identify whether an operator A is the infinitesimal generator of a strongly continuous semigroup.

Theorem 3 (Hill-Yosida-Phillips)**.** *A linear operator A is the infinitesimal generator of a strongly continuous semigroup $\{T(t)\}_{t\geq 0}$ satisfying $\|T(t)\| \leq Me^{wt}$ if and only if*

1. *A is a closed operator and $Dom(A)$ is dense in X, and either*

2a. *$(w, \infty) \subseteq \rho(A)$ and*

$$\|R(\lambda, A)\| \leq \frac{M}{(\lambda - w)^n} \text{ for } \lambda > w$$

or

2b. *$\rho(A)$ contains complex numbers λ with $Re(\lambda) > w$ and*

$$\|R(\lambda, A) \leq \frac{M}{(Re\lambda - w)^n} \text{ for } Re\lambda w.$$

There is a more direct relation between a strongly continuous semigroup $\{T(t)\}_{t\geq 0}$ and the resolvent operator $R(\lambda, A)$ of its infinitesimal generator given by:

1. **Integral formula**

$$R(\lambda, A) = \int_0^\infty e^{-\lambda s} T(s)ds \text{ if } Re\lambda > w$$

2. **Exponential formula**

$$T(t)x = \lim_{n\to\infty} (I - t/nA)^{-n} x$$

for all $x \in X$, and the convergence is uniform in t.

2.2 Semilinear partial differential equations

Now we consider the theory of semilinear partial differential equations where one study abstract Cauchy problems such as

$$\begin{cases} \frac{dX(t)}{dt} = AX(t) + F(X,t), & \text{if } t > 0 \\ X(0) = X_0 \end{cases} \tag{2.2.1}$$

where A is the infinitesimal generator of a strongly continuous semigroup $\{T(t)\}_{t\geq 0}$, $X_0 \in X$ and $F : X \times [0,\tau) \to X$ for some $\infty \geq \tau > 0$.

Remark 1. *A continuous functions $X : [0,\tau) \to X$ is called a classical solution of 2.2.1 if and only if*

1. *$X(0) = X_0$ for all $x \in X$.*
2. *$X(t)$ is continuously differentiable for $t > 0$.*
3. *$X(t) \in Dom(A)$ for $t > 0$.*
4. *Satisfies 2.2.1*

Theorem 4. *Let A be a densely defined linear operator with a non-empty resolvent set $\rho(A)$. The initial value problem 2.2.1 with $F = 0$ has a unique solution $X(t) : [0,\infty) \to X$ for every $X_0 \in Dom(A)$ if and only if A is the infinitesimal generator of a strongly continuous semigroup.*

In general, it is hard to find a classical solution of 2.2.1 thus, we are satisfied with finding a weaker solution called a mild solution. The existence of such a solution, up to some hypothesis, is given by the following theorem.

Theorem 5. *Let $F : [0,\tau] \times X \to X$ be continuous and satisfy a Lipschitz condition*

$$\|F(t,\phi) - F(t,\phi')\| \leq L\|\phi - \phi'\|, \; t \in [0,\tau), \;\; \phi, \phi' \in X, \;\; L \geq 0.$$

Assume that $\{T(t)\}_{t\geq 0}$ is a strongly continuous semigroup on X satisfying $\|T(t)\| \leq Me^{wt}$ for $t \geq 0$. Then for a given $X_0 \in X$, there exists a unique function $X : [0,\tau) \to X$ which solves the following abstract integral equation,

$$X(t) = T(t)X_0 + \int_0^t T(t-s)F(s,X(s))ds. \tag{2.2.2}$$

Such an X is called the mild solution of 2.2.1.

2.3 Approximation for Semilinear differential Equations

We shall approximate the solution of 2.2.1 without any a priori information of X. We will seek approximations on spaces X_n of X, which are usually finite dimensional.

In this section, we assume that

A. $X_1, X_2, \dots$ are all Banach spaces over $\mathbb{K}$. We will denote all theirs norms as $\|\cdot\|$.

B. There exist $p, q \geq 0$ and bounded linear operators $P_n : X \to X_n$ and $E_n : X_n \to X$ for each $n \geq 1$ such that $\|P_n\| \leq p$ and $\|E_n\| \leq q$.

C. For all $x \in X$ and $n \geq 1$, $P_n E_n x = x$.

D. There exist $M \geq 0$, $w \in \mathbb{R}$ and bounded linear operators $A_n : X_n \to X_n$ such that $\|e^{A_n t}\| \leq M e^{wt}$ for all $t \geq 0$.

E. A is a densely defined linear operator in X, $\lambda_0 \in (w, \infty) \cap \rho(A)$ and

$$\lim_{n\to\infty} \|A_n P_n x - P_n A x\| = \lim_{n\to\infty} \|E_n P_n x - x\| = 0; \text{ for all } x \in X.$$

Lemma 1. *For all $x \in Dom(A)$*

$$\lim_{n\to\infty} \|E_n (A_n - \lambda_0)^{-1} P_n x - (A - \lambda_0)^{-1} x\| = 0.$$

Theorem 6. *Under the hypothesis of this section. A is the infinitesimal generator of a strongly continuous semigroup $\{T(t)\}_{t\geq 0}$. Moreover, $\|T(t)\| \leq pqMe^{wt}$ for $t \geq 0$ and*

$$\lim_{n\to\infty} \sup_{t\geq 0} e^{-bt} \|R_n e^{A_n t} P_n x - T(t)x\| = 0$$

for all $x \in X$ and $b \in (w, \infty) \subseteq \rho(A)$.

Now we also assume a Lipschitz condition for the non-linearity for a abstract Couchy problem. More precisely,

F. Assume that $F : [0, \tau] \times X \to X$ is continuous, $\tau \in (0, \infty)$, and there exists $L \geq 0$ such that

$$\|F(t, x) - F(t, x')\| \leq L\|x - x'\|; \text{ for all } x \in X, \ t \in [0, \tau].$$

Given $X_0 \in X$, let $X : [0, \tau] \to X$ be the mild solution of 2.2.1, and let X_n the solution of

$$\begin{cases} \frac{X_n}{dt} = A_n X_n + P_n F(t, E_N X_n), & t > 0, \\ X_n(0) = P_n X_0 \end{cases} \tag{2.3.1}$$

Theorem 7. *Under the hypothesis and notation we have introduced,*

$$\lim_{n\to\infty} \sup_{0\leq t\leq \tau} \|E_n X_n(t) - X(t)\| = 0. \tag{2.3.2}$$

Chapter 3

p-adic Cellular Neural Networks

We introduce the p-adic cellular neural networks which are mathematical generalizations of the classical cellular neural networks (CNNs) introduced by Chua and Yang. The new networks have infinitely many cells which are organized hierarchically in rooted trees, and also they have infinitely many hidden layers. Intuitively, the p-adic CNNs occur as limits of large hierarchical discrete CNNs. More precisely, the new networks can be very well approximated by hierarchical discrete CNNs. Mathematically speaking, each of the new networks is modeled by one integro-differential equation depending on several p-adic spatial variables and the time. We study the Cauchy problem associated to these integro-differential equations and also provide numerical methods for solving them.

3.1 p-Adic CNNs: basic definitions

We say that a function $f:\mathbb{R}\rightarrow\mathbb{R}$ is called a Lipschitz function if there exists a real constant $L(f)>0$ such that, for all $x,y\in\mathbb{R}$, $|f(x)-f(y)|\leq L(f)|x-y|$. A relevant example is

$$f(x)=\frac{1}{2}\left(|x+1|-|x-1|\right).$$

3.1.1 p-Adic discrete CNNs

By considering G_M^N as a subset of $\mathbb{Q}_p^N$, $\left(G_M^N,\|\cdot\|_p\right)$ becomes a finite ultrametric space.

Definition 2. *An element $\boldsymbol{i}$ of G_M^N is called a cell. A p-adic discrete CNN is a dynamical system $CNN_d(\mathbb{A},\mathbb{B},U,Z)$ on G_M^N. The state $X_{\boldsymbol{i}}(t)\in\mathbb{R}$ of cell $\boldsymbol{i}$ at time t is described by the following differential equations:*

(i) state equation:

$$\frac{dX(\boldsymbol{i},t)}{dt}=-X(\boldsymbol{i},t)+\sum_{\boldsymbol{j}\in G_M^N}\mathbb{A}(\boldsymbol{i},\boldsymbol{j})Y(\boldsymbol{j},t)+\sum_{\boldsymbol{j}\in G_M^N}\mathbb{B}(\boldsymbol{i},\boldsymbol{j})U(\boldsymbol{j})+Z(\boldsymbol{i}),\ \boldsymbol{i}\in G_M^N,$$

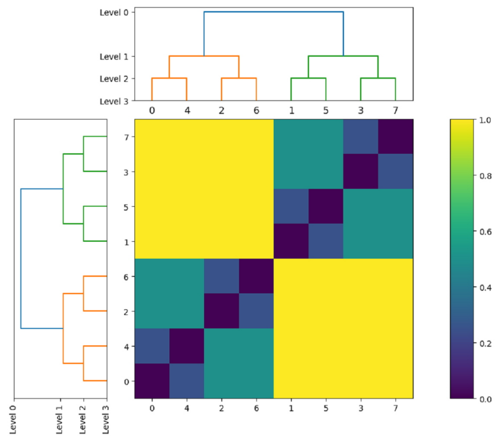

Figure 3.1: The heat map associated with the p-adic distance function on $\mathbb{Z}_2/2^3\mathbb{Z}_2$.

(ii) output equation:

$$Y(\boldsymbol{j},t) = f(X(\boldsymbol{j},t)),$$

where $Y(\boldsymbol{i},t) \in \mathbb{R}$ is the output of cell $\boldsymbol{i}$ at the time t, $f : \mathbb{R} \to \mathbb{R}$ is a bounded Lipschitz function satisfying $f(0) = 0$. The function $U(\boldsymbol{i}) \in \mathbb{R}$ is the input of the cell $\boldsymbol{i}$, $Z(\boldsymbol{i}) \in \mathbb{R}$ is the threshold of cell $\boldsymbol{i}$, and $\mathbb{A}, \mathbb{B} : G_M^N \times G_M^N \to \mathbb{R}$ are the feedback operator and feedforward operator, respectively.

Not all the cells of G_M^N are active. A cell $\boldsymbol{i}$ is connected with cell $\boldsymbol{j}$ if $\mathbb{A}(\boldsymbol{i},\boldsymbol{j}) \neq 0$ or $\mathbb{B}(\boldsymbol{i},\boldsymbol{j}) \neq 0$ for some $\boldsymbol{j} \in G_M^N$. Then, a p-adic discrete CNN is a dynamical system on

$$C_{N,M} := \left\{\boldsymbol{i} \in G_M^N; \mathbb{A}(\boldsymbol{i},\boldsymbol{j}) \neq 0 \text{ or } \mathbb{B}(\boldsymbol{i},\boldsymbol{j}) \neq 0 \text{ for some } \boldsymbol{j} \in G_M^N\right\}.$$

The topology of a p-adic discrete CNN depends on the functions $\mathbb{A}$, $\mathbb{B} : G_M^N \times G_M^N \to \mathbb{R}$. For general matrices $\mathbb{A}$, $\mathbb{B}$, it is difficult to give a graph-type description of the topology of the network. Our p-adic CNNs contain as a particular case the CNNs of Chua and Yang, see e.g. [18], [59]. In this article we focus on p-adic CNNs satisfying

$$\mathbb{A}(\boldsymbol{i},\boldsymbol{j}) = \mathbb{A}(\|\boldsymbol{i}-\boldsymbol{j}\|_p),\ \mathbb{B}(\boldsymbol{i},\boldsymbol{j}) = \mathbb{B}(\|\boldsymbol{i}-\boldsymbol{j}\|_p), \tag{3.1.1}$$

which are discrete CNNs having the space-invariant property. The fact that $\mathbb{A}$ and $\mathbb{B}$ are radial functions of $\|\cdot\|_p$ implies that the cells are organized in a tree like-structure with many layers.

3.1.2 p-Adic continuous CNNs

Definition 3. *Given $A(x,y)$, $B(x,y) \in L^1(\mathbb{Q}_p^N \times \mathbb{Q}_p^N)$, and U, $Z \in \mathcal{X}_\infty$, a p-adic continuous CNN, denoted as CNN(A,B,U,Z), is the dynamical system given by the following differential equations: (i) state equation:*

$$\frac{\partial X(x,t)}{\partial t} = -X(x,t) + \int\limits_{\mathbb{Q}_p^N} A(x,y)Y(y,t)d^Ny + \int\limits_{\mathbb{Q}_p^N} B(x,y)U(y)d^Ny + Z(x), \tag{3.1.2}$$

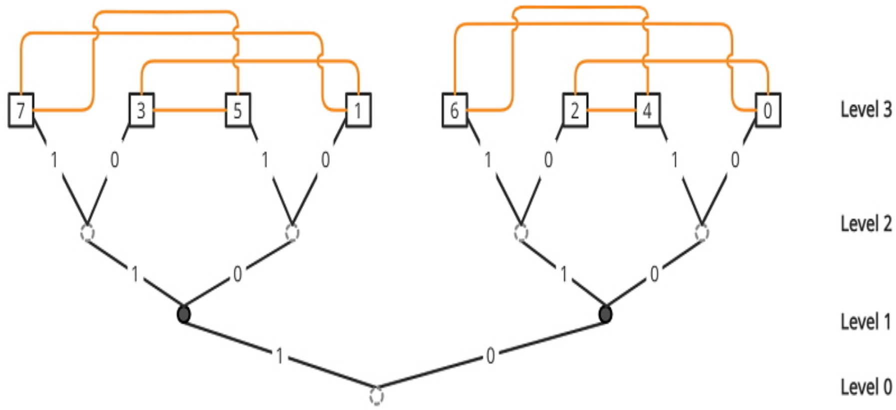

Figure 3.2: A 1-dimensional discrete 2-adic CNN with 8 cells: $C_{1,3} = \{0, 1, 2, 3, 4, 5, 7\} \subset \mathbb{Z}_2/2^3\mathbb{Z}_2 \subset 2^{-3}\mathbb{Z}_2/2^3\mathbb{Z}_2$. We set $\mathbb{B} = 0$ and $\mathbb{A}(\boldsymbol{i}, \boldsymbol{j}) = [a_{\boldsymbol{i},\boldsymbol{j}}]$, with $a_{\boldsymbol{i},\boldsymbol{j}} \neq 0$ if $|\boldsymbol{i} - \boldsymbol{j}|_2 = 1/2$ and $\boldsymbol{i}$, $\boldsymbol{j} \in C_{1,3}$; $a_{\boldsymbol{i},\boldsymbol{j}} = 0$ otherwise.

where $x \in \mathbb{Q}_p^N$, $t \geq 0$, and (ii) output equation: $Y(x,t) = f(X(x,t))$, $f : \mathbb{R} \to \mathbb{R}$ is a bounded Lipschitz function satisfying $f(0) = 0$. We say that $X(x,t) \in \mathbb{R}$ is the state of cell x at the time t, $Y(x,t) \in \mathbb{R}$ is the output of cell x at the time t. Function $A(x,y)$ is the kernel of the feedback operator, while function $B(x,y)$ is the kernel of the feedforward operator. Function U is the input of the CNN, while function Z is the threshold of the CNN.

We focus mainly in continuous CNNs having the space invariant property, i.e. $A(x,y) = A(\|x-y\|_p)$ and $B(x,y) = B(\|x-y\|_p)$ for some $A, B \in L^1$, however our results are valid for general p-adic continuous CNNs. Along this chapter the function $f(x) = \frac{1}{2}(|x+1| - |x-1|)$ will be fixed, for this reason it does not appear in the list of parameters of the CNNs.

3.1.3 Discretization of p-adic continuous CNNs

A central result of the present work is the fact that p-adic continuous CNNs are 'continuous versions' of p-adic discrete CNNs. More precisely, p-adic discrete CNNs are very good approximations of p-adic continuous CNNs for sufficiently large M. We discuss here the discretization process in an intutive way (a formal theorem will be provided later on, see Theorem 11).

Intuitively, a discretization of a p-adic continuous CNN(A, B, U, Z) is obtained assuming

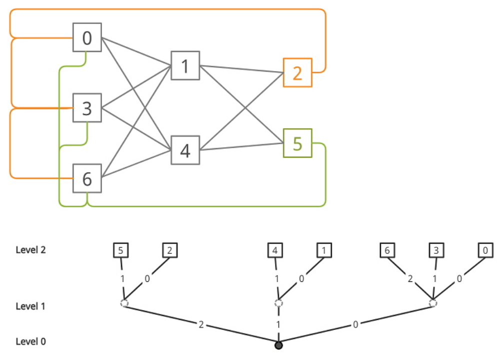

Figure 3.3: A 1-dimensional 3-adic CNN with 7 cells, $C_{1,2} = \{0,1,2,3,4,5,6\} \subset \mathbb{Z}_3/3^2\mathbb{Z}_3 \subset 3^{-2}\mathbb{Z}_3/3^2\mathbb{Z}_3$. We set $\mathbb{B} = 0$ and $\mathbb{A}(\boldsymbol{i},\boldsymbol{j}) = [a_{\boldsymbol{i},\boldsymbol{j}}]$, with $a_{\boldsymbol{i},\boldsymbol{j}} \neq 0$ if $|\boldsymbol{i}-\boldsymbol{j}|_3 = 1$ and $\boldsymbol{i},\boldsymbol{j} \in C_{1,2}$; $a_{\boldsymbol{i},\boldsymbol{j}} = 0$ otherwise.

that $X(\cdot,t)$, A, $Y(\cdot,t)$, B, U and Z belong to $\mathcal{D}^M$ (see Section 1.5), i.e.

$$X(x,t) = \sum_{\boldsymbol{i}\in G_M^N} X(\boldsymbol{i},t)\Omega\left(p^M \|x-\boldsymbol{i}\|_p\right), \quad Y(x,t) = \sum_{\boldsymbol{i}\in G_M^N} Y(\boldsymbol{i},t)\Omega\left(p^M \|x-\boldsymbol{i}\|_p\right),$$
$$U(x) = \sum_{\boldsymbol{i}\in G_M^N} U(\boldsymbol{i})\Omega\left(p^M \|x-\boldsymbol{i}\|_p\right), \quad Z(x) = \sum_{\boldsymbol{i}\in G_M^N} Z(\boldsymbol{i})\Omega\left(p^M \|x-\boldsymbol{i}\|_p\right),$$
$$A(x,y) = \sum_{\boldsymbol{i}\in G_M^N}\sum_{\boldsymbol{j}\in G_M^N} A(\boldsymbol{i},\boldsymbol{j})\Omega\left(p^M \|x-\boldsymbol{i}\|_p\right)\Omega\left(p^M \|y-\boldsymbol{j}\|_p\right),$$
$$B(x,y) = \sum_{\boldsymbol{i}\in G_M^N}\sum_{\boldsymbol{j}\in G_M^N} B(\boldsymbol{i},\boldsymbol{j})\Omega\left(p^M \|x-\boldsymbol{i}\|_p\right)\Omega\left(p^M \|y-\boldsymbol{j}\|_p\right).$$

Notice that if $f:\mathbb{R}\to\mathbb{R}$, then

$$f\left(X(x,t)\right) = \sum_{\boldsymbol{i}\in G_M^N} f(X(\boldsymbol{i},t))\Omega\left(p^M \|x-\boldsymbol{i}\|_p\right) = Y(x,t).$$

Now,

$$\frac{\partial}{\partial t}X(x,t) = \sum_{\boldsymbol{i}\in G_M^N} \frac{\partial}{\partial t}X(\boldsymbol{i},t)\Omega\left(p^M \|x-\boldsymbol{i}\|_p\right),$$

and

$$\int_{\mathbb{Q}_p^N} A(x,y) f\left(X(y,t)\right) d^N y$$

$$= \sum_{\boldsymbol{i}\in G_M^N} \left\{ \sum_{\boldsymbol{j}\in G_M^N} A(\boldsymbol{i},\boldsymbol{j}) f(X(\boldsymbol{j},t)) \int_{\mathbb{Q}_p^N} \Omega\left(p^M \left\|y-\boldsymbol{j}\right\|_p\right) d^N y \right\} \Omega\left(p^M \left\|x-\boldsymbol{i}\right\|_p\right)$$

$$= p^{-MN} \sum_{\boldsymbol{i}\in G_M^N} \left\{ \sum_{\boldsymbol{j}\in G_M^N} A(\boldsymbol{i},\boldsymbol{j}) Y(\boldsymbol{j},t)) \right\} \Omega\left(p^M \left\|x-\boldsymbol{i}\right\|_p\right).$$

Similarly,

$$\int_{\mathbb{Q}_p^N} B(x,y)U(y) d^N y = p^{-MN} \sum_{\boldsymbol{i}\in G_M^N} \left\{ \sum_{\boldsymbol{j}\in G_M^N} B(\boldsymbol{i},\boldsymbol{j}) U(\boldsymbol{j})) \right\} \Omega\left(p^M \left\|x-\boldsymbol{i}\right\|_p\right).$$

Therefore,

$$\frac{\partial}{\partial t} X(\boldsymbol{i},t) = -X(\boldsymbol{i},t) + \sum_{\boldsymbol{j}\in G_M^N} p^{-MN} A(\boldsymbol{i},\boldsymbol{j}) Y(\boldsymbol{j},t)$$
$$+ \sum_{\boldsymbol{j}\in G_M^N} p^{-MN} B(\boldsymbol{i},\boldsymbol{j}) U(\boldsymbol{j}) + Z(\boldsymbol{i}), \text{ for } \boldsymbol{i}\in G_M^N,$$

and $Y(\boldsymbol{i},t) = f(X(\boldsymbol{i},t))$, for $\boldsymbol{i}\in G_M^N$. This is exactly a p-adic discrete CNN with $\mathbb{A}(\boldsymbol{i},\boldsymbol{j}) = p^{-MN} A(\boldsymbol{i},\boldsymbol{j})$, $\mathbb{B}(\boldsymbol{i},\boldsymbol{j}) = p^{-MN} B(\boldsymbol{i},\boldsymbol{j})$.

Intuitively a p-adic continuous CNN has infinitely many layer. Each layer corresponds to some M, and the layers are organized in a hierarchical structure. For practical purposes, a p-adic continuous CNN is realized as a p-adic discrete CNN for M sufficiently large.

3.2 Stability of p-adic continuous CNN

Lemma 2. *Let f be a Lipschitz function on $\mathbb{R}$ with $f(0)=0$ and let E be a radial function in $L^1(\mathbb{Q}_p^N)$. Then, the mappings*

$$F_0 : g \rightarrow \int_{\mathbb{Q}_p^N} E(\|x-y\|_p) f(g(y)) d^N y$$
$$F_1 : g \rightarrow \int_{\mathbb{Q}_p^N} E(\|x-y\|_p) g(y) d^N y$$

are well defined bounded operators from $\mathcal{X}_\infty$ into itself.

Proof. We first notice that for all $g \in \mathcal{X}_\infty$, $F_0(g)(x)$ exists for all $x \in \mathbb{Q}_p^N$, since

$$|E(\|y\|_p)|\ |f(g(x-y))| \leq L(f)\|g\|_\infty\ |E(\|y\|_p)|\,, \tag{3.2.1}$$

where $E(\|y\|_p) \in L^1(\mathbb{Q}_p^N)$. To show the continuity of $F_0(g)(x)$, we take a sequence $\{x_m\}_{m\in\mathbb{N}} \subset \mathbb{Q}_p^N$ such that $x_m \to x$. By using (3.2.1) and the dominated convergence theorem,

$\lim_{m\to\infty} F_0(g)(x_m) = F_0(g)(x)$. Finally, we show that $F_0(g) \in \mathcal{X}_\infty$. By contradiction, assume that $F_0(g) \notin \mathcal{X}_\infty$. Then, there is a sequence $\{x_m\}_{m\in\mathbb{N}} \subset \mathbb{Q}_p^N$ such that $\lim_{m\to\infty} \|x_m\|_p = \infty$ and $\epsilon > 0$ such that $F_0(g)(x_m) > \epsilon$ for all $m \in \mathbb{N}$. By using (3.2.1) and the dominated convergence theorem, we have

$$\begin{aligned}\epsilon \leq \lim_{m\to\infty} |F_0(g)(x_m)| &= \lim_{m\to\infty} \left| \int_{\mathbb{Q}_p^N} E(\|y\|_p) f(g(x_m - y)) d^N y \right| \\ &= \left| \int_{\mathbb{Q}_p^N} E(\|y\|_p) \left\{ \lim_{m\to\infty} f(g(x_m - y)) \right\} d^N y \right| = 0\end{aligned}$$

which contradicts the fact $\epsilon > 0$. The same argument allow us to show that $F_1(g) \in \mathcal{X}_\infty$ for any $g \in \mathcal{X}_\infty$. □

Lemma 3. *Assume $A, B \in L^1(\mathbb{Q}_p^N)$ are radial functions and that U, $Z \in \mathcal{X}_\infty$. For $g \in \mathcal{X}_\infty$, set*

$$\boldsymbol{H}(g)(x) := \int_{\mathbb{Q}_p^N} A(\|x-y\|_p) f\left(g(y)\right) d^N y + \int_{\mathbb{Q}_p^N} B(\|x-y\|_p) U(y) d^N y + Z(x).$$

Then $\boldsymbol{H} : \mathcal{X}_\infty \to \mathcal{X}_\infty$ is a well-defined operator satisfying

$$\|\boldsymbol{H}(g) - \boldsymbol{H}(g')\|_\infty \leq L(f)\|A\|_1 \|g - g'\|_\infty, \text{ for } g,\ g' \in \mathcal{X}_\infty,$$

where $L(f)$ is the Lipschitz constant of f.

Proof. By Lemma 2, $\boldsymbol{H} : \mathcal{X}_\infty \to \mathcal{X}_\infty$ is a well-defined operator. Take g, $g' \in \mathcal{X}_\infty$, then

$$\begin{aligned}|\boldsymbol{H}(g)(x) - \boldsymbol{H}(g')(x)| &= \left| \int_{\mathbb{Q}_p^N} A(\|x-y\|_p) \left(f\left(g(y)\right) - f\left(g'(y)\right) \right) d^N y \right| \\ &\leq \int_{\mathbb{Q}_p^N} |A(\|x-y\|_p)| |f\left(g(y)\right) - f\left(g'(y)\right)| d^N y \leq L(f)\|g-g'\|_\infty \int_{\mathbb{Q}_p^N} |A(\|x-y\|_p)| d^N y \\ &= L(f)\|A\|_1 \|g - g'\|_\infty.\end{aligned}$$

□

Remark 2. *(i) Lemma 2 remains valid if we replace the condition E is radial and integrable by the condition $E(x,y)$ is a continuous function with compact support.*

(ii) Under the hypothesis of part (i), Lemma 3 is valid for operators of the form

$$\boldsymbol{L}g(x) = \int\limits_{\mathbb{Q}_p^N} A(x,y) f\left(g(y)\right) d^N y + \int\limits_{\mathbb{Q}_p^N} B(x,y) U(y) d^N y + Z(x),$$

for $g \in \mathcal{X}_\infty$.

Proposition 1. *Assume that A, $B \in L^1(\mathbb{Z}_p)$, and that U, $Z \in \mathcal{X}_\infty$. Let τ be a fixed positive real number. Then for each $X_0 \in \mathcal{X}_\infty$ there exists a unique $X \in C([0,\tau], \mathcal{X}_\infty)$ which satisfies*

$$X(x,t) = e^{-t} X_0\left(x\right) + \int_0^t e^{-(t-s)} \boldsymbol{H}(X(x,s)) ds \tag{3.2.2}$$

where

$$\boldsymbol{H} X(x,t) = \int\limits_{\mathbb{Q}_p^N} A(\|x-y\|_p) f(X(y,t)) d^N y + \int\limits_{\mathbb{Q}_p^N} B(\|x-y\|_p) U(y) d^N y + Z(x). \tag{3.2.3}$$

The function $X(x,t)$ is differentiable in t for all x, and it is a solution of equation (3.1.2) with initial datum X_0.

Proof. The result follows from Lemma 3, by using standard techniques in PDEs, see e.g. [46, Theorem 5.1.2]. To make the treatment comprehensive, we provide some details here. First, define

$$\boldsymbol{T}(Y) = X_0 e^{-t} + \int_0^t e^{-(t-s)} \boldsymbol{H}(Y(x,s)) ds,$$

and $\mathcal{Y} = C([0,\tau], \mathcal{X}_\infty)$ which is a Banach space with the norm $\|\cdot\|_\infty$. By Lemma 3, $\boldsymbol{T} : \mathcal{Y} \to \mathcal{Y}$. If Y, $Y_1 \in \mathcal{Y}$, then

$$\|\boldsymbol{T}(Y)(t) - \boldsymbol{T}(Y_1)(t)\|_\infty = \left\| \int_0^t e^{-(t-s)} \left\{ \boldsymbol{H}(Y)(s) - \boldsymbol{H}(Y_1)(s) \right\} ds \right\|_\infty$$

$$\leq \int_0^t e^{-(t-s)} \|\boldsymbol{H}(Y)(s) - \boldsymbol{H}(Y_1)(s)\|_\infty \, ds \leq L(f) \|A\|_1 \int_0^t \|Y - Y_1\|_\infty ds.$$

Now, for $M \geq 1$, it verifies that

$$\|\boldsymbol{T}^M(Y)(t) - \boldsymbol{T}^M(Y_1)(t)\|_\infty \leq \frac{\tau^M L(f)^M \|A\|_1^M}{M!} \|Y - Y_1\|_\infty,$$

By the Stirling approximation formula for $M!$, it holds that $0 < \frac{\tau^M L(f)^M \|A\|_1^M}{M!} < 1$ for some M sufficiently large, and by the contraction mapping theorem applied to $\boldsymbol{T}^M$, there is a unique $X \in \mathcal{Y}$ which $\boldsymbol{T}(X) = X$, see e.g. [46, Theorem 1.1.3]. Moreover, since the right-hand side of (3.2.2) is differentiable in t, X is a solution of (3.1.2) with initial condition. □

Remark 3. *The contraction mapping theorem provides an iterative formula for approximating $X(x,t)$. Set $X_1(x,t) = X_0\left(x\right)$ and*

$$X_{L+1}(x,t) = e^{-t} X_0\left(x\right) + \int_0^t e^{-(t-s)} H(X_L(x,s)) ds, \text{ for } L = 1, 2, \ldots,$$

then $\lim_{L\to\infty} \|X_L\left(\cdot,t\right) - X\left(\cdot,t\right)\|_\infty = 0$ for each $t \leq \tau$, see e.g. [46, Theorem 5.2.2].

Theorem 8. *Assume A, $B \in L^1(p^{-M_0}\mathbb{Z}_p^N)$ are radial functions, for some $M_0 \in \mathbb{N}$, and that U, Z, $X_0 \in \mathcal{X}_{M_0}$. Then there is a unique $X \in C([0,\tau], \mathcal{X}_{M_0}) \cap C^1([0,\tau], \mathcal{X}_{M_0})$ satisfying (3.2.2), which is a solution of equation (3.1.2) with initial datum X_0.*

Remark 4. *This theorem remains valid if $A(x,y)$, $B(x,y)$ are continuous functions with compact support, see Remark 2.*

Proof. Since $\mathcal{X}_{M_0}$ is a subspace of $\mathcal{X}_\infty$, by applying Proposition 1, there exists a unique $X \in C([0,\tau], \mathcal{X}_\infty) \cap C^1([0,\tau], \mathcal{X}_\infty)$ that satisfies all the announced properties. By Remark 3, $\lim_{L\to\infty} \|X_L(\cdot,t) - X(\cdot,t)\|_\infty = 0$, where

$$X_{L+1}(x,t) = e^{-t}X_0(x) + \int_0^t e^{-(t-s)}H(X_L(x,s))ds, \text{ for } L = 1, 2, \ldots.$$

By induction on L, if $X_L(\cdot,s) \in \mathcal{X}_{M_0}$, i.e. if

$$X_L(x,s) = \sum_{\boldsymbol{i}\in G_{M_0}^N} X_L(\boldsymbol{i},s)\Omega\left(p^{M_0}\|x-\boldsymbol{i}\|_p\right),$$

$$f(X_L(x,s)) = \sum_{\boldsymbol{i}\in G_{M_0}^N} Y_L(\boldsymbol{i},s)\Omega\left(p^{M_0}\|x-\boldsymbol{i}\|_p\right)$$

by using that

$$\int_0^t e^{-(t-s)}H(X_L(x,s))ds$$

$$= \sum_{\boldsymbol{i}\in G_{M_0}^N}\left(\int_0^t e^{-(t-s)}Y_L(\boldsymbol{i},s)ds\right)\left(\int_{\mathbb{Q}_p^N} A(\|x-y\|_p)\Omega\left(p^{M_0}\|y-\boldsymbol{i}\|_p\right)d^Ny\right)$$

$$+ \sum_{\boldsymbol{i}\in G_{M_0}^N} U(\boldsymbol{i})(1-e^{-t})\int_{\mathbb{Q}_p^N} B(\|x-y\|_p)\Omega\left(p^{M_0}\|y-\boldsymbol{i}\|_p\right)d^Ny$$

$$+ \sum_{\boldsymbol{i}\in G_{M_0}^N}(1-e^{-t})Z(\boldsymbol{i})\Omega\left(p^{M_0}\|x-\boldsymbol{i}\|_p\right),$$

and that for any $E \in L^1(p^{-M_0}\mathbb{Z}_p^N)$ are radial function, with the convention that the support of E is the ball $p^{-M_0}\mathbb{Z}_p^N$,

$$\int_{\mathbb{Q}_p^N} E(\|x-y\|_p)\Omega\left(p^{M_0}\|y-\boldsymbol{i}\|_p\right)d^Ny = \int_{\boldsymbol{i}+p^{M_0}\mathbb{Z}_p^N} E(\|x-y\|_p)d^Ny$$

$$= \begin{cases} 0 & \text{if } x \notin p^{-M_0}\mathbb{Z}_p^N \\ \int_{p^{M_0}\mathbb{Z}_p^N} E(\|z\|_p)d^Nz & \text{if } x \in \boldsymbol{i}+p^{M_0}\mathbb{Z}_p^N \\ p^{-M_0N}E(\|\boldsymbol{i}-\boldsymbol{j}\|_p) & \text{if } x \in \boldsymbol{j}+p^{M_0}\mathbb{Z}_p^N,\ \boldsymbol{i}\neq\boldsymbol{j}, \end{cases}$$

we conclude that

$$X_{L+1}(x,t) = e^{-t}X_0\left(x\right) + \tag{3.2.4}$$
$$\sum_{\boldsymbol{j}\in G_{M_0}^N}\left\{\sum_{\substack{\boldsymbol{i}\in G_{M_0}^N\\ \boldsymbol{i}\neq\boldsymbol{j}}} a\left(\boldsymbol{i},t\right)p^{-M_0N}A(\|\boldsymbol{i}-\boldsymbol{j}\|_p)\right\}\Omega\left(p^{M_0}\left\|y-\boldsymbol{j}\right\|_p\right)+$$
$$\sum_{\boldsymbol{j}\in G_{M_0}^N} a\left(\boldsymbol{j},t\right)\left(\int_{p^{M_0}\mathbb{Z}_p^N} A(\|z\|_p)d^Nz\right)\Omega\left(p^{M_0}\left\|y-\boldsymbol{j}\right\|_p\right)+$$
$$\sum_{\boldsymbol{i}\in G_{M_0}^N}\left\{\sum_{\substack{\boldsymbol{i}\in G_{M_0}^N\\ \boldsymbol{i}\neq\boldsymbol{j}}} U(\boldsymbol{i})(1-e^{-t})B(\|\boldsymbol{i}-\boldsymbol{j}\|_p)\right\}\Omega\left(p^{M_0}\left\|y-\boldsymbol{j}\right\|_p\right)+$$
$$\sum_{\boldsymbol{i}\in G_{M_0}^N} U\left(\boldsymbol{j}\right)\left(1-e^{-t}\right)\left(\int_{p^{M_0}\mathbb{Z}_p^N} B(\|z\|_p)d^Nz\right)\Omega\left(p^{M_0}\left\|y-\boldsymbol{j}\right\|_p\right)+(1-e^{-t})Z(\boldsymbol{i}),$$

i.e. $X_{L+1}(\cdot,s)\in\mathcal{X}_M$. Consequently, $\{X_L(\cdot,t)\}_{L\in\mathbb{N}\smallsetminus\{0\}}$ is a sequence in $\mathcal{X}_M$. Since $\mathcal{X}_M$ is closed in $\mathcal{X}_\infty$, $X\left(\cdot,t\right)\in\mathcal{X}_M$ for any $t\leq\tau$. □

Remark 5. *By using that*

$$p^{MN}\int_{p^M\mathbb{Z}_p^N} A(\|z\|_p)d^Nz\rightarrow A(0),\ p^{MN}\int_{p^M\mathbb{Z}_p^N} B(\|z\|_p)d^Nz\rightarrow B(0)$$

as $M\rightarrow\infty$, see e.g. [62, Theorem 1.14], (3.2.4) provides an explicit approximation of the continuous CNN described in Theorem 8.

Lemma 4. *Let τ be a fixed positive real number, let $X(x,t)$ be the solution given in Proposition 1, with $X(x,0)=X_0$. Then, for all $x,y\in\mathbb{Q}_p^N$ and $t\in(0,\tau)$,*

$$|X(x,t)-X(y,t)|\leq|X_0(x)-X_0(y)|e^{\|A\|_1L(f)t}.$$

Moreover, if X_0 is a locally-constant function, i.e. $X_0(x)=X_0(y)$ for $y\in B_l(x)$, with $l=l(x)\in\mathbb{Z}$, for any $x\in\mathbb{Q}_p^N$, then $X(\cdot,t)$ is a locally-constant function and $X(x,t)=X(y,t)$ for $y\in B_l(x)$ for any $x\in\mathbb{Q}_p^N$.

Proof. Fix $x,y\in\mathbb{Q}_p^N$, the by Proposition 1 and Lemma 3, for all $t\in(0,\tau]$

$$\begin{aligned}|X(x,t)-X(y,t)|&\leq e^{-t}|X_0(x)-X_0(y)|+\int_0^t e^{-(t-s)}|\boldsymbol{H}(X(x,s))-\boldsymbol{H}(X(y,s))|ds\\&\leq|X_0(x)-X_0(y)|+L(f)\|A\|_1\int_0^t|X(x,s)-X(y,s)|ds.\end{aligned}$$

Thus, by Gronwall's theorem, see [46, Theorem 5.1.1],

$$|X(x,t) - X(y,t)| \leq |X_0(x) - X_0(y)| e^{L(f)\|A\|_1 t}$$

for all $t \in (0, \tau)$. □

Definition 4. *A function $X_{stat}(x) := X_{stat}(x; A, B, U, Z) \in \mathcal{X}_\infty$ is called a stationary state of a p-adic continuous CNN(A, B, U, Z), if*

$$X_{stat}(x) = \int_{\mathbb{Q}_p^N} A(\|x-y\|_p) Y(y) d^N y + \int_{\mathbb{Q}_p^N} B(\|x-y\|_p) U(y) d^N y + Z(x),$$

where $Y(x) = f(X_{stat}(x))$ and $x \in \mathbb{Q}_p^N$.

Remark 6. *If a p-adic continuous CNN(A, B, U, Z) satisfies that $\|A\|_1 L(f) < 1$, then the CNN(A, B, U, Z) has a unique stationary state. This follows by the fact that, under this condition, $\boldsymbol{H}(X)$ becomes a contraction map in $\mathcal{X}_\infty$, cf. Lemmas 2, 3.*

Theorem 9. *All the states $X(x,t)$ of a p-adic continuous CNN(A, B, U, Z) are bounded for all time $t \geq 0$. More precisely, if*

$$X_{\max} := \|X_0\|_\infty + \|f\|_\infty \|A\|_1 + \|U\|_\infty \|B\|_1 + \|Z\|_\infty,$$

then

$$|X(x,t)| \leq X_{\max} \text{ for all } t \geq 0 \text{ and for all } x \in \mathbb{Q}_p^N. \tag{3.2.5}$$

In addition

$$X_-(x) := \liminf_{t\to\infty} X(x,t) \leq X(x,t) \leq \limsup_{t\to\infty} X(x,t) =: X_+(x),$$

for $x \in \mathbb{Q}_p^N$. If $X_-(x) = X_+(x) := X^*(x)$,then $X^*(x)$ is a stationary solution of the CNN(A, B, U, Z) and

$$X^*(x) \geq -\|f\|_\infty \|A\|_1 - \|U\|_\infty \|B\|_1 + Z(x). \tag{3.2.6}$$

Remark 7. *Condition (3.2.5) implies that $X(x,t)$ does not blow-up at finite time. The existence of a stationary state $X^*(x)$ means that the state of each cell of a p-adic continuous CNN most settle at stable equilibrium point after the transient has decayed to zero.*

Proof. By Proposition 1, see (3.2.2)-(3.2.3), by using that $|Y(y,t)| = |f(X(x,t))| \leq \|f\|_\infty$, we have

$$\begin{aligned}|\boldsymbol{H}(X(x,t))| &\leq \int_{\mathbb{Q}_p^N} |A(\|x-y\|_p)||Y(y,t)| d^N y + \int_{\mathbb{Q}_p^N} |B(\|x-y\|_p)||U(y)| d^N y + |Z(x)| \\ &\leq \|f\|_\infty \|A\|_1 + \|B\|_1 \|U\|_\infty + \|Z\|_\infty.\end{aligned}$$

Therefore

$$\begin{aligned}\|X(x,t)\|_\infty &\le e^{-t}\|X_0\|_\infty + \int_0^t e^{-(t-s)}\|\boldsymbol{H}(X(x,s))\|_\infty ds\\ &\le \|X_0\|_\infty + \|f\|_\infty\|A\|_1 + \|B\|_1\|U\|_\infty + \|Z\|_\infty.\end{aligned}$$

This bound is valid for any $t \in [0,\tau]$, but τ is arbitrary, so the bound is valid for any $t \ge 0$.

The bound (3.2.5) implies existence of the functions:

$$\begin{aligned}X_+(x) &= \limsup_{t\to\infty} X(x,t) = \lim_{M\to\infty} \sup\{X(x,t); t > M\},\\ X_-(x) &= \liminf_{t\to\infty} X(x,t) = \lim_{M\to\infty} \inf\{X(x,t); t > M\}.\end{aligned}$$

Now assume that $X_+(x) = X_-(x) = X^*(x)$, then $\lim_{t\to\infty} X(x,t) = X^*(x)$ exists. By using that

$$\begin{aligned}\int_0^t e^{-(t-s)}\boldsymbol{H}(X(x,s))ds &= \int_0^t e^{-u}\boldsymbol{H}(X(x,t-u))du\\ &= \int_0^\infty 1_{[0,t]}(u)\, e^{-u}\boldsymbol{H}(X(x,t-u))du,\end{aligned}$$

and

$$\left|1_{[0,t]}(u)\, e^{-u}\boldsymbol{H}(X(x,t-u))\right| \le (\|f\|_\infty\|A\|_1 + \|B\|_1\|U\|_\infty + \|Z\|_\infty)\, e^{-u} \in L^1(\mathbb{R}),$$

and the dominated convergence theorem and Lemma 3, it follows from (3.2.2) that

$$\begin{aligned}\lim_{t\to\infty} X(x,t) &= \int_0^\infty e^{-u}\lim_{t\to\infty}\left\{1_{[0,t]}(u)\,\boldsymbol{H}(X(x,t-u))\right\}du = \int_0^\infty e^{-u}\boldsymbol{H}(X^*(x))du\\ &= \int_{\mathbb{Q}_p^N} A(\|x-y\|_p)f(X^*(x))d^Ny + \int_{\mathbb{Q}_p^N} B(\|x-y\|_p)U(y)d^Ny + Z(x).\end{aligned}$$

which shows that $X^*(x)$ is a stationary solution of the CNN(A,B,U,Z). □

3.3 Stability of p-adic discrete CNN and Approximation of Continuous CNNs

3.3.1 The operators $\boldsymbol{P}_M$, $\boldsymbol{E}_M$

We now define for $M \ge 1$, $\boldsymbol{P}_M : \mathcal{X}_\infty \to \mathcal{X}_M$ as

$$\boldsymbol{P}_M\varphi(x) = \sum_{\boldsymbol{i}\in G_M^N} \varphi(\boldsymbol{i})\,\Omega\left(p^M\|x-\boldsymbol{i}\|_p\right).$$

Therefore $\boldsymbol{P}_M$ is a linear bounded operator, indeed, $\|\boldsymbol{P}_M\| \le 1$.

We denote by $\boldsymbol{E}_M$, $M \ge 1$, the embedding $\mathcal{X}_M \to \mathcal{X}_\infty$. If $\mathcal{Z}$, $\mathcal{Y}$ are real Banach spaces, we denote by $\mathfrak{B}(\mathcal{Z},\mathcal{Y})$, the space of all linear bounded operators from $\mathcal{Z}$ into $\mathcal{Y}$. The following result is a consequence of the above observations.

Lemma 5. *[72, Lemma 2] With the above notation, the following assertions hold true:*

(i) $\mathcal{X}_\infty$, $\mathcal{X}_M$ *for* $M \geq 1$, *are real Banach spaces, all with the norm* $\|\cdot\|_\infty$;

(ii) $\boldsymbol{P}_M \in \mathfrak{B}(\mathcal{X}_\infty, \mathcal{X}_M)$ *and* $\|\boldsymbol{P}_M\varphi\|_\infty \leq \|\varphi\|_\infty$ *for any* $M \geq 1$, $\varphi \in \mathcal{X}_\infty$;

(iii) $\boldsymbol{E}_M \in \mathfrak{B}(\mathcal{X}_M, \mathcal{X}_\infty)$ *and* $\|\boldsymbol{E}_M\varphi\|_\infty = \|\varphi\|_\infty$ *for any* $M \geq 1$, $\varphi \in \mathcal{X}_M$;

(iv) $\boldsymbol{P}_M\boldsymbol{E}_M\varphi = \varphi$ *for* $M \geq 1$, $\varphi \in \mathcal{X}_M$;

(v) $\lim_{M\to\infty} \|\varphi - \boldsymbol{P}_M\varphi\|_\infty = 0$ *for any* $\varphi \in \mathcal{X}_\infty$;

(vi) $\lim_{M\to\infty} \|\boldsymbol{E}_M\boldsymbol{P}_M\phi - \phi\|_\infty = 0$ *for all* $\phi \in \mathcal{X}_\infty$.

Proposition 2. *Assume that* $A(\|x\|_p)$, $B(\|x-y\|_p)$, $U(x)$, $Z(x) \in \mathcal{X}_M$, $M \geq 1$. *Let* τ *be a fixed positive real number. Consider the initial value problem:*

$$\begin{cases} X \in C([0,\tau], \mathcal{X}_M) \cap C^1([0,\tau], \mathcal{X}_M) \\ \frac{\partial X(x,t)}{\partial t} = -X(x,t) + \int\limits_{\mathbb{Q}_p^N} A(\|x-y\|_p) f(X(x,t)) d^N y \\ + \int\limits_{\mathbb{Q}_p^N} B(\|x-y\|_p) U(y) d^N y + Z(x), \; x \in B_M^N, \; t \geq 0 \\ X(x,0) = X_0 \in \mathcal{X}_M. \end{cases} \tag{3.3.1}$$

There exists a unique $X \in C([0,\tau], \mathcal{X}_M)$ *which satisfies*

$$X(x,t) = e^{-t} X_0(x) + \int_0^t e^{-(t-s)} \boldsymbol{H}(X(x,s)) ds$$

where

$$\boldsymbol{H}(X)(x,t) = \int\limits_{\mathbb{Q}_p^N} A(\|x-y\|_p) f(X(x,t)) d^N y + \int\limits_{\mathbb{Q}_p^N} B(\|x-y\|_p) U(y) d^N y + Z(x).$$

The function $X(x,t)$ *is a solution of equation 3.3.1 with initial datum* X_0.

Proof. The result is established by using the argument given in the proof of Theorem 8. □

By the discussion presented in section 3.1.3, (3.3.1) describes a p-adic discrete CNN. Furthermore, Theorem 12 is also valid for discrete CNN in $\mathcal{X}_M$.

Remark 8. *By using the discretization procedure given in Section 3.1.3 and in the proof of Theorem 8, Proposition 2 implies that the initial value problem*

$$\begin{cases} X_M \in C([0,\tau], \mathcal{X}_M) \cap C^1([0,\tau], \mathcal{X}_M) \\ \frac{\partial X_M}{\partial t} = -X_M + \boldsymbol{P}_M \boldsymbol{H}(\boldsymbol{E}_M X_M) \\ X_M(0) = \boldsymbol{P}_M(X_0) \end{cases}$$

has a unique solution for an arbitrary $\tau > 0$.

Theorem 10. *All the states* $X(\boldsymbol{i}, t)$, $\boldsymbol{i} \in G_M^N$, *in a p-adic discrete CNN are bounded for all time* $t \geq 0$. *More precisely, if*

$$X_{\max} := \max_{\boldsymbol{i}\in G_M^N} |X_0(\boldsymbol{i})| + p^{-MN} \left(\max_{\boldsymbol{i}\in G_M^N} |f(\boldsymbol{i})| \right) \sum_{\boldsymbol{i}\in G_M^N} |A(\boldsymbol{i})| + p^{-MN} \left(\max_{\boldsymbol{i}\in G_M^N} |U(\boldsymbol{i})| \right) \sum_{\boldsymbol{i}\in G_M^N} |A(\boldsymbol{i})| + \max_{\boldsymbol{i}\in G_M^N} |Z(\boldsymbol{i})|,$$

then

$$|X(\boldsymbol{i}, t)| \leq X_{\max} \text{ for all } t \geq 0 \text{ and for all } \boldsymbol{i} \in G_M^N.$$

In addition

$$X_-(\boldsymbol{i}) := \lim \inf_{t\to\infty} X(\boldsymbol{i}, t) \leq X(\boldsymbol{i}, t) \leq \lim \sup_{t\to\infty} X(\boldsymbol{i}, t) =: X_+(\boldsymbol{i}),$$

for $\boldsymbol{i} \in G_M^N$. *If* $X_-(\boldsymbol{i}) = X_+(\boldsymbol{i}) := X^*(\boldsymbol{i})$, *then*

$$X^*(\boldsymbol{i}) = \sum_{\boldsymbol{j}\in G_M^N} p^{-MN} A(\|\boldsymbol{i} - \boldsymbol{j}\|_p) f(X^*(\boldsymbol{i})) + \sum_{\boldsymbol{j}\in G_M^N} p^{-MN} B(\|\boldsymbol{i} - \boldsymbol{j}\|_p) U(\boldsymbol{j}) + Z(\boldsymbol{i}), \text{ for } \boldsymbol{i} \in G_M^N,$$

and

$$X^*(\boldsymbol{i}) \geq -p^{-MN} \left(\max_{\boldsymbol{i}\in G_M^N} |f(\boldsymbol{i})| \right) \sum_{\boldsymbol{i}\in G_M^N} |A(\boldsymbol{i})| - p^{-MN} \left(\max_{\boldsymbol{i}\in G_M^N} |U(\boldsymbol{i})| \right) \sum_{\boldsymbol{i}\in G_M^N} |A(\boldsymbol{i})| + Z(\boldsymbol{i}) \text{ , for all } \boldsymbol{i} \in G_M^N.$$

Theorem 11. *Let* X *be the solution of a continuous p-adic CNN given by Theorem 1 with initial condition* X_0. *Let* X_M *be the solution of the Cauchy problem*

$$\begin{cases} \frac{dX_M}{dt} = -X_M + \boldsymbol{P}_M \boldsymbol{H}(\boldsymbol{E}_M X_M) \\ X_M(0) = \boldsymbol{P}_M(X_0), \end{cases} \tag{3.3.2}$$

cf. Proposition 2 and Remark 8. Then

$$\lim_{M\to\infty} \sup_{0\leq t\leq\tau} \|X_M(t) - X(t)\|_\infty = 0.$$

Proof. The result follows from Lemma 5, Propositions 1, 2, by using standard techniques of approximation for evolution equations, see e.g. [46, Theorem 5.4.7]. See also [72, Section 9.1 and Theorem 7] for an in-depth discussion of similar matters. □

3.4 Numerical Simulations of p-Adic Continuous CNNs

In this section we present some numerical simulations of the solutions of several p-adic continuous CNNs in dimension 1. We give two numerical schemes for the numerical approximation of the solutions. In the first scheme, we consider the case when all of the functions A, B, U, Z are radial functions. While the second one considers the case when one of these functions is a test function.

3.4.1 Numerical Scheme A

In section we present an approximation of the solution $X(x,t)$ of s p-adic continuous CNN(A,B,U,Z) when A, B, U, Z are radial functions.

Lemma 6. *Let $H(|\cdot|_p) \in L^1(\mathbb{Q}_p)$ and let $g \in \mathcal{X}_\infty$. We set $G_k = p^{-k}\mathbb{Z}_p/p^k\mathbb{Z}_p$, $k \in \mathbb{N}$. Then*

$$\int_{\mathbb{Q}_p} H(|x-y|)g(y)dy = \lim_{k\to\infty} \sum_{\boldsymbol{i}\in G_k;\ \boldsymbol{i}\neq x} g(\boldsymbol{i})p^{-k}H(|x-\boldsymbol{i}|_p) + g(x)(1-p^{-1})\sum_{l=k}^{\infty} H(p^{-l})p^{-l}.$$

Proof. By Lemma 5-(v), $\lim_{k\to\infty}\sum_{\boldsymbol{i}\in G_k} g(\boldsymbol{i})\Omega(p^k|x-\boldsymbol{i}|_p) = g(x)$, now by the dominated convergence theorem,

$$\begin{aligned}\int_{\mathbb{Q}_p} H(|x-y|_p)g(y)dy &= \lim_{k\to\infty}\sum_{\boldsymbol{i}\in G_k} g(\boldsymbol{i})\int_{\mathbb{Q}_p} H(|x-y|_p)\Omega(p^k|y-\boldsymbol{i}|_p)dy \\ &= \lim_{k\to\infty}\sum_{\boldsymbol{i}\in G_k} g(\boldsymbol{i}) \int_{x-\boldsymbol{i}+p^k\mathbb{Z}_p} H(|z|_p)dz.\end{aligned}$$

Now, if $|x-\boldsymbol{i}|_p > p^{-k}$, i.e. $x \neq \boldsymbol{i}$ in G_k, then

$$\int_{x-\boldsymbol{i}+p^k\mathbb{Z}_p} H(|z|_p)dz = p^{-k}H(|x-\boldsymbol{i}|_p).$$

If $|x-\boldsymbol{i}|_p \leq p^{-k}$, i.e. $x = \boldsymbol{i}$ in G_k, then

$$\int_{x-\boldsymbol{i}+p^k\mathbb{Z}_p} H(|z|_p)dz = \sum_{l=k}^{\infty} H(p^{-l})(1-p^{-1})p^{-l}.$$

□

We now assume that A, B are radial integrable functions, and that U, Z, $X_0 \in \mathcal{X}_\infty$. Based on the continuity of operators $\boldsymbol{A}, \boldsymbol{B} : \mathcal{X}_\infty \to \mathcal{X}_\infty$ and the formula given in Lemma 6, we can approximate the solution $X(x,t)$ of a p-adic continuous CNN(A,B,U,Z) by p^{2k} ODEs,

$k \geq 1$, of the form

$$\frac{d}{dx}X(\boldsymbol{i},t) = -X(\boldsymbol{i},t) + \sum_{\boldsymbol{j}\in G_k;\ \boldsymbol{j}\neq\boldsymbol{i}} f(X(\boldsymbol{j},t))p^{-k}A(|\boldsymbol{i}-\boldsymbol{j}|_p)+$$

$$f(X(\boldsymbol{i},t))(1-p^{-1})\sum_{l=k}^{k_{\max}} A(p^{-l})p^{-l} + \sum_{\boldsymbol{j}\in G_k;\ \boldsymbol{j}\neq\boldsymbol{i}} U(\boldsymbol{i})p^{-k}B(|\boldsymbol{i}-\boldsymbol{j}|_p)$$

$$+U(\boldsymbol{j})(1-p^{-1})\sum_{l=k}^{k_{\max}} B(p^{-l})p^{-l} + Z(\boldsymbol{i}), \text{ for } \boldsymbol{i}\in G_k.$$

In the simulations the parameters k, k_{max} were chosen by trial and error on a case by case approach. The sum $\sum_{l=k}^{k_{\max}} A(p^{-l})p^{-l}$ can be approximated by $A(p^{-k})p^{-k}$ in the cases where $A(p^{-k})p^{-k}$ is the dominant term in $\sum_{l=k}^{k_{\max}} A(p^{-l})p^{-l}$.

3.4.2 Numerical Scheme B

In section we present an approximation of the solution $X(x,t)$ of s p-adic continuous CNN(A,B,U,Z) when A,B,U,Z are test functions.

Lemma 7. *Let* $H(x) = \sum_{l=0}^{m} H_l\Omega(p^{k_l}|x-b_l|_p)$ *be a test function and let* $g \in \mathcal{X}_\infty$. *Take* $G_k = p^{-k}\mathbb{Z}_p/p^k\mathbb{Z}_p$, $k\in\mathbb{N}$, *as before. Then*

$$\int_{\mathbb{Q}_p} H(x-y)g(y)dy = \lim_{k\to\infty}\sum_{\boldsymbol{i}\in G_k} g(\boldsymbol{i})\sum_{l=0}^{m} H_l\int_{\mathbb{Q}_p}\Omega(p^{k_l}|x-\boldsymbol{i}-b_l-y|_p)\Omega(p^k|y|_p)dy$$

$$= \lim_{k\to\infty}\sum_{\boldsymbol{i}\in G_k} g(\boldsymbol{i})\sum_{l=0}^{m} H_l p^{\min(-k,-k_l)}\Omega\left(p^{-\max(-k,-k_l)}|x-\boldsymbol{i}-b_l|_p\right)$$

$$= \lim_{k\to\infty}\sum_{\boldsymbol{i}\in G_k} g(\boldsymbol{i})\sum_{l=0}^{m} H_l p^{-\max(k,k_l)}\Omega\left(p^{\min(k,k_l)}|x-\boldsymbol{i}-b_l|_p\right).$$

Proof. It is sufficient to consider the case where $H(x) = \Omega(p^{k_H}|x-b_H|_p)$ for some $k_H\in\mathbb{Z}$ and $b_H\in\mathbb{Q}_p$. Since $g(x) = \lim_{k\to\infty}\sum_{\boldsymbol{i}\in G_k} g(\boldsymbol{i})\Omega(p^k|x-\boldsymbol{a}|_p)$, we have

$$\int_{\mathbb{Q}_p} H(x-y)g(y)dy = \lim_{k\to\infty}\sum_{\boldsymbol{i}\in G_k} g(\boldsymbol{i})\int_{\mathbb{Q}_p}\Omega(p^{k_H}|x-b_H-y|_p)\Omega(p^k|y-\boldsymbol{i}|_p)dy$$

$$= \lim_{k\to\infty}\sum_{\boldsymbol{i}\in G_k} g(\boldsymbol{i})\int_{\mathbb{Q}_p}\Omega(p^{k_H}|(x-b_H-\boldsymbol{i})-y|_p)\Omega(p^k|y|_p)dy.$$

Without loss of generality, we may assume that $k_H \leq k$, and since any two balls are disjoint or one contains the other, then $B_{-k}\cap B_{-k_H}(x-b_H-a) = \emptyset$ or $B_{-k}\cap B_{-k_H}(x-b_H-\boldsymbol{i}) = B_{-k}$. The latter case occurs if and only if $0\in B_{-k_H}(x-b_H-\boldsymbol{i})$, i.e. when $|x-b_H-a|_p \leq p^{-k_H}$.

Therefore

$$\int_{\mathbb{Q}_p} \Omega(p^{k_H}|x - b_H - \boldsymbol{i} - y|_p)\Omega(p^k|y|_p)dy = p^{-k}\Omega\left(p^{k_H}|x - b_H - \boldsymbol{i}|_p\right).$$

□

We now assume that U, Z, $X_0 \in \mathcal{X}_\infty$ and that A, B are test functions of the form

$$A(x) = \sum_{l=0}^{m_A} A_l \Omega(p^{k_l}|x - a_l|_p), \quad B(x) = \sum_{l=0}^{m_B} B_l \Omega(p^{k_l}|x - b_l|_p.$$

Based on the continuity of operators $\boldsymbol{A}, \boldsymbol{B} : \mathcal{X}_\infty \to \mathcal{X}_\infty$ and the formula given in Lemma 7, we can approximate the solution $X(x,t)$ of a p-adic continuous CNN by p^{2k} ODEs, $k \geq 1$, of the form

$$\frac{d}{dx}X(\boldsymbol{i},t) = -X(\boldsymbol{i},t) + \sum_{\boldsymbol{j}\in G_k} f(X(\boldsymbol{j},t)) \sum_{l=0}^{m_A} A_l p^{-\max(k,k_l)}\Omega\left(p^{\min(k,k_l)}|\boldsymbol{i} - \boldsymbol{j} - a_l|_p\right)$$
$$+ \sum_{\boldsymbol{j}\in G_k} U(\boldsymbol{j}) \sum_{l=0}^{m_B} B_l p^{-\max(k,k_l)}\Omega\left(p^{\min(k,k_l)}|\boldsymbol{i} - \boldsymbol{j} - b_l|_p\right) + Z(\boldsymbol{i}), \text{ for } \boldsymbol{i} \in G_k.$$

It is possible to combine the approximations given in numeric schemes A, B.

3.4.3 A remark on the visualization of finite rooted trees

The discretizations to level k of the kernels A, B are functions on $G_k \times G_k$, while the input U and X_0 are functions on G_k. We use systematically heat maps [1] to present these functions. We always include a plot of the tree G_k. By convention we identify the leaves of the tree G_k with the set of rational numbers $\{0, 1/p^k, 2/p^k, \ldots, (p^{2k}-1)/p^k\}$. Furthermore, we label the levels of G_k with integers from the set $\{-k, -k+1, \ldots, 0, 1, \ldots k-1\}$. The level l consists of the cells $\boldsymbol{i}$, $\boldsymbol{j}$ such that

$$-\log_p(|\boldsymbol{i} - \boldsymbol{j}|_p) = (\text{the level of the first common ancestor of } \boldsymbol{i}, \boldsymbol{j}) = l.$$

3.4.4 First Simulation

In this example, we take $k = 2$, $p = 2$, which means that we use a tree with $2^4 = 16$ leaves and 4 levels. A basic application of the classical CNNs is image processing, see e.g. [18]. In this example we present a one-dimensional edge detector, which is a p-adic, one-dimensional analog of the examples 3.1 and 3.2 in [18]. The input U is an image having three levels:

$$U(x) = \sum_{\boldsymbol{i}\in G_2} U_{\boldsymbol{i}}\Omega(2^2|x - \boldsymbol{i}|_2), \quad U_{\boldsymbol{i}} = \begin{cases} -1 & \text{if} \quad \boldsymbol{i} = 1, 2, 1/4, 13/4 \\ 0 & \text{if} \quad \boldsymbol{i} = 1/2, 9/4, 5/4 \\ 1 & \text{otherwise}, \end{cases}$$

[1] A heat map is a data visualization technique showing a phenomenon's magnitude as color in two dimensions. The color in a cell represents the value of the function in that particular cell.

$x \in G_2 = 2^{-2}\mathbb{Z}_2/2^2\mathbb{Z}_2$. As in [18] we take $X_0(x) = 0$, $A(x) = 0$. We use

$$B(x) = 64\Omega(2^2|x|_2) - 4 \sum_{\boldsymbol{i} \in G_2;\ \boldsymbol{i} \neq 0} \Omega(2^2|x - \boldsymbol{i}|_2),\ x \in G_2.$$

Finally, we take $Z(x) = -\Omega(2^{-2}|x|_2)$, $f(x) = \frac{1}{2}(|x+1| - |x-1|)$. The output $Y(x,t)$ consists of the edges on the input U, see Figure 3.6.

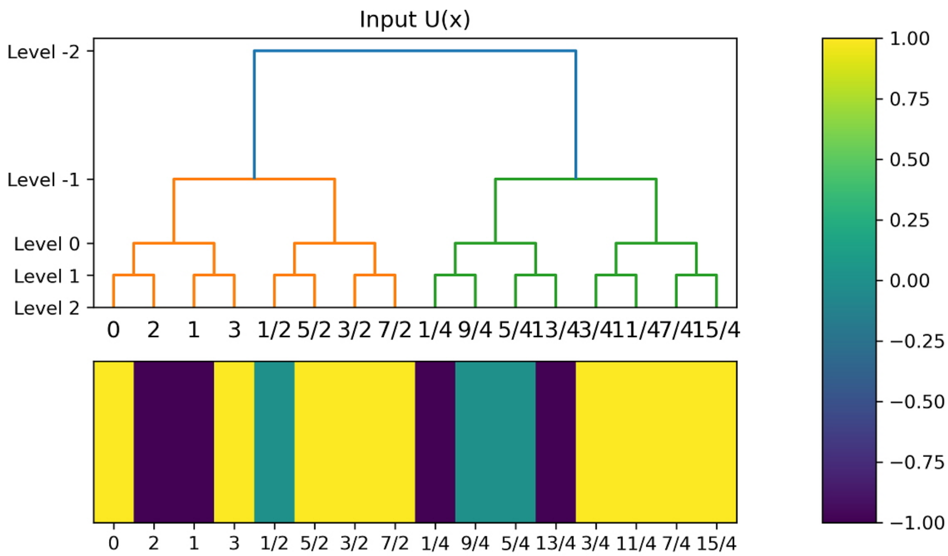

Figure 3.4: Simulation 1. Heat map $U(x)$.

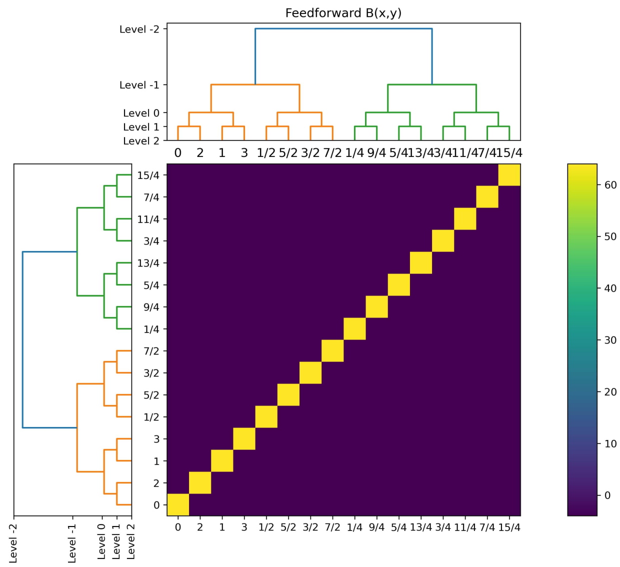

Figure 3.5: Simulation 1. Heat map of $B\left(|x-y|_2\right)$, x, $y \in G_2$.

3.4.5 Second Simulation

In this example, we take $k=2$, $p=2$, which means that we use a tree with $2^4=16$ leaves and 4 levels. We consider a CNN with the followin parameters:

$$A(x)=\Omega(2^2|x-2^{-2}|_2),\quad B(x)=U(x)=\Omega(2^2|x|_2),\ Z(x)=0,\ x\in G_{2.}$$

We set $X_0(x)=0$ and $\quad f(x)=\frac{1}{2}\left(|x+1|-|x-1|\right)$.

In this network, we have $A(\boldsymbol{i},\boldsymbol{j})=A(\boldsymbol{i}-\boldsymbol{j})=\Omega\left(2^2\left|\boldsymbol{i}-\boldsymbol{j}-2^{-1}\right|_2\right)$, $B(\boldsymbol{i},\boldsymbol{j})=B(|\boldsymbol{i}-\boldsymbol{j}|_2)=\Omega\left(2^2\left|\boldsymbol{i}-\boldsymbol{j}\right|_2\right)=\delta_{\boldsymbol{i},\boldsymbol{j}}$, where $\delta_{\boldsymbol{i},\boldsymbol{j}}$ denotes the Konecker delta function. This network does not have the space-invariant property because $A(\boldsymbol{i},\boldsymbol{j})=\Omega\left(2^2\left|\boldsymbol{i}-\boldsymbol{j}-2^{-1}\right|_2\right)$ is not a radial function. Due to this fact, $A(\boldsymbol{i},\boldsymbol{j})$ is not a symmetric matrix. For instance:

$$A(\frac{15}{4},0)=0,\ A(0,\frac{15}{4})=1,\quad A(\frac{1}{4},0)=0,\ A(0,\frac{1}{4})=1.$$

Our interpretation is that there is a connection from cell $\frac{15}{4}$ to cell 0, and a connection from cell 0 to cell $\frac{1}{4}$. This assertion is confirmed by the ouput $Y(x,t)$, see Figure 3.10. Notice that $Y(\frac{1}{2},t)\neq 0$ and $A(\frac{1}{2},0)=A(0,\frac{1}{2})=0$. But $A(\frac{1}{4},\frac{1}{2})=0$, $A(\frac{1}{2},\frac{1}{4})=1$, then there is a connection from cell $\frac{1}{4}$ to cell $\frac{1}{2}$, which explains the fact that $Y(\frac{1}{2},t)\neq 0$.

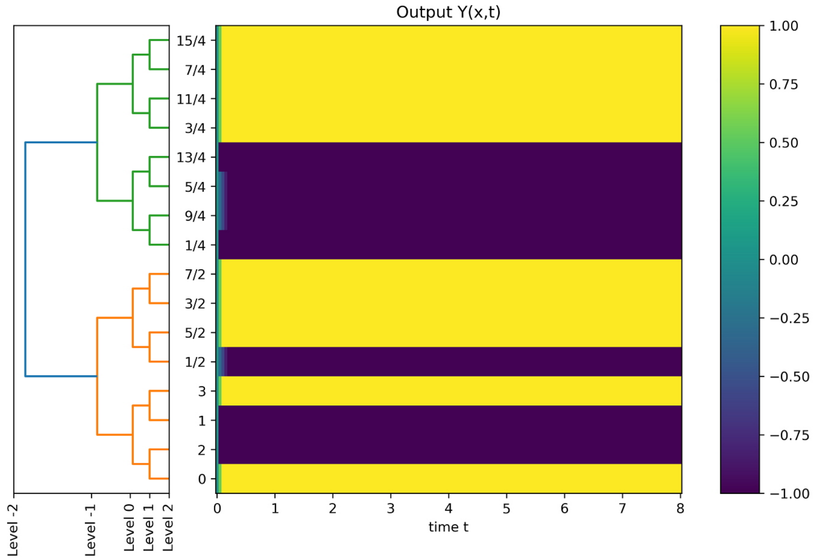

Figure 3.6: Simulation 1. Step 0.05.

The numerical solution is given in Figure 3.10. We now take $A(x) = B(x) = \Omega(2^2|x|_2)$. In this case the output $Y(x,t)$ changes completely, see Figure 3.11.

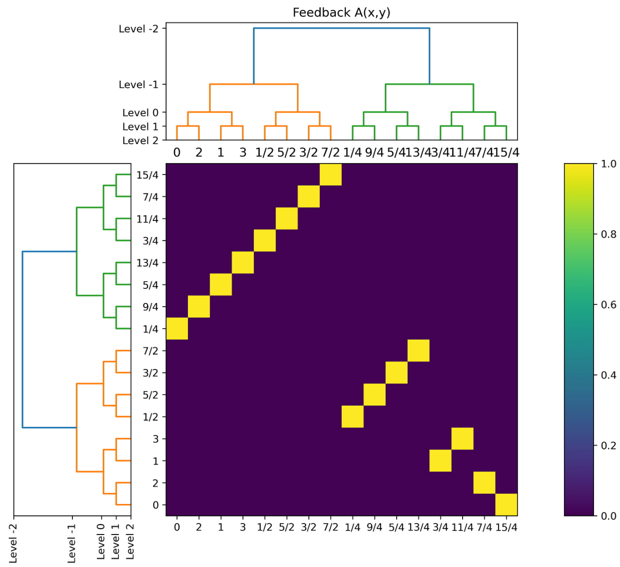

Figure 3.7: Simulation 2. Heat map $A(x-y)$ for $x, y \in G_2$.

3.4.6 Third Simulation

In this example, we take $k = 3$, $p = 2$, which means that we use a tree with $2^6 = 64$ leaves and 12 levels. We consider a CNN with the following parameters: $A(x) = \Omega(2^3|x - 2^{-2}|_2)$, $B(|x|_2) = \Omega(2^3|x|_2)$, $U(x) = \sin(p^4|x|_2)$, $Z(x) = 0.15\Omega(2^{-2}|x|_2)$ for $x \in G_3 = 2^{-3}\mathbb{Z}_3/2^3\mathbb{Z}_3$. We set $X_0(x) = 0$ and $f(x) = \frac{1}{2}(|x+1| - |x-1|)$.

As a consequence of the fractal nature of the p-adic numbers, the p-adic CNNs exhibit self-similarity in several ways. For instance, the graph of the kernel $A(x, y)$ is a self-similar set, this follows by comparing the graphs given in simulations 2 and 3 for this kernel. In addition, the output $Y(x, t) = 0$ when the norm $|x|_2$ is sufficiently large. In this simulation the CNN produces a pattern similar to the input, see Figure 3.13 and Figure 3.14.

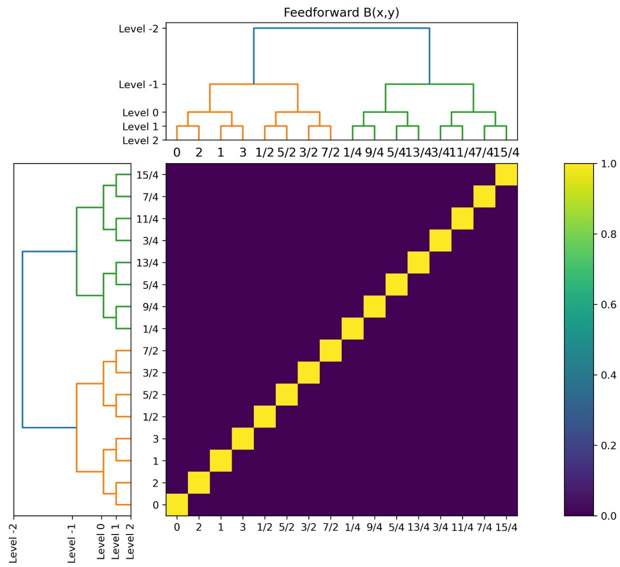

Figure 3.8: Simulation 2. Heat map of $B\left(|x-y|_2\right)$ for $x, y \in G_2$.

3.4.7 Fourth Simulation

In this example, we take $k=2$, $p=2$, which means that we use a tree with $2^4=16$ leaves and 4 levels. The parameters of the CNN are $A(x)=\Omega\left(2^2\left|x-2^{-2}\right|_2\right)$, $B(x)=U(x)=Z(x)=0$, we set $X_0(x)=\Omega\left(2^2|x|_2\right)$, $f(x)=\frac{1}{2}(|x+1|-|x-1|)$ for $x\in G_2$.

In this example, at time zero the cells near the origin are excited, which causes all the cells of the network to activate. The activation can be seen in the Fourier transform of the output. After some time the network returns to a state of rest.

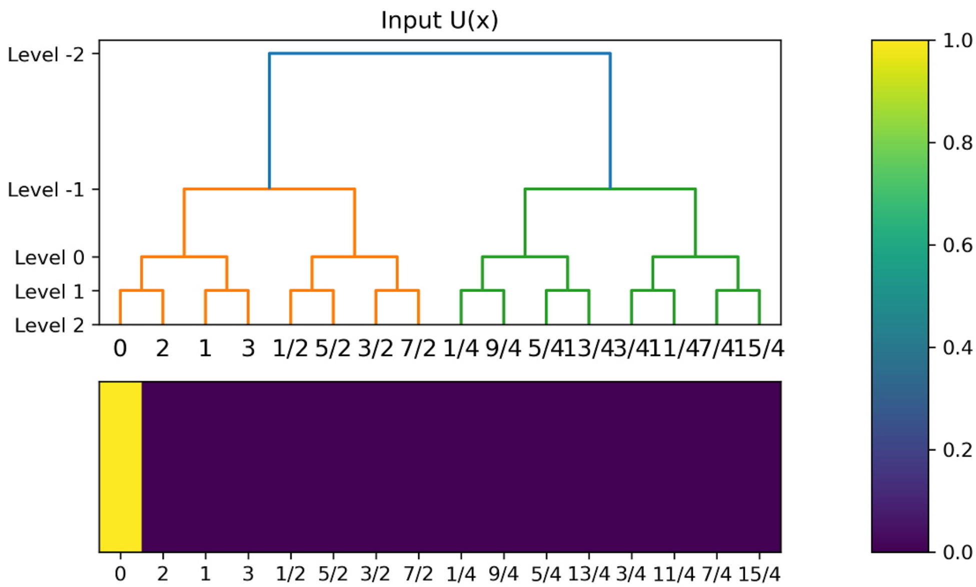

Figure 3.9: Simulation 2. Heat map of $U(x)$.

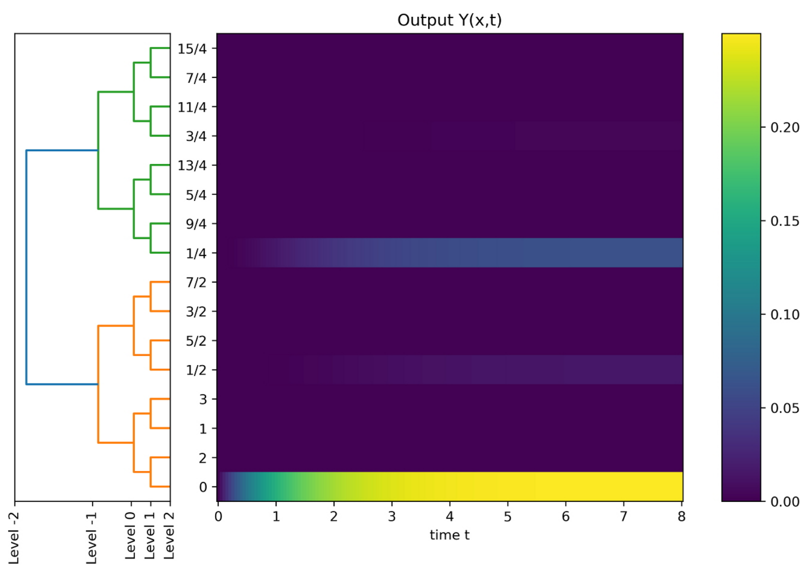

Figure 3.10: Simulation 2. Step 0.05.

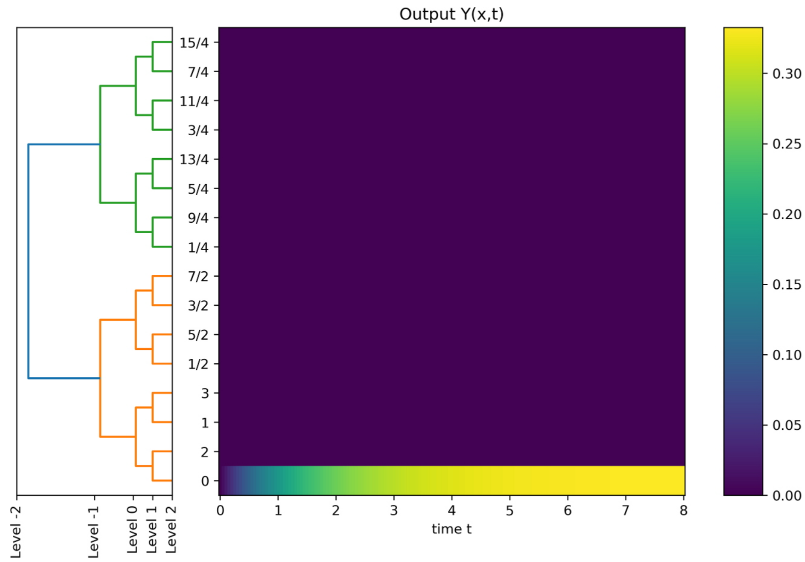

Figure 3.11: Simulation 2. Output with $A(x) = B(x) = \Omega(2^2|x|_2)$ and step 0.05.

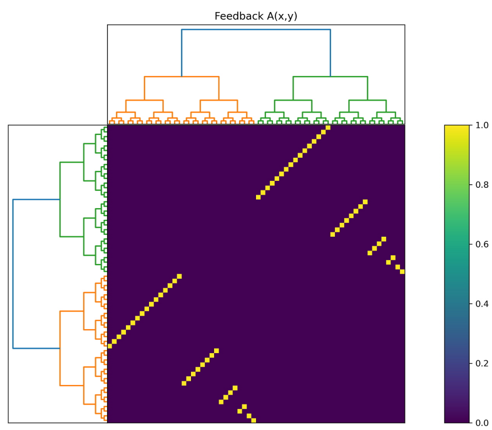

Figure 3.12: Simulation 3. Heat map of $A(x - y)$ for x, $y \in G_3$.

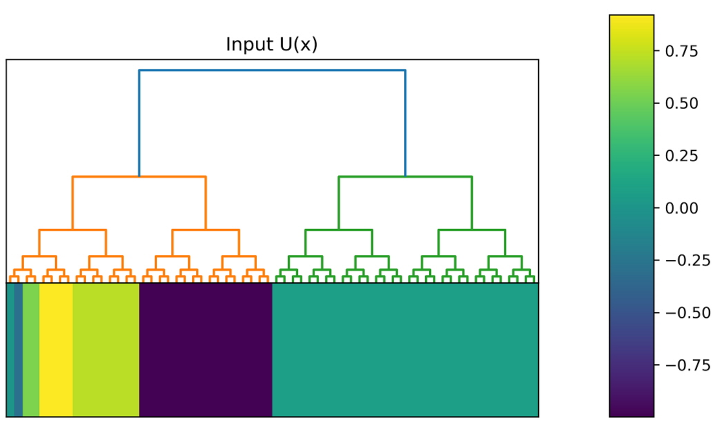

Figure 3.13: Simulation 3. Heat map of $U(x)$.

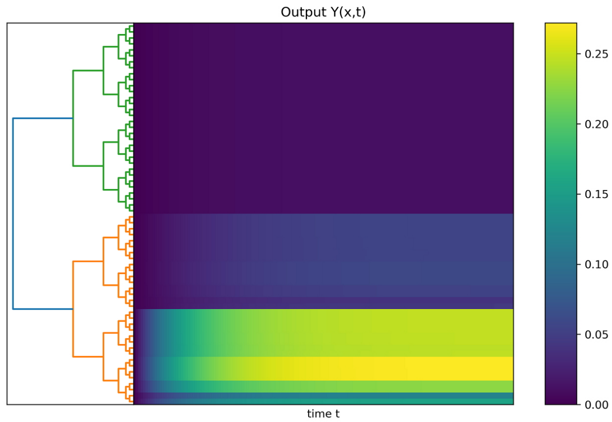

Figure 3.14: Simulation 3. Step 0.05.

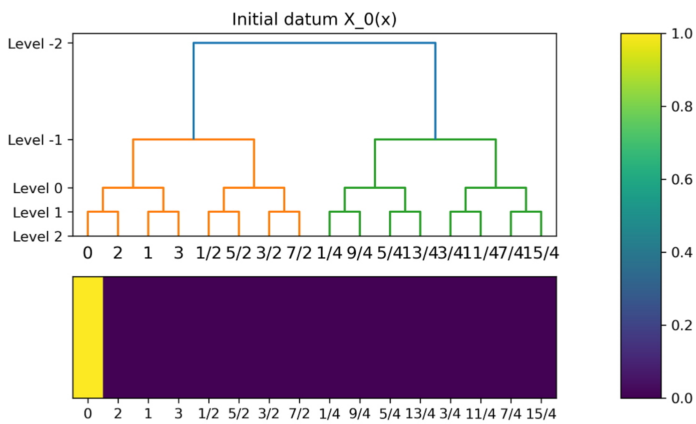

Figure 3.15: Simulation 4. Heat map of $X_0(x)$.

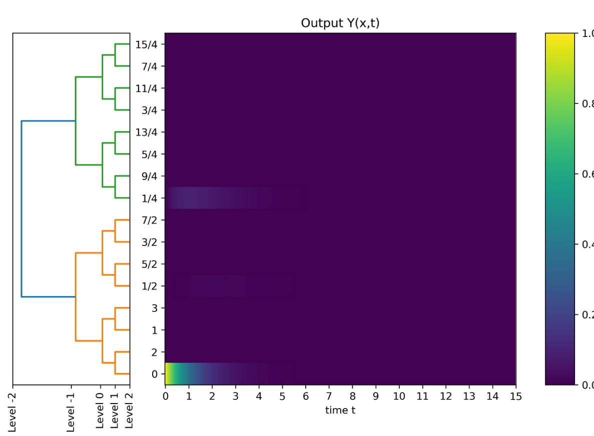

Figure 3.16: Simulation 4. Step 0.05.

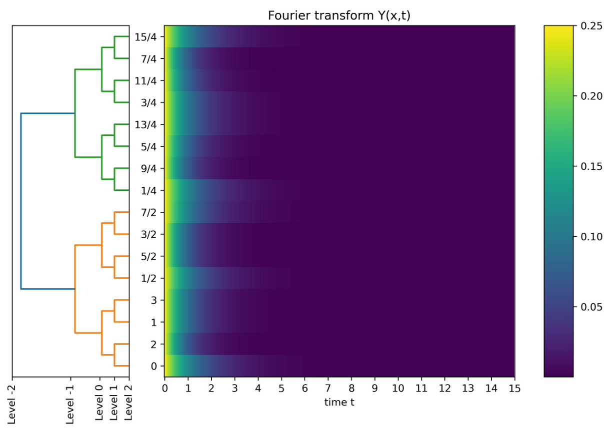

Figure 3.17: Simulation 4.

Chapter 4

p-adic Cellular Neural Network: Application to Image Processing

In this chapter, we present two new types of p-adic CNNs that can perform computations with real data, and whose dynamics can be understood almost completely. The first type can detect edges of gray images. The stationary states of these networks are organized hierarchically in a lattice structure, and that dynamics of any of these networks consists of transitions toward some minimal state in the lattice. The second type is a new class of reaction-diffusion networks. We investigate the stability of these networks and show that they can be used as filters to reduce noise, preserving the edges, in images polluted with additive Gaussian noise. The networks introduced here we found experimentally. They are abstract evolution equations on spaces of real-valued functions defined in the p-adic unit ball for some prime number p. In practical applications the prime p is determined by the size of image, and thus, only small primes are used. We provide several numerical simulations to show how these networks work.

4.1 A type p-adic continuous CNNs for edge detection

In this section we present new edge detectors[1] based on p-adic CNNs for gray images. We take $B \in L^1(\mathbb{Z}_p)$ and $U, Z \in \mathcal{C}(\mathbb{Z}_p)$, a, $b \in \mathbb{R}$, and fix the sigmoidal function $f(s) = \frac{1}{2}(|s+1| - |s-1|)$ for $s \in \mathbb{R}$. In this section we consider the following p-adic CNN:

$$\begin{cases} \frac{\partial}{\partial t} X(x,t) = -X(x,t) + aY(x,t) + (B * U)(x) + Z(x), \quad x \in \mathbb{Z}_p, t \geq 0; \\ \\ Y(x,t) = f(X(x,t)). \end{cases} \tag{4.1.1}$$

We denote this p-adic CNN as $CNN(a, B, U, Z)$, where a, B, U, Z are the parameters of the network. In applications to edge detection, we take $U(x)$ to be a gray image, and take the initial datum as $X(x, 0) = 0$.

[1]Edge detection includes a variety of mathematical methods that aim at identifying edges in a digital image at which the image brightness changes sharply.

4.1.1 Stationary states

We say that $X_{stat}(x)$ is a *stationary state* of network $CNN(a,B,U,Z)$, if

$$\begin{cases} X_{stat}(x) = aY_{stat}(x) + (B*U)(x) + Z(x), \quad x \in \mathbb{Z}_p; \\ \\ Y_{stat}(x) = f(X_{stat}(x)). \end{cases} \tag{4.1.2}$$

Remark 9. *Let $\tilde{X}(x)$ be any solution of (4.1.2). Then*

$$\widetilde{X}(x) = \begin{cases} a + (B*U)(x) + Z(x) & \text{if} \quad \widetilde{X}(x) > 1 \\ -a + (B*U)(x) + Z(x) & \text{if} \quad \widetilde{X}(x) < -1, \end{cases} \tag{4.1.3}$$

and

$$(1-a)\,\widetilde{X}(x) = (B*U)(x) + Z(x) \ \text{if} \ \left|\widetilde{X}(x)\right| \leq 1. \tag{4.1.4}$$

Lemma 8. *(i) If $a < 1$, then network $CNN(a,B,U,Z)$ has a unique stationary state $X_{stat}(x) \in \mathcal{C}(\mathbb{Z}_p)$ given by*

$$X_{stat}(x) = \begin{cases} a + (B*U)(x) + Z(x) & \text{if} \quad (B*U)(x) + Z(x) > 1-a \\ -a + (B*U)(x) + Z(x) & \text{if} \quad (B*U)(x) + Z(x) < -1+a \\ \frac{(B*U)(x)+Z(x)}{1-a} & \text{if} \quad |(B*U)(x) + Z(x)| \leq 1-a \end{cases} \tag{4.1.5}$$

(ii) If $a = 1$, then network $CNN(a,B,U,Z)$ has a unique stationary state $X_{stat}(x) \in L^1(\mathbb{Z}_p)$ given by

$$X_{stat}(x) = \begin{cases} 1 + (B*U)(x) + Z(x) & \text{if} \quad (B*U)(x) + Z(x) > 0 \\ -1 + (B*U)(x) + Z(x) & \text{if} \quad (B*U)(x) + Z(x) < 0 \\ 0 & \text{if} \quad (B*U)(x) + Z(x) = 0. \end{cases} \tag{4.1.6}$$

Proof. If $a < 1$, it follows from (4.1.3)-(4.1.4) that (4.1.5) is a continuous stationary state since by the dominated convergence theorem $(B*U)(x)$ is continuous. To establish the uniqueness of the solution, let $X(x) \in \mathcal{C}(\mathbb{Z}_p)$ be another stationary state. Consider a point $x_0 \in \mathbb{Z}_p$ such that $X(x_0) > 1$. Then by (4.1.3), $X(x_0) = a + (B*U)(x_0) + Z(x_0) > 1$ consequently $(B*U)(x_0) + Z(x_0) > 1-a$ and thus

$$X(x_0) = a + (B*U)(x_0) + Z(x_0) = X_{stat}(x_0).$$

The cases $X(x_0) < -1$ and $X\,|(x_0)| < 1$ are treated in a similar way.

The case $a = 1$ follows from (4.1.4), in this case we have that $X_{stat}(x) \in L^1(\mathbb{Z}_p)$ since $X_{stat}(x)$ is bounded. The continuity of $X_{stat}(x)$ requires further hypotheses on B, U, Z. □

Definition 5. *Assume that $a > 1$. Given*

$$I_+ \subseteq \{x \in \mathbb{Z}_p;\ 1-a < (B*U)(x) + Z(x)\},$$

$$I_- \subseteq \{x \in \mathbb{Z}_p;\ (B * U)(x) + Z(x) < a - 1\},$$

satisfying $I_+ \cap I_- = \varnothing$ *and*

$$\mathbb{Z}_p \smallsetminus (I_+ \cup I_-) \subseteq \{x \in \mathbb{Z}_p;\ 1 - a < (B * U)(x) + Z(x) < a - 1\},$$

we define the function

$$X_{stat}(x; I_+, I_-) = \begin{cases} a + (B * U)(x) + Z(x) & \text{if} \ \ x \in I_+ \\ -a + (B * U)(x) + Z(x) & \text{if} \ \ x \in I_- \\ \frac{(B*U)(x)+Z(x)}{1-a} & \text{if} \ \ x \in \mathbb{Z}_p \setminus (I_+ \cup I_-)\,. \end{cases} \tag{4.1.7}$$

Theorem 12. *Assume that* $a > 1$. *All functions of type (4.1.7) are stationary states of network* $CNN(a, B, U, Z)$. *Conversely, any stationary state of network* $CNN(a, B, U, Z)$ *has the form (4.1.7).*

Proof. We first verify that any function of type (4.1.7) is a stationary state. Take a point $x_0 \in \mathbb{Z}_p$. Since the sets I_+, I_-, $\mathbb{Z}_p \smallsetminus (I_+ \cup I_-)$ are disjoint, three cases occur.

Case 1: $x_0 \in I_+$.

If $x_0 \in I_+$, then $X_{stat}(x_0; I_+, I_-) = a + (B * U)(x_0) + Z(x_0)$ and by definition of I_+, $a + (B * U)(x_0) + Z(x_0) > 1$. Then

$$\begin{aligned} &af(X_{stat}(x_0; I_+, I_-)) + (B * U)(x_0) + Z(x_0) = \\ &a + (B * U)(x_0) + Z(x_0) = X_{stat}(x_0; I_+, I_-). \end{aligned}$$

Case 2: $x_0 \in I_-$.

If $x_0 \in I_-$, then $X_{stat}(x_0; I_+, I_-) = -a + (B * U)(x_0) + Z(x_0)$ and by definition of I_-, $-a + (B * U)(x_0) + Z(x_0) < -1$. Then

$$\begin{aligned} &af(X_{stat}(x_0; I_+, I_-)) + (B * U)(x_0) + Z(x_0) = \\ &- a + (B * U)(x_0) + Z(x_0) = X_{stat}(x_0; I_+, I_-). \end{aligned}$$

Case 3: $x_0 \in \mathbb{Z}_p \smallsetminus (I_+ \cup I_-)$.

If $x_0 \notin I_+ \sqcup I_-$, then $X_{stat}(x_0; I_+, I_-) = \frac{(B*U)(x_0)+Z(x_0)}{1-a}$ and by definition of $\mathbb{Z}_p \smallsetminus (I_+ \cup I_-)$, $-1 \leq \frac{(B*U)(x_0)+Z(x_0)}{1-a} \leq 1$, then

$$\begin{aligned} af(X_{stat}(x_0; I_+, I_-)) + (B * U)(x_0) + Z(x_0) &= \\ a\frac{(B * U)(x_0) + Z(x_0)}{1 - a} + (B * U)(x_0) + Z(x_0) &= \frac{(B * U)(x_0) + Z(x_0)}{1 - a} \\ &= X_{stat}(x_0; I_+, I_-). \end{aligned}$$

Therefore $X_{stat}(x_0; I_+, I_-)$ is a stationary state of the network $CNN(a, B, U, Z)$.

Now, suppose that $X_{stat}(x)$ is a stationary state of network $CNN(a,B,U,Z)$. Set

$$I_+ := X_{stat}^{-1}((1,\infty)), \qquad I_- := X_{stat}^{-1}((-\infty,-1)).$$

By using (4.1.3) and (4.1.4), we have

$$I_+ \subseteq (B*U+Z)^{-1}((1-a,\infty)),$$

$$I_- \subseteq (B*U+Z)^{-1}((-\infty,a-1)),$$

and

$$\mathbb{Z}_p \smallsetminus (I_+ \cup I_-) \subseteq (B*U+Z)^{-1}([1-a,a-1]).$$

Then $X_{stat}(x_0;I_+,I_-)$ is a well-defined function. Finally, using again (4.1.3) and (4.1.4), we conclude that $X_{stat}(x) = X_{stat}(x_0;I_+,I_-)$ for all $x \in \mathbb{Z}_p$. □

Remark 10. *Notice that*

$$Y_{stat}(x;I_+,I_-) := f\left(X_{stat}(x;I_+,I_-)\right) = \begin{cases} 1 & \text{if} \quad x \in I_+ \\ -1 & \text{if} \quad x \in I_- \\ \frac{(B*U)(x)+Z(x)}{1-a} & \text{if} \quad x \in \mathbb{Z}_p \setminus (I_+ \cup I_-)\,. \end{cases}$$

The function $Y_{stat}(x;I_+,I_-)$ is the output of the network. If $I_+ \cup I_- = \mathbb{Z}_p$, we say that $X_{stat}(x;I_+,I_-)$ is bistable. The set $\mathcal{B}\left(I_+,I_-\right) = \mathbb{Z}_p \backslash (I_+ \cup I_-)$ measures how far $X_{stat}(x;I_+,I_-)$ is from being bistable. We call set $\mathcal{B}\left(I_+,I_-\right)$ the set of bistability of $X_{stat}(x;I_+,I_-)$. If $\mathcal{B}\left(I_+,I_-\right) = \varnothing$, then $X_{stat}(x;I_+,I_-)$ is bistable.

Remark 11. *If $I_+ \cup I_- \subsetneqq \mathbb{Z}_p$, we say that $X_{stat}(x;I_+,I_-)$ is an unstable.*

4.2 Hierarchical structure of the space of stationary states

A relation $\preccurlyeq$ is *a partial order* on a set S if it satisfies: 1 (reflexivity) $f \preccurlyeq f$ for all f in S; 2 (antisymmetry) $f \preccurlyeq g$ and $g \preccurlyeq f$ implies $f = g$; 3 (transitivity) $f \preccurlyeq g$ and $g \preccurlyeq h$ implies $f \preccurlyeq h$. A *partially ordered set* $(S, \preccurlyeq)$ (or poset) is a set taken endowed with a partial order. A partially ordered set $(S, \preccurlyeq)$ is called a *lattice* if for every f, g in S, the elements $f \wedge g = \inf\{f,g\}$ and $f \vee g = \sup\{f,g\}$ exist. Here, $f \wedge g$ denotes the largest element in S satisfying $f \wedge g \preccurlyeq f$ and $f \wedge g \preccurlyeq g$; while $f \vee g$ denotes the smallest element in S satisfying $f \preccurlyeq f \vee g$ and $g \preccurlyeq f \vee g$. We say that $h \in S$ a *minimal* element of with respect to $\preccurlyeq$, if there is no element $f \in S$, $f \neq h$ such that $f \preccurlyeq h$.

Posets offer a natural way to formalize the notion of hierarchy.

We set

$$\mathcal{M} = \bigcup_{I_+,I_-} \left\{X_{stat}(x;I_+,I_-)\right\},$$

where I_+, I_- run trough all the sets given in Definition 5. Given $X_{stat}(x; I_+, I_-)$ and $X_{stat}(x; I_+, I_-)$ in $\mathcal{M}$, with $I_+ \cup I_- \neq \mathbb{Z}_p$ or $I'_+ \cup I'_- \neq \mathbb{Z}_p$, we define

$$X_{stat}(x; I'_+, I'_-) \preccurlyeq X_{stat}(x; I_+, I_-) \text{ if } I_+ \cup I_- \subseteq I'_+ \cup I'_-. \tag{4.2.1}$$

In the case $I_+ \cup I_- = \mathbb{Z}_p$ and $I'_+ \cup I'_- = \mathbb{Z}_p$, the corresponding stationary states $X_{stat}(x; I_+, I_-)$, $X_{stat}(x; I_+, I_-)$ are not comparable. Since the condition $I_+ \cup I_- \subseteq I'_+ \cup I'_-$ is equivalent to $\mathcal{B}\left(I'_+, I'_-\right) = \mathbb{Z}_p \setminus (I'_1 \cup I'_{-1}) \subseteq \mathcal{B}\left(I_1, I_{-1}\right) = \mathbb{Z}_p \setminus (I_1 \sqcup I_{-1})$, condition (4.2.1) means that the set of bistability of $X_{stat}(x; I'_+, I'_-)$ is smaller that the set of of bistability of $X_{stat}(x; I_+, I_-)$. Also, the condition $I_+ \cup I_- \subseteq I'_+ \cup I'_-$implies that

$$X_{stat}(x; I'_+, I'_-)(x) = X_{stat}(x; I_+, I_-)(x) \text{ for all } x \in I_+ \cup I_- \cup \mathcal{B}\left(I'_+ \cup I'_-\right).$$

By using this observation, one verifies that (4.2.1) defines a partial order in $\mathcal{M}$. This means that the set of stationary states of the network $CNN(a, B, U, Z)$, $a > 1$, has a hierarchical structure, where the bistable stationary states are the minimal ones. Intuitively, the bistable stationary states are at the deepest level of $\mathcal{M}$. Furthermore, $(\mathcal{M}, \preccurlyeq)$ is a lattice. Indeed, given $X_{stat}(x; I'_+, I'_-)$, $X_{stat}(x; I_+, I_-)$,in $\mathcal{M}$, it verifies that

$$X_{stat}(x; I'_+, I'_-) \wedge X_{stat}(x; I_+, I_-) = X_{stat}(x; I''_+, I''_-),$$

where $I''_+ = I_+ \cup I'_+$, $I''_- = I_- \cup I'_-$, and

$$X_{stat}(x; I'_+, I'_-) \vee X_{stat}(x; I_+, I_-) = X_{stat}(x; I'''_+, I'''_-),$$

where $I'''_+ = I_+ \cap I'_+$, $I'''_- = I_- \cap I'_-$. Therefore, we have established the following result:

Theorem 13. *$(\mathcal{M}, \preccurlyeq)$ is a lattice. Furthermore, the set of minimal elements of $(\mathcal{M}, \preccurlyeq)$ agrees with the set of bistable states of $CNN(a, B, U, Z)$.*

4.3 Edge detection

4.3.1 A new class of edge detectors

We take $a > 1$, $X(x, 0) = 0$, and $U(x) \in \mathcal{D}(\mathbb{Z}_p)$ to be a gray image. We argue that network (4.1.1) works as an edge detector. By Theorem 12, network $CNN(a, B, U, Z)$, $a > 1$ has steady states of the form

$$Y_{stat}(x) = f(X_{stat}(x)) = \begin{cases} +1 & \text{if} \quad (B * U)(x) + Z(x) > \text{Threshold}_1 \\ -1 & \text{if} \quad (B * U)(x) + Z(x) < \text{Threshold}_2 \end{cases} \tag{4.3.1}$$

where Threshold_2, Threshold_1 are real numbers. This type of outputs occur for networks with stationary states where $I_+ \sqcup I_- = \mathbb{Z}_p$. For instance, when $I_+ \subseteq (B*U+Z)^{-1}((\text{Threshold}_1, \infty))$ and $I_- \subseteq (B * U + Z)^{-1}((-\infty, \text{Threshold}_2))$. If $U(x)$ is sufficiently small, then $(B * U)(x) + Z(x)$ gives a measure of dispersion of the image intensities; if this value is larger than Threshold_1, the networks ouputs $+1$ to indicate the existence of an edge, if value is smaller than Threshold_2, the network ouputs -1 to indicate the non existence of an edge.

We conducted several numerical experiments with gray images presented in Section 4.4. We implemented a numerical method for solving the initial value problem attached to network $CNN(a,B,U,Z)$, with $X(x,0)=0$ and $U(x)$ a gray image. The simulations show that after a sufficiently long time the network outputs a white and black image approximating the edges of the original image $U(x)$. This means that for t sufficiently large $X(x,t)$ is close to a bistable stationary state $X_{stat}(x;I_{+},I_{-})$. Furthermore, after a certain sufficiently large time, the outputs of the network do not show a difference perceivable by the human eye. We interpret this result as the bistable stationary states are asymptotically stable; of course this is a mathematical conjecture.

We now give an intuitive picture of the dynamics of the network, for t sufficiently large, using $(\mathcal{M},\preccurlyeq)$ as an *asymptotic landscape for* $CNN(a,B,U,Z)$. For t sufficiently large, the network performs transitions between stationary states $X_{stat}(x;I_{+},I_{-})$ belonging to a small neighborhood $\mathcal{N}$ around a bistable state $X_{stat}^{(0)}(x;I_{+},I_{-})$, $I_{+}\cup I_{-}=\mathbb{Z}_{p}$. The dynamics of the network consists of transitions in a hierarchically organized landscape $(\mathcal{M},\preccurlyeq)$ toward of some minimal state. This is a reformulation of the classical paradigm asserting that the dynamics of a large class of complex systems can be modeled as a random walk on its energy landscape, see e.g. [21, 23, 29, 34, 41, 52, 64, 72]

4.3.2 Discretization

To process an image $U(x)$, we use a discrete version of network $CNN(a,B,U,Z)$, $a>1$. In turn, this requires to determine suitable kernels $B(x)$. We address these matters on this section.

We take L to be a positive integer, and set $G_{L}=\mathbb{Z}_{p}/p^{L}\mathbb{Z}_{p}$. We identify $i\in G_{L}$ with an element of the form

$$i=i_{0}+i_{1}p+\ldots+i_{L-1}p^{L-1},$$

where the i_{k}s belong to the set $\{0,1,\ldots,p-1\}$. We denote by $\mathcal{D}_{L}\left(\mathbb{Z}_{p}\right)$ the $\mathbb{R}$-vector space of test functions of the form

$$\varphi\left(x\right)=\sum_{i\in G_{L}}\varphi\left(i\right)\Omega\left(p^{L}\left\vert x-i\right\vert_{p}\right)$$

supported in the unit ball $\mathbb{Z}_{p}$ and $\Omega\left(p^{L}\left\vert x-i\right\vert_{p}\right)$ is the characteristic function of the ball $B_{-L}(i)$. Since $\Omega\left(p^{L}\left\vert x-i\right\vert_{p}\right)\Omega\left(p^{L}\left\vert x-j\right\vert_{p}\right)=0$ for $i\neq j$, the set

$$\left\{\Omega\left(p^{L}\left\vert x-i\right\vert_{p}\right)\right\}_{i\in G_{L}}$$

is a basis of $\mathcal{D}_{L}\left(\mathbb{Z}_{p}\right)$. Notice that the dimension of $\mathcal{D}_{L}\left(\mathbb{Z}_{p}\right)$ is p^{L}.

Assuming that $B\left(x\right),U(x),Z(x)\in\mathcal{D}_{L}\left(\mathbb{Z}_{p}\right)$, the initial value problem

$$\begin{cases}\frac{\partial}{\partial t}X(x,t)=-X(x,t)+aY(x,t)+(B\ast U)(x)+Z(x), & x\in\mathbb{Z}_{p},t\geq0;\\ \\ X(x,0)=X_{0}\in\mathcal{D}_{L}\left(\mathbb{Z}_{p}\right). & \end{cases}\tag{4.3.2}$$

has unique solution

$$X(x,t)=\sum_{i\in G_L}X(i,t)\Omega\left(p^L\left|x-i\right|_p\right) \tag{4.3.3}$$

in $\mathcal{D}_L(\mathbb{Z}_p)$ for $t\geq 0$, see Theorem 8.

This result allow us to obtain a discretization of (4.3.2) and (4.1.1) as follows. Take

$$U(x)=\sum_{i\in G_L}U(i)\Omega(p^L|x-i|), \tag{4.3.4}$$

$$Z(x)=\sum_{i\in G_L}Z(i)\Omega(p^L|x-i|), \tag{4.3.5}$$

and

$$B(x)=p^{M_2-M_1}\Omega(p^{M_2}|x|_p)-\Omega(p^{M_1}|x|_p) \tag{4.3.6}$$

for some integers $M_1\leq M_2\leq L$.

We now take i, $j\in G_L$ and an integer $M\leq L$, then

$$|i-j+p^Lz|_p=|i-j|_p \text{ for any } z\in\mathbb{Z}_p.$$

By using this observation, one gets that

$$\Omega(p^M|x|_p)*U(x)= \tag{4.3.7}$$

$$=\sum_{i\in G_L}\left\{\sum_{j\in G_L}U(j)\int_{\mathbb{Z}_p}\Omega(p^M|i-y|_p)\Omega(p^L|y-j|_p)dy\right\}\Omega(p^L|x-i|_p)$$

$$=\sum_{i\in G_L}\left\{\sum_{j\in G_L}U(j)\int_{j+p^L\mathbb{Z}_p}\Omega(p^M|i-y|_p)dy\right\}\Omega(p^L|x-i|_p)$$

$$=\sum_{i\in G_L}\left\{p^{-L}\sum_{j\in G_L}U(j)\Omega(p^M|i-j|_p)\right\}\Omega(p^L|x-i|_p).$$

Now, from (4.3.6)-(4.3.7), we get the following formula:

$$(B*U)(x)= \tag{4.3.8}$$

$$\sum_{i\in G_l}p^{-L}\left(p^{M_2-M_1}\sum_{j\in G_l}\Omega(p^{M_2}|i-j|_p)U(j)-\sum_{j\in G_l}\Omega(p^{M_1}|i-j|_p)U(j)\right)\Omega(p^L|x-i|_p).$$

We now replace (4.3.3)-(4.3.8) in the equation in (4.3.2) and use that $\{\Omega(p^L|x-i|)\}_{i\in G_L}$ is a basis of $\mathcal{D}_L(\mathbb{Z}_p)$, to get a discretization of (4.3.2):

$$\begin{cases}\frac{dX(i,t)}{dt}=-X(i,t)+aY(i,t)+p^{-L}\left(\mathcal{L}U\right)(i)+Z(i), & i\in G_L\\ X(i,0)=X_0(i),\end{cases} \tag{4.3.9}$$

where

$$Y(i,t) = f\left(X(i,t)\right),\ i \in G_L,$$

and

$$\left(\mathcal{L}U\right)(i) := p^{M_2 - M_1} \sum_{j \in G_l} \Omega(p^{M_2}|i-j|_p)U(j) - \sum_{j \in G_l} \Omega(p^{M_1}|i-j|_p)U(j),\ i \in G_L. \quad (4.3.10)$$

Graph Laplacians

Let $G = (V, E)$ be a simple finite graph with vertices V and edges E. Let $\phi : V \to \mathbb{R}$ be a function on the graph. The graph Laplacian Δ acting on ϕ is defined as

$$\left(\Delta\phi\right)(v) = \sum_{\substack{w \in V \\ dist(w,v)=1}} \left[\phi\left(v\right) - \phi\left(w\right)\right],$$

where $\operatorname{dist}(w, v)$ is the distance on the graph, e.i., the distance between w and v in G is the number of edges in a shortest path, see [53]. Now, let $N\left(v\right)$ be a fixed neighborhood of v, for instance,

$$\mathcal{N}\left(v\right) = \left\{w \in V; \operatorname{dist}(w, v) \leq M\right\},$$

for positive integer M, a generalization of operator Δ is

$$\left(\Delta_{\mathcal{N}}\phi\right)(v) = \sum_{w \in \mathcal{N}(v)} \left(\Delta\phi\right)(w). \quad (4.3.11)$$

The operator $\mathcal{L}$ has the form (4.3.11). Indeed, the following formula holds for operator $\left(\mathcal{L}U\right)(i)$:

$$\left(\mathcal{L}U\right)(i) = \sum_{\substack{j \in G_L \\ |i-j|_p \leq p^{-M_2}}} \left[\sum_{\substack{k \in G_L \\ p^{-M_2} < |j-k|_p \leq p^{-M_1}}} \left[U(j) - U(k)\right]\right],\ i \in G_L. \quad (4.3.12)$$

In particular, taking $M_1 = 0$, $M_2 = 1$, one gets that

$$\sum_{\substack{k \in G_L \\ p^{-1} < |j-k|_p \leq 1}} \left[U(j) - U(k)\right] = \sum_{\substack{k \in G_L \\ |j-k|_p = 1}} \left[U(j) - U(k)\right],$$

which is the graph Laplacian on $G_L = \mathbb{Z}_p / p^L \mathbb{Z}_p$ with the distance induced by $|\cdot|_p$.

Finally, we establish formula (4.3.12). We use that

$$\#\left\{k \in G_L; p^{-M_2} < |j-k|_p \leq p^{-M_1}\right\} = p^{M_2 - M_1},$$

since $i = i_0 + i_1 p + \ldots + i_{L-1} p^{L-1}$. Now $\left|i-j\right|_p \leq p^{-M_2}$ and $p^{-M_2} < |j-k|_p \leq p^{-M_1}$ implies that

$$\left|i-k\right|_p = \max\left\{\left|i-j\right|_p, \left|j-k\right|_p\right\} = |j-k|_p \leq p^{-M_1},$$

by ultrametric property of $|\cdot|_p$. Then,

$$\sum_{\substack{j\in G_L\\ |i-j|_p\leq p^{-M_2}}}\left[\sum_{\substack{k\in G_L\\ p^{-M_2}<|j-k|_p\leq p^{-M_1}}}[U(j)-U(k)]\right]=$$

$$\sum_{\substack{j\in G_L\\ |i-j|_p\leq p^{-M_2}}}\left[\#\left\{k\in G_L;p^{-M_2}<|j-k|_p\leq p^{-M_1}\right\}\right]U(j)$$

$$-\sum_{\substack{j\in G_L\\ |i-j|_p\leq p^{-M_2}}}\sum_{\substack{k\in G_L\\ p^{-M_2}<|j-k|_p\leq p^{-M_1}}}U(k)=$$

$$\sum_{\substack{j\in G_L\\ |i-j|_p\leq p^{-M_2}}}p^{M_2-M_1}U(j)-\sum_{\substack{k\in G_L\\ |i-k|_p\leq p^{-M_1}}}U(k)=\left(\mathcal{L}U\right)(i).$$

4.4 Numerical Examples

To construct an edge detector using (4.3.9), it requires an algorithm for splitting a large image into smaller sub-images. Given an image I of size (n,m), a prime p and an integer K, the algorithm divides image I into sub-images I_r' of size (p^K,p^K) or less. Then, we use another algorithm to codify sub-image I_r' as a test function $Test(I_r')$. These algorithms are presented in the Section 4.7. We process the test function $Test(I_r')=U$ using network

$$\begin{cases}\frac{dX(i,t)}{dt}=-X(i,t)+aY(i,t)+\sum_{j=0}^{8}\left\{U(i)-U(i+j3^2)\right\}+z_0, & i\in G_L\\ X(i,0)=0\\ Y(i,t)=f(X(i,t)),\end{cases}\tag{4.4.1}$$

with $p=3$, $L=4$, $M_1=2$, $M_2=4$, and $Z(i)=z_0\in\mathbb{R}$, for $i\in G_L$, and rescaling $\left(\mathcal{L}U\right)(i)$ as $3^4\left(\mathcal{L}U\right)(i)$, for $i\in G_L$, to get another test function $X(i,t_0;Test(I_r'))$ taking values in $\{\pm1\}$. Each test function $X(i,t_0;Test(I_r'))$ is transformed into an image I_r^{edges}, at the final step, we concatenate all the images I_r^{edges} to obtain a full image I^{edges}, which is the output image. The time t_0 is chosen on a case-by-case basis so that the edges are as sharp as possible. See Figures 4.1, 4.2.

4.5 Reaction-diffusion Cellular Neural Networks

4.5.1 The p-adic heat equation

For $\alpha>0$, the Vladimirov-Taibleson operator $\boldsymbol{D}^\alpha$ is defined as

$$\begin{array}{ccc}\mathcal{D}(\mathbb{Q}_p) & \to & L^2(\mathbb{Q}_p)\cap\mathcal{C}\left(\mathbb{Q}_p\right)\\ \varphi & \to & \boldsymbol{D}^\alpha\varphi,\end{array}$$

Figure 4.1: Left side, the original image. Right side, edges obtained by using a Canny edge detector. See Section B.1

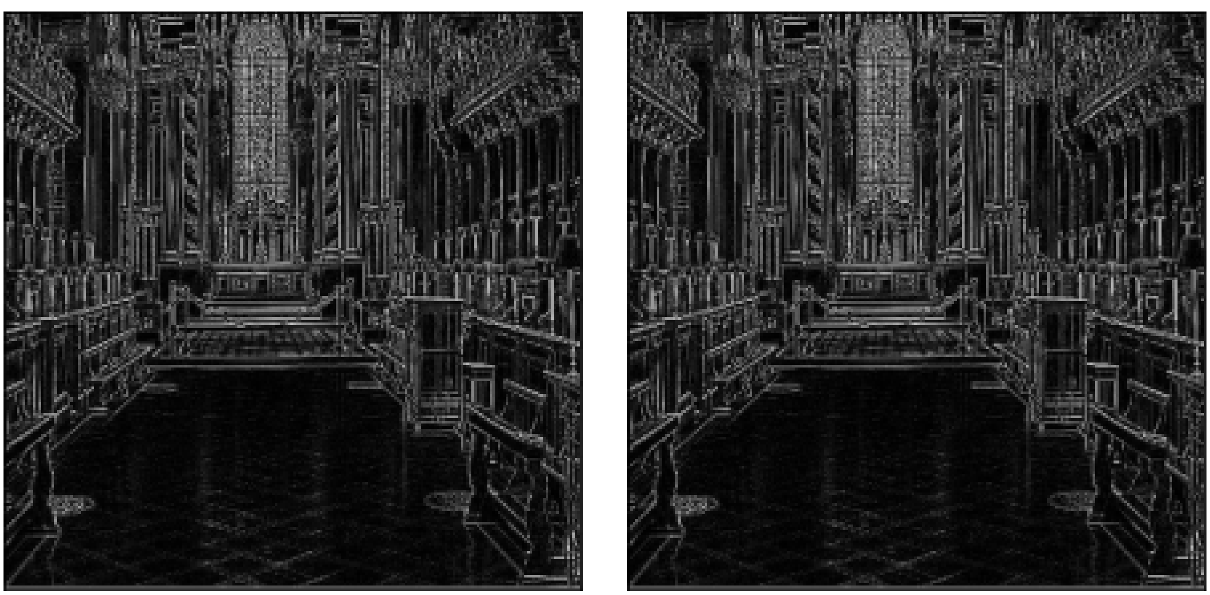

Figure 4.2: Left side, edges obtained by using CNN (4.4.1), with $z_0 = -1$ and 6 steps. Right side, edges obtained by using the CNN (4.4.1), with $z_0 = -1$ and 10 steps.

where

$$(\boldsymbol{D}^{\alpha}\varphi)(x) = \frac{1-p^{\alpha}}{1-p^{-\alpha-1}} \int_{\mathbb{Q}_p} \frac{[\varphi(x-y)-\varphi(x)]}{|y|_p^{\alpha+1}} dy.$$

The p-adic analogue of the heat equation is

$$\frac{\partial u(x,t)}{\partial t} + a\boldsymbol{D}^{\alpha} u(x,t) = 0, \text{ with } a > 0.$$

The solution of the Cauchy problem attached to the heat equation with initial datum $u(x,0) = \varphi(x) \in \mathcal{D}(\mathbb{Q}_p)$ is given by

$$u(x,t) = \int_{\mathbb{Q}_p} Z(x-y,t)\,\varphi(y)\,dy,$$

where $Z(x,t)$ is the *p-adic heat kernel* defined as

$$Z(x,t) = \int_{\mathbb{Q}_p} \chi_p(-x\xi)\, e^{-at|\xi|_p^{\alpha}} d\xi, \tag{4.5.1}$$

where $\chi_p(-x\xi)$ is the standard additive character of the group $(\mathbb{Q}_p, +)$. The p-adic heat kernel is the transition density function of a Markov stochastic process with space state $\mathbb{Q}_p$, see, e.g., [38, 75].

4.5.2 The p-adic heat equation on the unit ball

We define the operator $\boldsymbol{D}_0^{\alpha}$ $\alpha > 0$, by restricting $\boldsymbol{D}^{\alpha}$ to $\mathcal{D}(\mathbb{Z}_p)$ and considering $(\boldsymbol{D}^{\alpha}\varphi)(x)$ only for $x \in \mathbb{Z}_p$. It satisfies that

$$\boldsymbol{D}_0^{\alpha}\varphi(x) = \lambda\varphi(x) + \frac{1-p^{\alpha}}{1-p^{-\alpha-1}} \int_{\mathbb{Z}_p} \frac{\varphi(x-y)-\varphi(x)}{|y|_p^{\alpha+1}} dy,$$

for $\varphi \in \mathcal{D}(\mathbb{Z}_p)$, with $\lambda = \frac{p-1}{p^{\alpha+1}-1}p^{\alpha}$.

Consider the Cauchy problem

$$\begin{cases} \frac{\partial u(x,t)}{\partial t} + \boldsymbol{D}_0^{\alpha} u(x,t) - \lambda u(x,t) = 0, & x \in \mathbb{Z}_p, \quad t > 0; \\ u(x,0) = \varphi(x), & x \in \mathbb{Z}_p, \end{cases}$$

where $\varphi \in \mathcal{D}(\mathbb{Z}_p)$. The solution of this problem is given by

$$u(x,t) = \int_{\mathbb{Z}_p} Z_0(x-y,t)\varphi(y)\,dy,\ x \in \mathbb{Z}_p,\ t > 0,$$

where

$$Z_0(x,t) := e^{\lambda t} Z(x,t) + c(t),\ x \in \mathbb{Z}_p,$$
$$c(t) := 1 - (1-p^{-1}) e^{\lambda t} \sum_{n=0}^{\infty} \frac{(-1)^n}{n!} t^n \frac{1}{1-p^{-n\alpha-1}}$$

and $Z(x,t)$ is given (4.5.1). The function $Z_0(x,t)$ is non-negative for $x \in \mathbb{Z}_p$, $t > 0$, and

$$\int_{\mathbb{Z}_p} Z_0(x,t)dx = 1,$$

see [38]. Furthermore, $Z_0(x,t)$ is the transition density function of a Markov process with space state $\mathbb{Z}_p$.

The family

$$\begin{array}{rccl} T_t: & L^1(\mathbb{Z}_p) & \longrightarrow & L^1(\mathbb{Z}_p), \\ & \phi(x) & \longmapsto & T_t\phi(x) := \int_{\mathbb{Z}_p} Z_0(x-y,t)\phi(y)dy, \end{array} \tag{4.5.2}$$

is a C^0-semigroup of contractions with generator $\boldsymbol{D}_0^{\alpha} - \lambda I$ on $L^1(\mathbb{Z}_p)$, see [32, Proposition 4, Proposition 5]

4.5.3 Reaction-diffusion CNNs

Definition 6. *Given $\mu \in \mathbb{R}$, $\alpha > 0$, $A(x)$, $B(x)$, $U(x)$, $Z(x) \in \mathcal{C}(\mathbb{Z}_p)$, a p-adic reaction-diffusion CNN, denoted as $CNN(\mu, \alpha, A, B, U, Z)$, is the dynamical system given by the following integro-differential equation:*

$$\frac{\partial X(x,t)}{\partial t} = \mu X(x,t) + (\lambda I - \boldsymbol{D}_0^{\alpha}) X(x,t) + \int_{\mathbb{Z}_p} A(x-y) f(X(y,t))dy \tag{4.5.3}$$
$$+ \int_{\mathbb{Z}_p} B(x-y)U(y)dy + Z(x),$$

where $x \in \mathbb{Z}_p$, $t \geq 0$. We say that $X(x,t) \in \mathbb{R}$ is the state of cell x at the time t. Function A is the kernel of the feedback operator, while function B is the kernel of the feedforward operator. Function U is the input of the CNN, while function Z is the threshold of the CNN.

Notice that if $\mu = 0$ and $A = B = U = Z = 0$, (4.5.3) becomes the p-adic heat equation in the unit ball. Then, in (4.5.3), $(\lambda I - \boldsymbol{D}_0^{\alpha})$ is the diffusion term, while the other terms are the reaction ones, which describe the interaction between $X(x,t)$, $U(x)$, and $Z(x)$.

Remark 12. *In this section, we assume that f is an arbitrary Lipschitz function, $f(0) = 0$, i.e., $|f(s) - f(t)| \leq L(f)\,|s-t|$, for s, $t \in \mathbb{R}$, where $L(f)$ is a positive constant.*

Lemma 9. *Let A, B, U, $Z \in \mathcal{C}(\mathbb{Z}_p)$.*

(i) Set

$$\boldsymbol{H}(g) := \int_{\mathbb{Z}_p} A(x-y) f\left(g(y)\right) dy + \int_{\mathbb{Z}_p} B(x-y) U(y) dy + Z(x), \tag{4.5.4}$$

for $g \in L^1(\mathbb{Z}_p)$. Then $\boldsymbol{H} : L^1(\mathbb{Z}_p) \to L^1(\mathbb{Z}_p)$ is a well-defined operator satisfying

$$\|\boldsymbol{H}(g) - \boldsymbol{H}(g')\|_1 \leq L(f)\|A\|_\infty \|g - g'\|_1, \text{ for } g,\ g' \in L^1(\mathbb{Z}_p).$$

(ii) The restriction of $\boldsymbol{H}$ to $\mathcal{C}(\mathbb{Z}_p)$ satisfies

$$\|\boldsymbol{H}(g) - \boldsymbol{H}(g')\|_\infty \leq L(f)\|A\|_1 \|g - g'\|_\infty, \text{ for } g,\ g' \in \boldsymbol{C}(\mathbb{Z}_p),$$

so $\boldsymbol{H} : \mathcal{C}(\mathbb{Z}_p) \to \mathcal{C}(\mathbb{Z}_p)$ is well-defined operator.

Proof. Take $g, g' \in L^1(\mathbb{Z}_p)$, then

$$\|\boldsymbol{H}(g) - \boldsymbol{H}(g')\|_1 = \|\int_{\mathbb{Z}_p} A(x-y) \left\{ f\left(g(y)\right) - f\left(g'(y)\right) \right\} dy\|_1$$

$$\leq \int_{\mathbb{Z}_p} \left\{ \int_{\mathbb{Z}_p} |A(x-y)| \quad |f\left(g(y)\right) - f\left(g'(y)\right)| \, dy \right\} dx \leq L(f)\|A\|_\infty \int_{\mathbb{Z}_p} |g(y) - g'(y)| \, dy$$

$$\leq L(f)\|A\|_\infty \|g - g'\|_1.$$

This inequality also proves that $\boldsymbol{H}$ is well-defined. The second part is established in a similar way. □

Proposition 3. *Let A, B, $U(x)$, $Z \in \mathcal{C}(\mathbb{Z}_p)$. Take $X_0(x) \in L^1(\mathbb{Z}_p)$ as the initial datum for the Cauchy problem attached to (4.5.3). Then there exists $\tau = \tau\left(X_0\right) \in (0, \infty]$ and a unique $X(t) \in \mathcal{C}([0,\tau], L^1(\mathbb{Z}_p))$ satisfying*

$$\begin{cases} X(t) = e^{\mu t} T_t X_0 + \int_0^t e^{\mu(t-s)} T_{t-s} \boldsymbol{H}(X(s)) ds \\ X(0) = X_0. \end{cases} \tag{4.5.5}$$

Proof. By [32, Proposition 4], $(\boldsymbol{D}_0^\alpha - \lambda I)$ is the generator of a strongly continuous semigroup $\{T_t\}_{t\geq 0}$ of contraction on $L^1(\mathbb{Z}_p)$. Then $(\boldsymbol{D}_0^\alpha - \lambda I) + \mu I$ is the generator of a strongly continuous semigroup $\{e^{\mu t} T_t\}_{t\geq 0}$ on $L^1(\mathbb{Z}_p)$, see [46, Theorem 4.3-(10)]. Since $\|e^{\mu t} T_t\| \leq e^{\mu t}$ and $\boldsymbol{H}$ is a Lipschitz nonlinearity, see Lemma 9-(i), there exits a unique mild solution $X(t) \in \mathcal{C}([0,\tau], L^1(\mathbb{Z}_p))$ satisfying (4.5.5), see, e.g., [46, Thorem 5.1.2]. □

Lemma 10. *Let A, B, U, $Z \in \mathcal{C}(\mathbb{Z}_p)$. Take $X_0 \in \mathcal{C}(\mathbb{Z}_p)$. Then, the integral equation (4.5.5) has unique solution $\mathcal{C}([0,\infty), \mathcal{C}(\mathbb{Z}_p))$.*

Proof. It is sufficient to show that (4.5.5) has a unique solution in $\mathcal{C}([0,T],\mathcal{C}(\mathbb{Z}_p))$, where $T>0$ is an arbitrary time horizon. Indeed, if $X_0(t)\in\mathcal{C}([0,T_0],\mathcal{C}(\mathbb{Z}_p))$ and $X_1(t)\in\mathcal{C}([0,T_1],\mathcal{C}(\mathbb{Z}_p))$, with $T_0\leq T_1$ are mild solutions, then $X_0(t)=X_1(t)$ for $t\in[0,T_1]$, see [46, Theorem 5.2.3].

We set $\mathcal{Y}:=\mathcal{C}([0,T],\mathcal{C}(\mathbb{Z}_p))$, which is a Banach space with norm

$$\sup_{0\leq t\leq T}\|Y(t)\|_\infty=\sup_{0\leq t\leq T}\left[\sup_{x\in\mathbb{Z}_p}|Y(x,t)|\right].$$

We now set

$$\boldsymbol{G}g(t):=e^{\mu t}T_tX_0+\int_0^t e^{\mu(t-s)}T_{t-s}\boldsymbol{H}\left(g(s)\right)ds,$$

for $g(t)\in\mathcal{C}([0,T],\mathcal{C}(\mathbb{Z}_p))$. By using that $Z_0(x,t)\in L^1(\mathbb{Z}_p)$, one gets $T_tg\in\mathcal{C}([0,T],\mathcal{C}(\mathbb{Z}_p))$, and by Lemma 9-(ii), $\boldsymbol{G}:\mathcal{Y}\rightarrow\mathcal{Y}$. We now set

$$\boldsymbol{G}^n=\underbrace{\boldsymbol{G}\circ\boldsymbol{G}\circ\cdots\circ\boldsymbol{G}}_{n-times}.$$

We show that for n sufficiently large $\boldsymbol{G}^n$ is a contraction. We first notice that

$$\|\boldsymbol{G}g(t)-\boldsymbol{G}g(t)\|_\infty\leq L(f)e^{\mu T}\|A\|_1\|g(t)-g'(t)\|_\infty.$$

By a well-known argument, see e.g. [46, Proof of Theorem 5.1.2], one gets that

$$\|\boldsymbol{G}^ng(t)-\boldsymbol{G}^ng(t)\|_\infty\leq\frac{(e^{\mu T}L(f)\|A\|_1T)^n}{n!}\|g(t)-g'(t)\|_\infty,$$

with $\frac{(e^{\mu T}L(f)\|A\|_1T)^n}{n!}<1$, for n sufficiently large. Therefore $\boldsymbol{G}$ has a unique fixed point $X(t)$ in $\mathcal{Y}$, see, e.g., [46, Theorem 1.1.3]. □

Theorem 14. *Let $X(t)\in\mathcal{C}([0,\infty),\mathcal{C}(\mathbb{Z}_p))$ be the unique solution of (4.5.5), with initial condition $X_0\in\mathcal{C}(\mathbb{Z}_p)$. Then,*

$$\|X(t)\|_\infty\leq e^{\mu t}\|X_0\|_\infty+\frac{(e^{\mu t}-1)}{\mu}\left(\|A\|_1\|f\|_\infty+\|B\|_1\|U\|_\infty+\|Z\|_\infty\right),\tag{4.5.6}$$

if $\mu\neq0$, otherwise

$$\|X(t)\|_\infty\leq\|X_0\|_\infty+\tau\left(\|A\|_1\|f\|_\infty+\|B\|_1\|U\|_\infty+\|Z\|_\infty\right).\tag{4.5.7}$$

Proof. By using that $\|B*U\|\leq\|B\|_1\|U\|_\infty$, cf. [62, Theorem 1.7], and Lemma 9-(ii), we get that

$$\|\boldsymbol{H}(g)\|_\infty\leq L(f)\|A\|_1\|g\|_\infty+\|B\|_1\|U\|_\infty+\|Z\|_\infty\text{ for }g,\in\boldsymbol{C}(\mathbb{Z}_p).$$

Now, the stated formula follows from (4.5.5), by Lemma 10, by using that $\|A\|_1\leq\|A\|_\infty$ and $\|B\|_1\leq\|B\|_\infty$. The bound (4.5.7) is established in a similar way. □

Figure 4.3: On the left side, the original image $X(x, 0)$. On the right side $X(x, 3)$.

4.6 Denoising

In this section, we present a new denoising technique based on certain reaction-diffusion CNNs. We first consider the initial value problem

$$\begin{cases} \frac{\partial X(x,t)}{\partial t} + \boldsymbol{D}_0^1 X(x,t) - \lambda X(x,t) = 0, & x \in \mathbb{Z}_p, \quad t > 0 \\ X(x,0) = X_0(x), & x \in \mathbb{Z}_p, \end{cases} \tag{4.6.1}$$

where $X_0(x) \in [0, 1]$ is a gray image codified as a test function supported in the unit ball $\mathbb{Z}_p$. The algorithm for this coding is discussed at the end of this section. The output image $X(x, t)$ is similar to the one produced by the classical Gaussian filter. See Figure 4.3.

We propose the following reaction-diffusion CNN for denoising gray images polluted with normal additive noise:

$$\frac{\partial X(x,t)}{\partial t} = 3X(x,t) + (\lambda I - \boldsymbol{D}_0^{\alpha})X(x,t) + 3B * [X_0(x) - f(X(x,t))], \tag{4.6.2}$$

where $\alpha = 0.75$, $f(x) = 0.5(|x + 1| - |x - 1|)$, $B(x) = (\Omega(p^2|x|_p) - \Omega(|x|_p))$, and $-1 \leq X_0(x) \leq 1$. Notice that we are using the interval $[-1, 1]$ as a gray scale. This equation was found experimentally. Natively, the reaction term $3X(x,t) + 3B * [X_0(x) - f(X(x,t))]$ gives an estimation of the edges of the image, while the diffusion term $(\lambda I - \boldsymbol{D}_0^{\alpha})X(x,t)$ produces a smoothed version of the image.

The processing of an image $X_0(x)$ using (4.4.1) requires solving the corresponding Cauchy problem with initial datum $X(x, 0) = X_0(x)$. Given an image I, i.e., a matrix of size (n, m), and a pixel (i, j) of I , for the processing this pixel we use a neighborhood $I_{i,j}$ centered at this pixel, which is sub-image $I_{i,j}$ of size of $\left(p^K, p^K\right)$, where p^{2K} is the number of pixels in the sub-image $I_{i,j}$. We use small primes, $p = 2, 3$ to get sub-images of size 2×2 and 3×3. The choosing of the prime p is completely determined by the image size, then, only small primes are required. Now, we codify the sub-image $I_{i,j}$ a test function $Tes(I_{i,j})$ and solve numerically the Cauchy problem attached to (4.4.1) with initial datum $Tes(I_{i,j})$. We pick a time t_0, on a case by case basis, and take the test function $X(x, t_0; I_{i,j})$ as the output of the network. At the final step, we transform $X(x, t_0; I_{i,j})$ into an image $I'_{i,j}$, and take the pixel processed image at (i, j) as the center of $I'_{i,j}$. See Figures 4.4, 4.5.

Figure 4.4: Left side, the original image. Right side, the image plus Gaussian noise, mean zero and variance 0.05.

4.7 Images and test functions

We show the existence of a bijective correspondence between images and test functions. We first show the existence of a bijective correspondence between finite disjoint unions of balls contained in $\mathbb{Z}_p$, for some prime p with weighted rooted trees of valence p. The connection between clustering, trees and ultrametric spaces is well-known, see e.g., [34, Chapter 2] and the references therein. Then we show the existence of a bijective correspondence between finite, regular rooted trees of valence p with images.

4.7.1 Finite rooted trees and test functions

By a *finite rooted tree* $\mathcal{T}$, we mean a finite undirected graph in which any two vertices are connected by exactly one path. The vertices $V(\mathcal{T})$ of $\mathcal{T}$ are organized in disjoint *levels*:

$$V(\mathcal{T}) = \bigsqcup_{j=0}^{M} Level_j\,(\mathcal{T})\,,$$

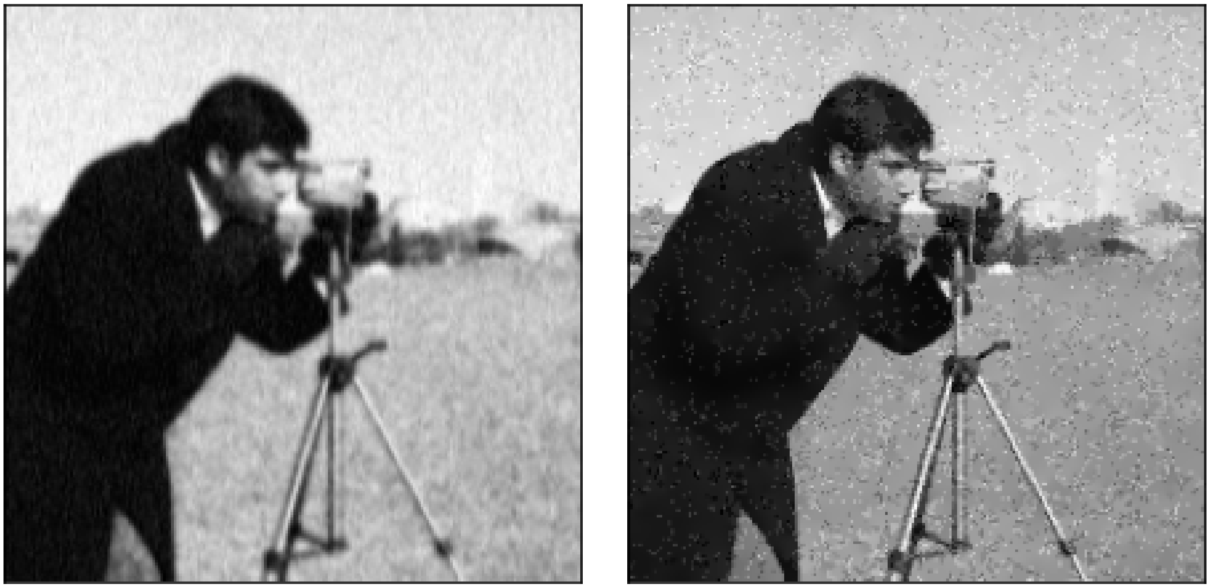

Figure 4.5: Left side, filtered image using Equation 4.6.2. Right side, filtered image obtained by using Perona-Malik equation with $\lambda = 0.04$, $\delta_t = 0.075$, and $t = 100$ iterations, and $g_1(s)$, Section B.2.

where $Level_j(\mathcal{T}) := Level_j = \{v_{j,0}, v_{j,1}, \ldots, v_{j,k_j}\}$, $k_j \geq 1$, are the vertices of $\mathcal{T}$ at level j. At level 0 there is exactly one vertex v_0, *the root of the tree*. The vertices at the level 1 are the *descendants* of the root, which means that there is path $v_0 \to v_{1,i}$ for any vertex $v_{1,i} \in Level_1$. Inductively, the vertices at level j, $1 \leq j \leq M$, are the the descendants of the vertices at level $j-1$. The vertices at level M do not have descendants.

We denote by $\gamma(v)$, $v \in V(\mathcal{T})$, the number of edges emanating from v. We set

$$\gamma_{\mathcal{T}} := \max_{v \in V(\mathcal{T})} \{\gamma(v)\}.$$

We fix a prime number defined as $p_{\mathcal{T}} := \min_p \{p \text{ prime};\ \gamma_{\mathcal{T}} \leq p\}$. For the sake of simplicity we use $p := p_{\mathcal{T}}$. Given any vertex $v_{j,i_j} \in Level_j$, $1 \leq j \leq M$, there is exactly one path connecting v_{j,i_j} with v_0:

$$v_0 \to v_{1,i_1} \to \ldots \to v_{j-1,i_{j-1}} \to v_{j,i_j}. \tag{4.7.1}$$

We attach to v_{j,i_j} the p-adic integer

$$I_{v_{j,i_j}} := i_1 + i_2 p + \ldots + i_{j-1} p^{j-2} + i_j p^{j-1}, \tag{4.7.2}$$

where the digits i_k belong to $\{0, 1, \ldots, p-1\}$. Then, there is a bijection between the vertices of $\mathcal{T}$ and the p-adic integers of form (4.7.2). Given a vertex v at level L_v denote the corresponding p-adic number as

$$I_v = i_1 + i_2 p + \ldots + i_{L_v - 1} p^{L_v - 1}, \ \ L_v \leq M. \tag{4.7.3}$$

Now we attach to $\mathcal{T}$ the following family of balls:

$$B(\mathcal{T}) := \left\{ I_v + p^{L_v}\mathbb{Z}_p,\, v \in V(\mathcal{T}) \smallsetminus \{v_0\} \right\} \bigsqcup \left\{ \mathbb{Z}_p \right\},$$

where the unit ball $\mathbb{Z}_p$ correspond to the case $v = v_0$. The tree $\mathcal{T}$ and the collection of balls $B(\mathcal{T})$ are equivalent data. Indeed, given a finite collection B of balls contained in $\mathbb{Z}_p$ such that $\mathbb{Z}_p \in B$, there is a finite rooted tree $\mathcal{T}$ that represents the partial order induced by $\subseteq$ in B.

We say that a vertex v is a leaf of $\mathcal{T}$ if v does not have descendants. In particular, all the vertices in $Level_M$ are leaves. We denote by $Leaf(\mathcal{T})$ the set of all leaves of $\mathcal{T}$. Finally, we attach to $\mathcal{T}$ the open compact subset

$$\mathcal{K}(\mathcal{T}) = \bigsqcup_{v \in Leaf(\mathcal{T})} \left(I_v + p^{L_v}\mathbb{Z}_p \right). \tag{4.7.4}$$

Now, given a finite disjoint union of balls of the form $\bigsqcup_{v \in \mathcal{G}} \left(I_v + p^{L_v}\mathbb{Z}_p \right)$, there is a unique tree $\mathcal{T}$ having $\{I_v; v \in \mathcal{G}\}$ as a set of leaves. The other vertices correspond to truncations of the numbers I_vs. And given a tree $\mathcal{T}$, (4.7.4) attaches a unique finite disjoint union of balls to $\mathcal{T}$.

We define a *weighted tree* as a pair $(\mathcal{T}, w)$, where $w : Leaf(\mathcal{T}) \to \mathbb{R}_+ := \{x \in \mathbb{R}; x \geq 0\}$. We denote by $\Omega\left(p^{L_v}\left|x - I_v\right|_p\right)$ the characteristic function of the ball $\left(I_v + p^{L_v}\mathbb{Z}_p\right)$. Given a test function from $\mathcal{D}_{L_v}(\mathbb{Z}_p)$ of the form

$$\Phi\left(x\right) = \sum_{v \in \mathcal{G}} c_v \Omega\left(p^{L_v}\left|x - I_v\right|_p\right), \quad x \in \mathbb{Z}_p, \tag{4.7.5}$$

we attach to it the unique weighted tree with leaves $\{I_v; v \in \mathcal{G}\}$ and weights $v \to c_v$, for $v \in \mathcal{G}$. Conversely, given a weighted tree $(\mathcal{T}, w)$, with leaves $\mathcal{G} = \{I_v; v \in Leaf(\mathcal{T})\}$, and $w(v) = c_v$ for $v \in \mathcal{G}$, (4.7.5) defines a unique test function $\Phi\left(x\right)$ from $\mathcal{D}_{L_v}(\mathbb{Z}_p)$.

4.7.2 Images and finite rooted trees

We propose an algorithm for coding an image as a finite, weighted, regular, rooted tree of valence p, where p a prime number. The input is an image I, a (n, m) matrix, and a prime number p satisfying $p \leq m, n$. The output is a finite, weighted, regular tree $Tree(I)$. We use two functions. The function d_H divides an image into p horizontal sub-images, and the function d_V divides an image into p vertical sub-images. The tree has at most $L := \lfloor \log_p(nm) \rfloor$ levels. The level zero contains just the root of the tree. Each vertex of the tree corresponds to a sub-image I' of I, and the descendants of this vertex, in the next level, are sub-images of I' obtained by using the function d_H or d_V.

1. The tree $Tree(I)$ corresponding to an image I is construct recursively as follows:
2. Level 0: there is one vertex, the root of the tree which corresponds to I.
3. Level $2l + 1$: the descendants of a vertex I' at the level $2l$ correspond to the elements of $d_H(I')$.

4. Level $2l$: the descendants of a vertex I' at the level $2l-1$ correspond to the elements of $d_V(I')$.
5. Level L: all the vertices (leaves) at the level L are pixels. The gray intensity of each pixel gives a the weight of the corresponding leaf.

We now define the operator d_V. Let m_0, r_0 nonnegative integers such that $m = pm_0 + r_0$. If $m_0 \neq 0$, we define

$$I_s = [I_{i,j}]_{\substack{0\le i<n \\ sm_0\le j\le m_0(s+1)}} \quad \text{for } s = 0,\dots,r_0,$$
$$I_s = [I_{i,j}]_{\substack{0\le i<n \\ m_0 s+r_0\le j<m_0 s}} \quad \text{for } s = r_0+1,\dots,p-1,$$

and

$$d_V(I) = [I_s]_{s=0,\dots,p-1}.$$

If $m_0 = 0$, we define

$$I_s = [I_{i,j}]_{\substack{0\le i<n \\ j=s}} \text{ for } s = 0,\dots,r_0, \text{ and } d_V(I) = [I_s]_{s=0,\dots,p-1}.$$

Thus the operator d_V divides the image I into p vertical sub-images.

We now define operators d_H. Let n_0, q_0 be non-negative integers satisfying $n = (p-1)n_0 + q_0$. If $n_0 \neq 0$. We define

$$I_s = [I_{i,j}]_{\substack{sn_0\le i\le n_0(s+1) \\ 0\le j<m}} \quad \text{for } s = 0,\dots,q_0,$$
$$I_s = [I_{i,j}]_{\substack{n_0 s+q_0\le i<n_0 s \\ 0\le j<m}} \quad \text{for } s = q_0+1,\dots,p-1,$$

and

$$d_H(I) = [I_s]_{s=0,\dots,p-1}.$$

If $n_0 = 0$, we define

$$I_s = (I_{i,j})_{i=s;0\le j<m} \text{ for } s = 0,\dots,q_0, \text{ and } d_H(I) = [I_s]_{s=0,\dots,p-1}.$$

Thus the operator d_H divides the image I into p horizontal sub-images.

Consequently, the correspondence between images and weighted, finite, regular, rooted trees of valence p, is a bijection. Figure 4.6 shows the correspondence between images and test functions.

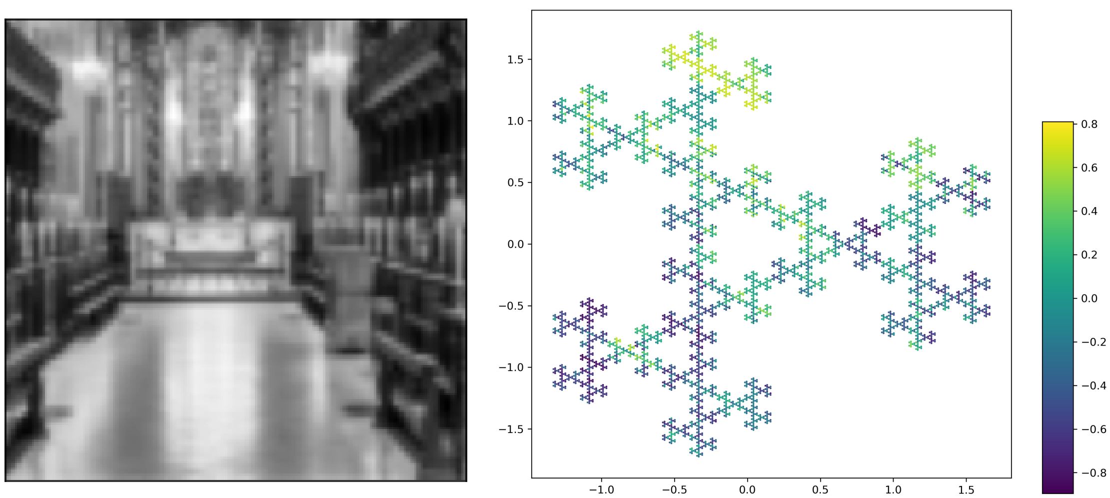

Figure 4.6: Left side, original image 81×81. Right side, the representation of the image as a test function. We use $p = 3$, $L = 8$.

Chapter 5

Conclusions

In this thesis, we presented a mathematical generalization of the CNNs of Chua and Yang called *p-adic cellular neural networks*. The p-adic continuous CNNs offered a theoretical framework to study the emergent patterns of hierarchical discrete CNNs having arbitrary many hidden layers.

A p-adic Cellular Neural Network is

$$\frac{\partial X(x,t)}{\partial t} = -X(x,t) + \int_{\mathbb{Q}_p} A(|x-y|_p) Y(y,t) dy + \int_{\mathbb{Q}_p} B(|x-y|_p) U(y) dy + Z(x), \qquad (5.0.1)$$

with $Y(x,t) = f(X(x,t))$. We studied the case where $A(|x|_p)$, $B(|x|_p)$ are integrable, and U, Z are continuous functions vanishing at infinity. Under these hypotheses the initial value problem attached to (5.0.1), with initial datum X_0 (a continuous function vanishing at infinity) has a unique solution $X(x,t)$ which is a continuous function vanishing at infinity in x for any $t \geq 0$, satisfying $|X(x,t)| \leq X_{\max}$, where the constant $X_{\max}$ is completely determined by A, B, U, Z and f. We also presented a large number of numerical simulations. Such simulations required solving integro-differential equations on a tree.

We also showed that p-adic CNNs can process real gray images, and that the dynamics can be understood almost completely. We presented two types of p-adic CNNs, one type for edge detection of gray images, and the other, for denoising of gray images polluted with Gaussian noise. The performance of this edge detector is comparable to the Canny detector. But most importantly, we can explain, reasonably well, how the network detects the edges of an image. On the other hand, although the image denoising performance is not as good as the results obtained using the Perona-Malik equation, the mathematical analysis of the network presented is more feasible than the mathematical analysis in the case of Perona-Malik.

This thesis open a path for different applications of p-adic Cellular Neural Networks or more general Neural Networks.

There are some paths to continue this work. One is to use fuzzy operators in p-adic CNN, which combines images' low and high-level information. This line of research is connected with the morphological operators in image processing. Another is to study p-adic versions of the Perona-Malik Equation. More generally, anisotropic p-adic diffusion equation. These approximations can present betters results for denoising in image processing and new mathematical challenges.

Appendix A

Cellular Neural Networks

Cellular neural network (CNN) was introduced by Leon O. Chua and Linc Yang in [20] as a new circuit architecture. This CNN presents some of the critical features of neural networks and has some significant potential applications in such areas as *image processing*, *patter recognition*, and *partial differential equations*, among others.
The primary circuit unit is called a cell, where any cell is connected only to its neighbor cells. The adjacent cells can interact directly with each other. However, cells not directly connected may indirectly affect each other because of the continuous time dynamics' propagation effect. For an in-depth review cellular neural network, the reader may consult [18, 20, 59], and the references therein.

The following section is taking directly from [61].

A.1 General Cellular Neural Network

We introduce 1-dimensional cellular neural networks (1D-CNN). A 1D-CNN cell will be denoted by $\mathfrak{C}_i$, where $i \in \{1, 2, \dots, N\}$. Each cell in the 1D-CNN architecture is a dynamic system and is locally coupled only to the neighboring cells that lie inside $S_i(r)$, sphere of influence, of radio r.

$$S_i(r) := \{\mathfrak{C}_k : \max(|i-k|) \leq r,\ 1 \leq k \leq N\}. \tag{A.1.1}$$

The cell dynamics are defined by the state equation

$$\begin{cases} \dot{X}_i = g(X_i, Z_i, U_i(t), I_i^s) \\ Y_I = f(X_i) \end{cases} \tag{A.1.2}$$

with **State vector** $X_i \in \mathbb{R}^{m_x}$, **Output vector** $Y_i \in \mathbb{R}^{m_y}$, **threshold** $Z_i \in \mathbb{R}^{m_z}$, and **Input vector** $U_i \in \mathbb{R}^{m_u}$ of the i-th cell $\mathfrak{C}_i$.

- $I_i^s \in \mathbb{R}^{m_I}$ is a **Synaptic law** of the cell $\mathfrak{C}_i$.
- $f : \mathbb{R}^{m_x} \to \mathbb{R}^{m_y}$ is a nonlinear output function.

- $g : \mathbb{R}^{m_x} \times \mathbb{R}^{m_z} \times \mathbb{R}^{m_y} \times \mathbb{R}^{m_I} \to \mathbb{R}^{m_x}$.

The synaptic law defines the coupling between the considered cell $\mathfrak{C}_i$ and all the cells within the sphere of influence $S_i(r)$.

$$\begin{aligned} I_i^s := \sum_{k \in S_i(r)} \Big[& \hat{A}_{i,k} X_k(t) + A_{i,k} Y_k(t) + B_{i,k} U_k(t) + A_{i,k}^{\tau} Y_k(t-\tau) \\ & + B_{i,k}^{\tau} U_k(t-\tau) + A_{i,k}^{n}(Y_i, Y_k) + B_{i,k}^{n}(U_i, U_k) + C_{i,k}^{n}(X_i, X_k) \Big] \end{aligned} \tag{A.1.3}$$

The synaptic law is uniquely specify by synaptic matrices $\hat{A}_{i,k} \in \mathbb{R}^{m_I \times m_X}$, $A_{i,k} \in \mathbb{R}^{m_I \times m_y}$, $B_{i,k} \in \mathbb{R}^{m_I \times m_u}$, $A_{i,k}^{\tau} \in \mathbb{R}^{m_I \times m_y}$, $B_{i,k}^{\tau} \in \mathbb{R}^{m_I \times m_u}$ and nonlinear functions

$$\begin{aligned} A_{i,k}^{n} &: \mathbb{R}^{m_y} \times \mathbb{R}^{m_y} \to \mathbb{R}^{m_I} \\ B_{i,k}^{n} &: \mathbb{R}^{m_u} \times \mathbb{R}^{m_u} \to \mathbb{R}^{m_I} \\ C_{i,k}^{n} &: \mathbb{R}^{m_x} \times \mathbb{R}^{m_x} \to \mathbb{R}^{m_I}. \end{aligned}$$

It is usually listed these matrices as entries of the following matrices:

- **State template** $\hat{A} := (\hat{A}_{i,k})$.
- **Feedback template** $A := (A_{i,k})$.
- **Feedforward template** $B = (B_{i,k})$.
- **Delay-type feedback template** $A^{\tau} = (A_{i,k}^{\tau})$.
- **Delay-type feedforward template** $B^{\tau} = (B_{i,k}^{\tau})$.
- **Nonlinear feedback template** $A^n(Y_i, Y_k) = \big(A_{i,k}^n(Y_i, Y_k)\big)$.
- **Nonlinear feedforward template** $B^n(U_i, U_k) = \big(B_{i,k}^n(U_i, U_k)\big)$.
- **Nonlinear state template** $C^n(X_i, X_k) = \big(C_{i,k}^n(X_i, X_k)\big)$.

The superscripts τ and n of a template indicate that the template is a delay-type and nonlinear type. In general, an n-dimensional cellular neural network (nD-CNN) is defined the same way as 1D- CNN, but we put $i \in N_1 \times \ldots \times N_n$ on the State equation and Synaptic equation.

A.2 Chua-Yang CNN model

The cell dynamics of the Chua-Yang CNN model, see [20], is governed by the following 2-dimensional state equation

$$\begin{aligned} C\dot{x}_{ij} &= -a x_{ij} + z + I_{ij}^s \\ y_{ij} &= f(x_{ij}) = 1/2(|x_{ij} - 1| - |x_{ij} + 1|) \\ I_{ij}^s &= \sum_{(k,l) \in S_{ij}(r)} a_{ij,kl} y_{kl} + b_{ij,kl} u_{kl} \end{aligned} \tag{A.2.1}$$

with the following constraint conditions:

- $u_{ij}(t)$ are contestants on time.
- $|x_{ij}(0)|, |u_{ij}| \leq 1$.
- $a > 0$.

We gather some results of Chua-Yang CNN presented in [20].

Theorem 15. *[20, Theorem 1] All states x_{ij} in a CNN A.2.1 are bounded for all time $t > 0$ and the bound x_{max} can be computed by the following formula for any CNN*

$$x_{max} = 1 + (1/a)z_{max} + (1/a) \max_{1 \leq i \leq N_1,\, 1 \leq j \leq N_2} \left(\sum_{(k,l) \in S_{(i,j)}(r)} (|a_{ij,kl}| + |b_{ij,kl}|) \right) \tag{A.2.2}$$

Proposition 4. *[20, Corollary 1] After the transient of a CNN A.2.1 has decayed to zero, we always obtain a constant output, e.i.*

$$\lim_{t \to \infty} y_{ij}(t) = constant.$$

Theorem 16. *[20, Theorem 5] If the circuit parameters satisfy*

$$a_{ij,kl} > a$$

then each cell of a CNN most settle at a stable equilibrium point after the transient has decayed to zero ($t \to \infty$). Moreover, the magnitude of all stable equilibrium point is greater than 1. In other words, we have the following properties:

$$\lim_{t \to \infty} |x_{ij}(t)| > 1$$

and

$$\lim_{t \to \infty} y_{ij}(t) = \pm 1.$$

Appendix B

Image processing

Following [13] a image is a function that maps every point in some domain of definition to a certain color values. An gray image u is a map from an image domain Ω to some color space F: $u : \Omega \to F$. where $F \subseteq \mathbb{R}$. One can distinguish between discrete and continuous image domains:

- discrete gray d-dimensional images, for example $\Omega = \{1, \dots, N_1\} \times \cdots \times \{1, \dots, N_d\}$.
- continuous gray d-dimensional images, for example $\Omega \subseteq \mathbb{R}^d$ (domain), or specifically $\Omega = [0, a_1] \times \cdots \times [0, a_d]$.

When partial differential equations are applied, continuous 2-dimensional gray images are used as a theoretical object in image processing. But, discrete 2-dimensional gray images, which are $N_1 \times N_2$ matrices, are the best representations of the (real) images we want to process.

B.1 Canny Edge detector

We follow section is taken from [68].

The edge is the most basic feature of an image, which refers to the set of pixels that have a sudden change in the gray level. Edge detection is a basic method to recognize and segment the edges of images based on gray discontinuous points. The Canny operator is a multiply-scale edge detection algorithm proposed by John F.Canny in 1986, the goal is to find an optimal edge detection algorithm, which is widely used in the field of image processing, and are constantly improved and innovated.

Using Canny edge detection, there are usually several steps:

1. Denoise image vefore detecting edge of the image, and usually use the Gauss smoothing filter to reduce noise, according to

$$G(x, y) = \frac{1}{2\pi\sigma^2} e^{\frac{x^2+y^2}{2\sigma^2}} \tag{B.1.1}$$

2. Calculate the gradient amplitude and direction, usually the gradient direction takes the four angles, according to

$$G = \sqrt{G_x^2 + G_y^2} \tag{B.1.2}$$

$$\theta = \arctan\left(\frac{G_y}{G_x}\right) \tag{B.1.3}$$

where G_x and G_y are the first derivative (as neighbor of a pixel) in the horizontal direction and the vertical direction, respectively, e.i., $G_x = [1/2\ 0\ \ -1/2]G$ and $G_y = [1/2\ 0\ \ -1/2]^T G$.

3. Non maximum suppression, which eliminates non edge pixels, leaving only a few fine lines. For this, at every pixel, pixel is checked if it is a local maximum in its neighborhood in the direction of gradient.

4. Select the hysteresis threshold, hysteresis threshold needs two threshold which retain or exclude pixels to select the edge.

If the amplitude of the pixel position if higher than the high threshold, the pixel is reserved as an edge pixel.

If the amplitude of the pixel position is less than the high threshold, the pixel is exclude.

If the amplitude of the pixel position is between the two threshold, the pixel is reserved only when connected to a pixel higher than high threshold.[1]

B.2 Perona-Malik Equation

We follow [13, 66] to write this section.

The idea of Perona and Malik [50] was to slow down diffution at edges, where edges can be describe as points where the gradient has a large magnitude. They apply an inhomogeneous process that reduces the diffusivity at those locations which have a large likehood to be edges. This likehood is measured by $| \bigtriangledown u|^2$. The Perona-Malik is based on the equation

$$\partial_t u = div(g(| \bigtriangledown u|^2) \bigtriangledown u) \tag{B.2.1}$$

where it is usual to take

$$g_1(s) = \frac{1}{1 + \frac{s^2}{\lambda^2}}, \quad g_2(s) = e^{-\frac{s^2}{2\lambda^2}}, \tag{B.2.2}$$

the parameter λ says how fast the function tends to zero. One problem when $g(s)$ is be taken as $g_i(s)$ is that Equation B.2.1 is not always a well-posedness process for some initial conditions, e.g., see [36].

[1] https://docs.opencv.org/4.x/da/d22/tutorial_py_canny.html

Bibliography

[1] S. Albeverio, A. Khrennikov, and B. Tirozzi, *p-adic dynamical systems and neural networks*, Mathematical models and methods in applied sciences, 9 (1999), pp. 1417–1437.

[2] S. Albeverio, A. Y. Khrennikov, and V. M. Shelkovich, *Theory of p-adic distributions: linear and nonlinear models*, no. 370, Cambridge University Press, 2010.

[3] L. Alvarez, F. Guichard, P.-L. Lions, and J.-M. Morel, *Axioms and fundamental equations of image processing*, Archive for rational mechanics and analysis, 123 (1993), pp. 199–257.

[4] P. Arena, S. Baglio, L. Fortuna, and G. Manganaro, *Chua's circuit can be generated by cnn cells*, IEEE Transactions on Circuits and Systems I: Fundamental Theory and Applications, 42 (1995), pp. 123–125.

[5] P. Arena, S. Baglio, L. Fortuna, and G. Manganaro, *Dynamics of state controlled cnns*, in 1996 IEEE International Symposium on Circuits and Systems. Circuits and Systems Connecting the World. ISCAS 96, vol. 3, IEEE, 1996, pp. 56–59.

[6] P. Arena, S. Baglio, L. Fortuna, and G. Manganaro, *Generation of n-double scrolls via cellular neural networks*, International Journal of circuit theory and applications, 24 (1996), pp. 241–252.

[7] V. Avetisov, A. Bikulov, S. Kozyrev, and V. A. Osipov, *p-adic models of ultrametric diffusion constrained by hierarchical energy landscapes*, Journal of Physics A: Mathematical and General, 35 (2002), p. 177.

[8] V. Avetisov, A. K. Bikulov, and V. Al Osipov, *p-adic description of characteristic relaxation in complex systems*, Journal of Physics A: Mathematical and General, 36 (2003), p. 4239.

[9] O. M. Becker and M. Karplus, *The topology of multidimensional potential energy surfaces: Theory and application to peptide structure and kinetics*, The Journal of chemical physics, 106 (1997), pp. 1495–1517.

[10] J. Benois-Pineau and A. Khrennikov, *Significance delta reasoning with p-adic neural networks: application to shot change detection in video*, The Computer Journal, 53 (2010), pp. 417–431.

[11] J. Benois-Pineau, A. Khrennikov, and N. Kotovich, *Segmentation of images in p-Adic and Euclidean Metrics*, Doklady Mathematics, 64 (2001), pp. 450–455.

[12] M. Bocardo-Gaspar, H. García-Compeán, and W. Zúñiga-Galindo, *Regularization of p-adic string amplitudes, and multivariate local zeta functions*, Letters in Mathematical Physics, 109 (2019), pp. 1167–1204.

[13] K. Bredies, D. Lorenz, et al., *Mathematical Image Processing*, Springer, 2018.

[14] ——, *Mathematical Image Processing*, Springer, 2018.

[15] T. Cazenave and A. Haraux, *An introduction to semilinear evolution equations*, vol. 13, Oxford University Press on Demand, 1998.

[16] D. Chistyakov, *Fractal geometry for images of continuous embeddings of p-adic numbers and solenoids into euclidean spaces*, Theoretical and Mathematical Physics, 109 (1996), pp. 1495–1507.

[17] L. O. Chua, *CNN: A paradigm for complexity*, vol. 31, World Scientific, 1998.

[18] L. O. Chua and T. Roska, *Cellular neural networks and visual computing: foundations and applications*, Cambridge university press, 2002.

[19] L. O. Chua and L. Yang, *Cellular neural networks: Applications*, IEEE Transactions on circuits and systems, 35 (1988), pp. 1273–1290.

[20] ——, *Cellular neural networks: Theory*, IEEE Transactions on circuits and systems, 35 (1988), pp. 1257–1272.

[21] B. Dragovich, A. Y. Khrennikov, S. V. Kozyrev, and I. V. Volovich, *On p-adic mathematical physics*, P-Adic Numbers, Ultrametric Analysis, and Applications, 1 (2009), pp. 1–17.

[22] S. Espejo, R. Carmona, R. Domínguez-Castro, and A. Rodríguez-Vázquez, *A vlsi-oriented continuous-time cnn model*, International Journal of Circuit Theory and Applications, 24 (1996), pp. 341–356.

[23] C. W. S. Frauenfelder H, Chan S. S., *The physics of proteins*, (2010).

[24] L. Goras and L. O. Chua, *Turing patterns in cnns. ii. equations and behaviors*, IEEE Transactions on Circuits and Systems I: Fundamental Theory and Applications, 42 (1995), pp. 612–626.

[25] L. GoraS, L. O. Chua, and D. Leenaerts, *Turing patterns in cnns. i. once over lightly*, IEEE Transactions on Circuits and Systems I: Fundamental Theory and Applications, 42 (1995), pp. 602–611.

[26] L. Goras, L. O. Chua, and L. Pivka, *Turing patterns in cnns. iii. computer simulation results*, IEEE Transactions on Circuits and Systems I: Fundamental Theory and Applications, 42 (1995), pp. 627–637.

[27] C. Guzelis and L. O. Chua, *Stability analysis of generalized cellular neural networks*, International Journal of Circuit Theory and Applications, 21 (1993), pp. 1–33.

[28] P. R. Halmos, *Measure Theory*, D. Van Nostrand Company, Inc., New York, N. Y., 1950.

[29] H. Hua and L. Hovestadt, *p-adic numbers encode complex networks*, Scientific Reports, 11 (2021), pp. 1–11.

[30] J.-i. Igusa, *An introduction to the theory of local zeta functions*, vol. 14 of AMS/IP Studies in Advanced Mathematics, American Mathematical Society, Providence, RI; International Press, Cambridge, MA, 2000.

[31] A. Y. Khrennikov, *Information dynamics in cognitive, psychological, social, and anomalous phenomena*, vol. 138, Springer Science & Business Media, 2013.

[32] A. Y. Khrennikov and A. N. Kochubei, *p-adic analogue of the porous medium equation*, Journal of Fourier Analysis and Applications, 24 (2018), pp. 1401–1424.

[33] A. Y. Khrennikov, N. Kotovich, and E. Borzistaya, *Compression of images with the aid of representation by p-adic maps and approximation by mahler's polynomials*, in Dokl. Akad. Nauk, vol. 396, 2004, pp. 305–308.

[34] A. Y. Khrennikov, S. V. Kozyrev, and W. A. Zúñiga-Galindo, *Ultrametric pseudodifferential equations and applications*, vol. 168, Cambridge University Press, 2018.

[35] A. Y. Khrennikov and B. Tirozzi, *Learning of p-adic neural networks*, Can. Math. Soc. Proc. Ser, 29 (2000), pp. 395–401.

[36] S. Kichenassamy, *The perona–malik paradox*, SIAM Journal on Applied Mathematics, 57 (1997), pp. 1328–1342.

[37] N. Koblitz, *p-adic Numbers, p-adic Analysis, and Zeta-Functions*, vol. 58, Springer Science & Business Media, 2012.

[38] A. N. Kochubei, *Pseudo-differential equations and stochastics over non-Archimedean fields*, CRC Press, 2001.

[39] ——, *Linear and nonlinear heat equations on p-adic ball*, Ukrainian Mathematical Journal, 70 (2018), pp. 217,231.

[40] N. Kotovich and A. Y. Khrennikov, *Representation and compression of images with the aid of m-adic coordinate systems*, in Doklady. Mathematics, vol. 66, 2002, pp. 330–334.

[41] S. Kozyrev, *Methods and applications of ultrametric and p-adic analysis: From wavelet theory to biophysics*, Proceedings of the Steklov Institute of Mathematics, 274 (2011), pp. 1–84.

[42] M. Lakra and S. Kumar, *Solving a generalized order improved diffusion equation of image denoising using a cenn-based scheme*, Multimedia Tools and Applications, (2022), pp. 1–28.

[43] E. León-Cardenal and W. Zúñiga-Galindo, *An introduction to the theory of local zeta functions from scratch*, Revista Integración, 37 (2019), pp. 45–76.

[44] P. H. Long and P. T. Cat, *Real-time image processing by cellular neural network using reaction-diffusion model*, in 2009 International Conference on Knowledge and Systems Engineering, IEEE, 2009, pp. 93–99.

[45] A. McAndrew, *An introduction to digital image processing with matlab notes for scm2511 image processing 1 semester 1, 2004*, (2004).

[46] M. Miklavčič, *Applied functional analysis and partial differential equations*, Allied Publishers, 1998.

[47] H. Nakao and A. S. Mikhailov, *Turing patterns in network-organized activator–inhibitor systems*, Nature Physics, 6 (2010), pp. 544–550.

[48] A. Nomura, M. Ichikawa, K. Okada, H. Miike, and T. Sakurai, *Edge detection algorithm inspired by pattern formation processes of reaction-diffusion systems*, International Journal of Circuits, Systems and Signal Processing, 5 (2011), pp. 105–115.

[49] M. A. Nowak, *Evolutionary dynamics: exploring the equations of life*, Harvard university press, 2006.

[50] P. Perona, T. Shiota, and J. Malik, *Anisotropic diffusion*, in Geometry-driven diffusion in computer vision, Springer, 1994, pp. 73–92.

[51] C. B. Price, P. Wambacq, and A. Oosterlinck, *Applications of reaction-diffusion equations to image processing*, in Third International Conference on Image Processing and its Applications, 1989., IET, 1989, pp. 49–53.

[52] R. Rammal, G. Toulouse, and M. A. Virasoro, *Ultrametricity for physicists*, Reviews of Modern Physics, 58 (1986), p. 765.

[53] M. Reuter, S. Biasotti, D. Giorgi, G. Patanè, and M. Spagnuolo, *Discrete laplace–beltrami operators for shape analysis and segmentation*, Computers & Graphics, 33 (2009), pp. 381–390.

[54] T. Roska and L. O. Chua, *Cellular neural networks with non-linear and delay-type template elements and non-uniform grids*, International Journal of Circuit Theory and Applications, 20 (1992), pp. 469–481.

[55] T. Roska, L. O. Chua, D. Wolf, T. Kozek, R. Tetzlaff, and F. Puffer, *Simulating nonlinear waves and partial differential equations via cnn. i. basic techniques*, IEEE Transactions on Circuits and Systems I: Fundamental Theory and Applications, 42 (1995), pp. 807–815.

[56] L. Ruthotto and E. Haber, *Deep neural networks motivated by partial differential equations*, Journal of Mathematical Imaging and Vision, 62 (2020), pp. 352–364.

[57] G. Sapiro, *Geometric partial differential equations and image analysis, cambridgeuniv*, Press, Cambridge, UK, (2001).

[58] G. Sapiro, *Geometric partial differential equations and image analysis*, Cambridge university press, 2006.

[59] A. Slavova, *Cellular neural networks: dynamics and modelling*, vol. 16, Springer Science & Business Media, 2003.

[60] I. M. Stamova and S. Simeonov, *Delayed reaction–diffusion cellular neural networks of fractional order: Mittag–leffler stability and synchronization*, Journal of Computational and Nonlinear Dynamics, 13 (2018), p. 011015.

[61] J. A. Suykens, J. Vandewalle, et al., *Cellular neural networks, multi-scroll chaos and synchronization*, vol. 50, World scientific, 2005.

[62] M. H. Taibleson, *Fourier Analysis on Local Fields.(MN-15)*, Princeton University Press, 2015.

[63] A. Torresblanca-Badillo and W. Zúñiga-Galindo, *Ultrametric diffusion, exponential landscapes, and the first passage time problem*, Acta Applicandae Mathematicae, 157 (2018), pp. 93–116.

[64] V. S. Vladimirov, I. V. Volovich, and E. I. Zelenov, *p-adic Analysis and Mathematical Physics*, World Scientific, 1994.

[65] W. Wang, *Finite-time synchronization for a class of fuzzy cellular neural networks with time-varying coefficients and proportional delays*, Fuzzy Sets and Systems, 338 (2018), pp. 40–49.

[66] J. Weickert et al., *Anisotropic diffusion in image processing*, vol. 1, Teubner Stuttgart, 1998.

[67] J. WU, *Theory and applications of partial functional differential equations*, Appl. Math. Sci., 119 (1996).

[68] Z. Xu, X. Baojie, and W. Guoxin, *Canny edge detection based on open cv*, in 2017 13th IEEE international conference on electronic measurement & instruments (ICEMI), IEEE, 2017, pp. 53–56.

[69] T. Yang, L.-B. Yang, C. W. Wu, and L. O. Chua, *Fuzzy cellular neural networks: theory*, in 1996 Fourth IEEE International Workshop on Cellular Neural Networks and Their Applications Proceedings (CNNA-96), IEEE, 1996, pp. 181–186.

[70] B. Zambrano-Luna and W. A. Zuniga-Galindo, *p-adic cellular neural networks*, Journal of Nonlinear Mathematical Physics, (2022), pp. 1–37.

[71] B. A. Zambrano-Luna and W. A. Zúñiga-Galindo, *p-adic cellular neural networks: Applications to image processing*, arXiv preprint arXiv:2210.14132, (2022).

[72] W. Zúñiga-Galindo, *Non-archimedean reaction-ultradiffusion equations and complex hierarchic systems*, Nonlinearity, 31 (2018), p. 2590.

[73] ——, *Non-archimedean replicator dynamics and eigen's paradox*, Journal of Physics A: Mathematical and Theoretical, 51 (2018), p. 505601.

[74] ——, *Reaction-diffusion equations on complex networks and turing patterns, via p-adic analysis*, Journal of Mathematical Analysis and Applications, 491 (2020), p. 124239.

[75] W. A. Zúñiga-Galindo, *Pseudodifferential equations over non-Archimedean spaces*, vol. 2174, Springer, 2016.

[76] W. A. Zuniga-Galindo, *Ultrametric diffusion, rugged energy landscapes and transition networks*, Physica A: Statistical Mechanics and its Applications, 597 (2022), pp. 127–221.